UNDERSTANDING AND MAPPING VARIABILITY OF THE NIOBRARA FORMATION ACROSS WATTENBERG FIELD, DENVER BASIN

by

Nicholas Matthies

A thesis submitted to the Faculty and the Board of Trustees of the Colorado School of Mines in partial fulfillment of the requirements for the degree of Master of Science (Geology).

Golden, Colorado

Date_____

Signed:_____
Nicholas Matthies

Signed:_____
Dr. Stephen A. Sonnenberg
Thesis Advisor

Golden, Colorado

Date:_____

Signed:_____
Dr. Paul Santi
Professor and Head
Department of Geology and Geological Engineering

ABSTRACT

Wattenberg Field has been a prolific producer of oil and gas since the 1970s, and a resurgence of activity in recent years in the Niobrara Formation has created the need for a detailed study of this area. This study focuses on mapping regional trends in stratigraphy, structure, and well log properties using digital well logs, 3D seismic data, and core X-ray diffraction data.

Across Wattenberg, the Niobrara is divided into the Smoky Hill Member (made up of A Chalk, A Marl, B Chalk, B Marl, C Chalk, C Marl, and Basal Chalk/Marl) and the Fort Hays Limestone Member. Directly beneath the Niobrara, the Codell Sandstone is the uppermost part of the Carlile Formation. Stratigraphic trends in these units are primarily due to differential compaction and compensational sedimentation.

The largest structural trend is a paleo-high that runs east-west to northeast-southwest across the middle of the field. It has a relief of about 100 ft, and is 20 mi wide. The A Chalk and A Marl show evidence of submarine erosion over this area. Faults mapped from 3D seismic data are consistent with previously published data on a proposed polygonal fault system in the Denver Basin. Faults are 1000-10,000 ft long, have 30-150 ft vertical displacement, about 45° dip, and commonly form grabens 20-1000 ft wide. The faults and grabens have a northeast-southwest trend and are commonly seen en echelon. This orientation is interpreted to be the result of transtension.

Total organic carbon (TOC) was calculated from resistivity and density logs and mapped across Wattenberg Field. The high range of maturity limits the accuracy of the calculation, especially in the chalks. Mean TOC values are erroneously high at the edges of the field, where maturity is lower.

An anomalous resistivity low is recognized and mapped in the center of the field. Its primary cause is attributed to overpressuring as a result of higher thermal maturation. Petrophysical analysis on the well logs and geophysical analysis on the 3D seismic data are recommended for future work.

TABLE OF CONTENTS

LIST OF FIGURES

ACKNOWLEDGEMENTS

This thesis would not be complete without the support and guidance of many important people in my life. I would like to thank Dr. Steve Sonnenberg for being my advisor and helping me through the whole process of graduate school. I would also like to thank Dr. Tom Davis and Dr. John Humphrey for serving on my committee and for their work to improve my research. My colleagues in both the Niobrara Consortium and the Reservoir Characterization Project deserve thanks for their support, collaboration, and insight. I would also like to acknowledge Anadarko Petroleum Corporation and Bill Barrett Corporation for donating data for this work. On a personal note, I would like to thank my family, Mark, Donna, Kara, Larry, and Sally for their unwavering support. Finally, my wife Jenny deserves thanks for her sacrifices, encouragement, and love.

CHAPTER 1

INTRODUCTION

Wattenberg Field is located in the center of the Denver Basin in northeastern Colorado and is one of the largest oil and gas fields in the United States. With a long history of development, beginning in 1970, this field has entered a new phase of development since 2009 with the exploitation of the Niobrara Formation. Due to its low porosity and permeability, this "tight" formation is considered unconventional and requires new research approaches from both geologic and engineering perspectives to facilitate the greatest success. The work of this thesis aims to address this gap in knowledge by answering questions related to the geology of the Niobrara Formation in Wattenberg Field.

1.1 Objectives and Purpose

The objectives of this thesis are to:

- Describe and map Niobrara lithology and structure
- Use digital well logs to characterize the Niobrara
- Examine variability of stratigraphy and rock characteristics at large and small scales
- Integrate various types of data (e.g., well log, seismic, core) into a cohesive analysis

The purpose of this work is to provide a comprehensive analysis of the current state of Wattenberg Field by mapping and interpreting multiple variables that describe the Niobrara. This will be accomplished through the use of the petroleum systems approach and with the understanding of the modern, unconventional development of this field (horizontal and hydraulically fractured wells).

1.2 Study Area

The location of this research is limited to Wattenberg Field in Denver Basin, Colorado. In order to identify and interpret trends of different scales across this area, two different scales are employed. Specifically, regional-level research will be within the Greater Wattenberg Area (GWA) defined as T7N to T2S and R69W to R61W (Figure 1.1). Local-scale research will be limited to a 36 mi^2 area near the center of the GWA.

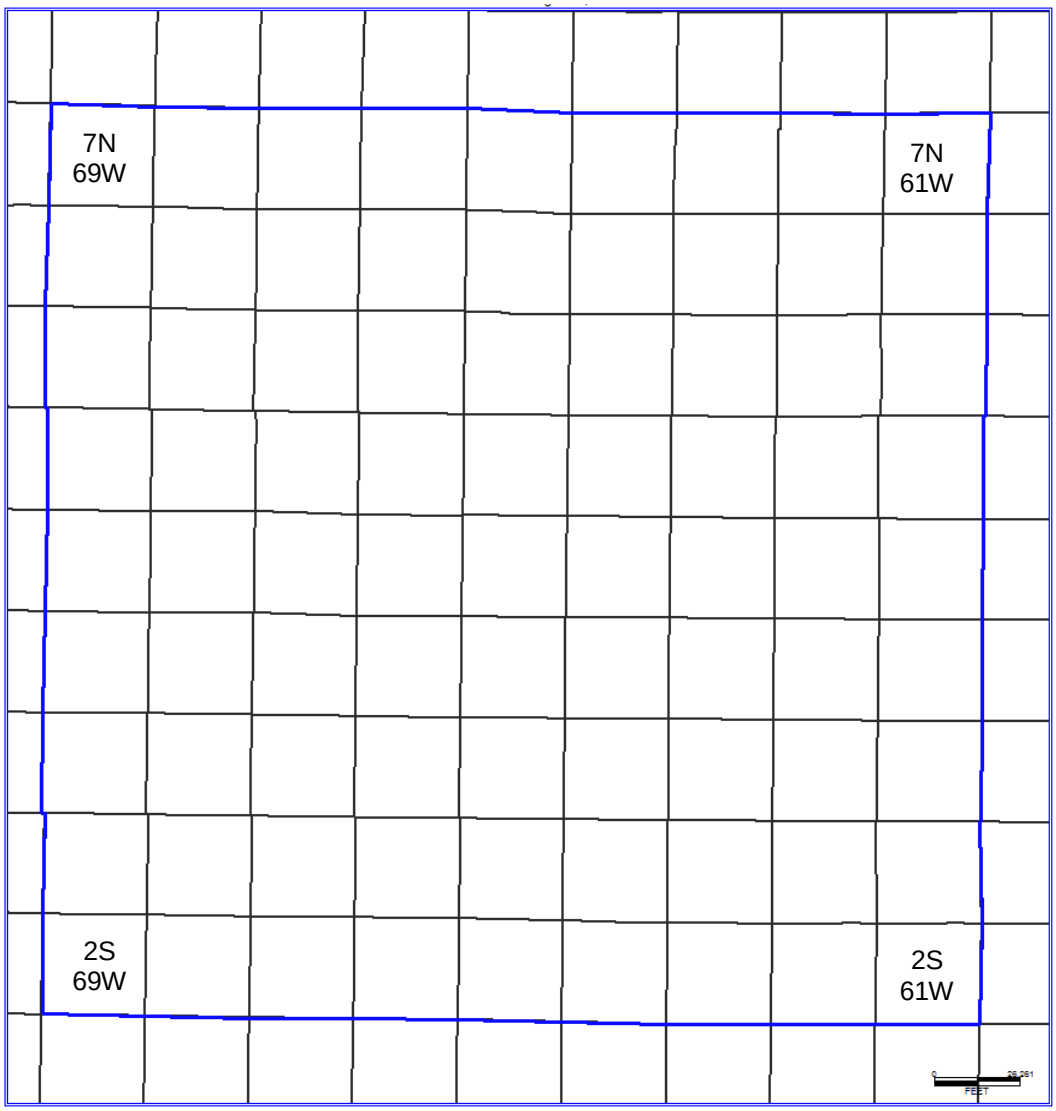

Figure 1.1. Blue outline shows the location of the Greater Wattenberg Area.

1.3 Dataset and Methodology

Two separate datasets are used in this study; one at each scale presented in the previous section. At the small-scale study area, a dataset of 2061 wells with digital logs was donated to the Colorado School of Mines Niobrara Consortium by the Bill Barrett Corporation. These logs include gamma ray, spontaneous potential, caliper, resistivity, neutron porosity, density porosity, and bulk density through the Niobrara Formation for the majority of the wells in the dataset. For the large-scale study area, data was donated to the Colorado School of Mines Reservoir Characterization Project by Anadarko Petroleum Corporation and is located within Wattenberg Field. This dataset includes 1344 wells with digital logs featuring a similar set of logs as the other dataset. Additionally, there is X-ray diffraction (XRD) data for one well within Wattenberg Field, and seismic data from a 50 mi^2 wide azimuth 3D P-wave survey. Data was also used from the USGS Core Research Center and IHS Energy U.S. well and production database.

The software IHS PETRA was used to organize and analyze the bulk of these data. Within PETRA, formation tops were picked from digital wells logs. Each interval of the Niobrara was assigned a zone and isopachs and log statistics were computed. XRD data was imported in to PETRA as digital logs for analysis. Transform and Petrel were used to create layouts of seismic data. Detailed work on the seismic data is being performed by other students within the Reservoir Characterization Project.

1.4 Research Questions

To organize the direction of this research, a selection of research questions was complied. The following questions help to fulfill the objectives and purpose and provide a direction for the conclusions of this thesis.

- What structural features are present in GWA and what are their causes?
- How does the stratigraphy of the Niobrara Formation vary across Wattenberg?
- How do structure and stratigraphy interact, particularly in relation to the thin in the A Chalk and A Marl?
- What patterns and variability in log data can be recognized across Wattenberg, and what are the causes of this variability?
- Chiefly, what are the causes of resistivity trends seen in Wattenberg?
- How do log-derived TOC calculations describe variability across Wattenberg?
- What are the characteristics of faults observable in the Niobrara?
- What additional evidence can be found to support theorized faulting styles in the Niobrara in the Denver Basin?
- Can growth strata be mapped to constrain the timing of observed faults?

CHAPTER 2

GEOLOGIC OVERVIEW OF WATTENBERG FIELD

A review of Wattenberg Field and the Niobrara Petroleum System allows for a background to this thesis. Additionally, the stratigraphy and structural styles of the Niobrara are reviewed.

2.1 History of Wattenberg Field Development

Wattenberg Field is by many measures one of the largest oil or gas fields in the Rocky Mountains. Its areal extent, reserves, well count, and years of development have made it a centerpiece of any discussion of petroleum in the Rocky Mountains, and especially in the Denver Basin. Even today, over 40 years since its discovery, Wattenberg is a focus of new research and development.

The first exploration done in the area that would become Wattenberg targeted the Permian Lyons Sandstone in the 1950s. From this early exploration, operators began to recognize the presence of a large accumulation of tight gas in the thick Cretaceous section of the Denver Basin. However, it was not until 1970 that Amoco and Vessels Oil and Gas began developing the J Sandstone. Early production was limited by poorly defined pay zones and inadequate fracture stimulations. By 1975, practices improved and successful development on 320-acre spacing continued through the end of the decade. In 1980, regulations changed to allow development on 160-acre spacing. This change prompted unimpeded development until 1994, as operators were able to improve well design to increase per well reserves to amounts higher than their preexisting 320-acre wells. In 1998, regulations were revised again to allow any Cretaceous formation to be completed in any well up to 5 wells per 160-acre tract (Ladd, 2001).

One of the many reasons Wattenberg is a unique field is its relatively continuous development since its discovery. As with the rest of the industry, Wattenberg has gone through boom cycles, but the field has experienced continuous drilling primarily due to the multiple productive formations. While the J Sandstone was the primary target for early development in Wattenberg, the potential of other Cretaceous formations was recognized with the Hygiene and Terry sandstones being targeted as early as 1971. Production from the Codell began in the 1970s, but poor reservoir quality and high gas oil ratios (GOR) from the first wells did not spark a large interest. Energy Oil began testing the Codell in 1981 and soon was able to improve well performance with completion procedures. A boom from 1991-1994 resulted in 4680 completions (Ladd, 2001). Other Cretaceous formations were developed to a limited extent during the first 30 years of Wattenberg's history, but the Niobrara would not make headlines until the 21st Century.

The Niobrara Formation's source rock potential and petroleum content has been known since the earliest delineation of Wattenberg Field. However, poor reservoir conditions due to the Niobrara's tight nature severely limited the number of wells. The most significant turning point in the development of the Niobrara in the Denver Basin was the Jake well discovery drilled by EOG Resources in October 2009. After producing 50,000 barrels of oil in the first 90 days, the well generated huge interest in this play (Matthews, 2011). Further successes were realized through the comparison of the Niobrara to other shale oil plays (like the Bakken and Eagle Ford) and through modern drilling techniques (horizontal drilling and hydraulic fracturing). Since this play expanded in 2009, significant research has been done to understand the Niobrara and to develop the field as efficiently as possible.

2.2 Stratigraphy

Before discussing the stratigraphy of the Niobrara, it is necessary to look at the regional setting during the Cretaceous. A seaway extended north-south across North America, splitting it into two landmasses (Figure 2.1). This seaway is called the Western Interior Cretaceous (WIC) Seaway. Sediments generally entered the basin from the west due to the uplifted Sevier Orogeny. A maximum of about 15,000 ft of sediment is preserved near the Utah-Colorado border (Kauffman, 1977). Siliciclastics dominated the western side of the seaway and marine shales with carbonate intervals dominated the eastern side. The Niobrara is one of the carbonate formations (Figure 2.2).

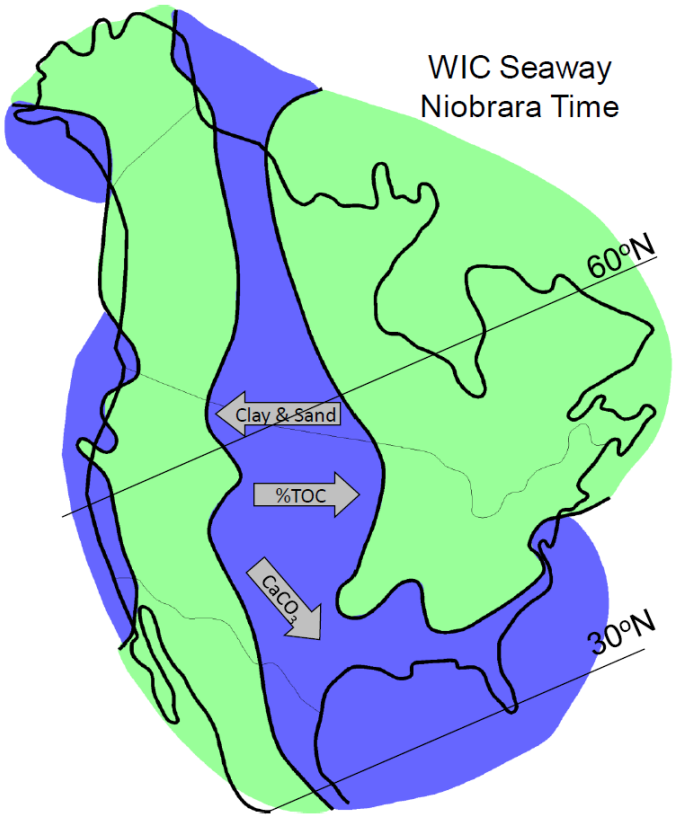

Figure 2.1. Location and characteristics of the Western Interior Cretaceous Seaway from Sonnenberg (2012) modified after Longman et al. (1998).

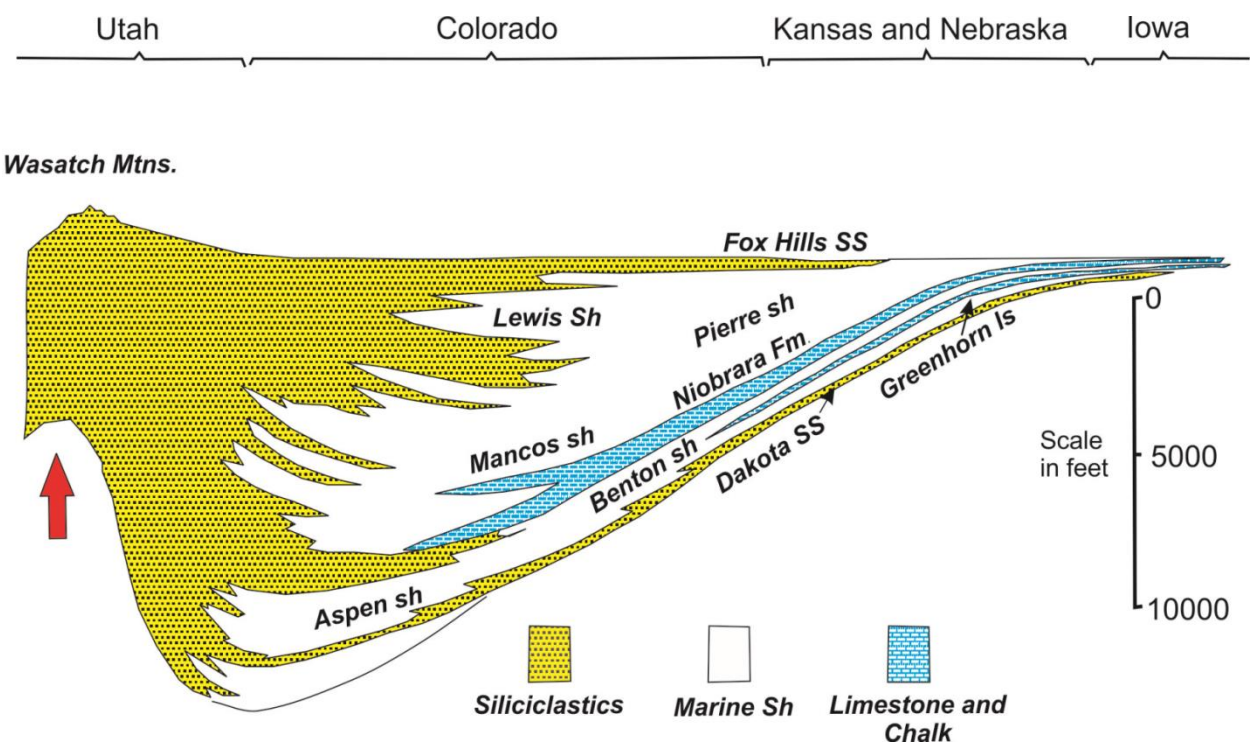

Figure 2.2. Cross section of WIC Seaway section showing lithology and thickness trends and the distribution of the Niobrara Formation. Note the increase of siliciclastics to the west and carbonates to the east. From Sonnenberg (2012) modified after Kauffman (1977).

In the GWA, the Cretaceous section begins with the productive Dakota Sandstone at a typical depth of 7800 ft (Figure 2.3). Producing intervals continue up to a typical depth of 4300 ft, including the J Sand, Codell Sand, Niobrara, Hygiene Sandstone, and Terry Sandstone. Source rock intervals include the Skull Creek Shale, Graneros Shale, Niobrara, and the Sharon Springs Member of the Pierre Shale.

While all of these formations produce significant amounts of oil and gas, the focus of this research is the Niobrara Formation. The Niobrara is a relatively continuous formation made up of two members: (a) the lower Fort Hays Limestone Member and (b) the upper Smoky Hill Member. The lower Fort Hays Limestone Member is a relatively pure limestone that is 20-30 ft thick in the GWA, thickening to the southeast (Weimer et al., 1986). The upper Smoky Hill Member is made up of alternating chalks and marls. In descending order, these individual units

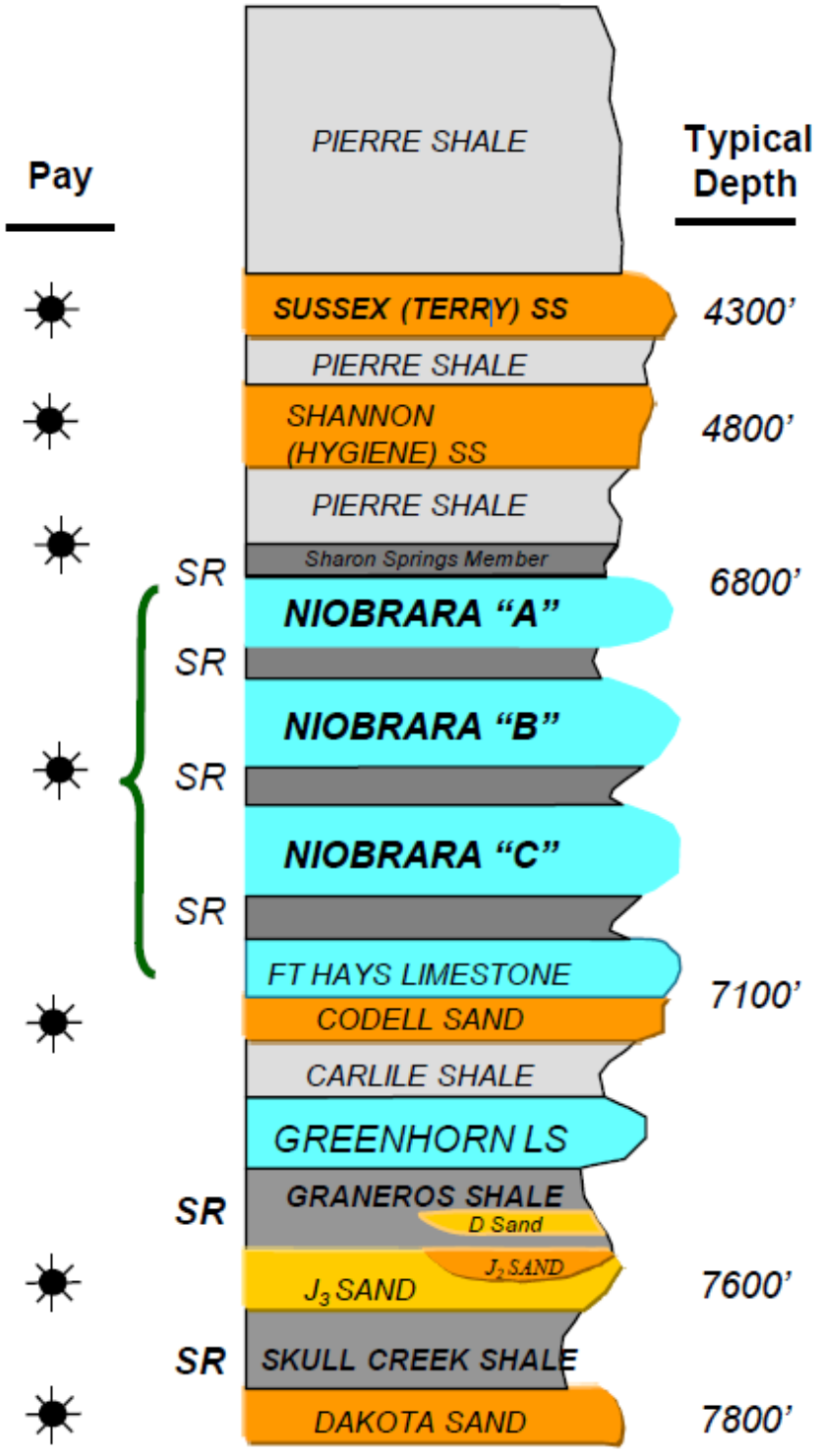

Figure 2.3. Cretaceous stratigraphic column showing the multiple pay zones, source rock (SR) intervals, and typical drilling depths (after Sonnenberg, 2012).

are called the A Chalk, A Marl, B Chalk, B Marl, C Chalk, and C Marl. In places, the B Chalk is divided into the B1 Chalk and B2 Chalk, and a Basal Chalk/Marl unit is present between the C Marl and Fort Hays.

A type log of the Niobrara in Wattenberg (Figure 2.4) shows typical log responses for the various chalks and marls within the formation. Compared to the marls, the chalks have a lower gamma ray, a higher resistivity, and neutron-density porosity crossover. This type log also shows typical thicknesses for each of the units, with the Niobrara as a whole about 300 ft thick (Weimer and Sonnenberg 1982; Drake and Hawkins, 2012). While these chalks and marls are generally continuous in the Denver Basin, care must be used with lithocorrelation. Contacts between chalks and marls are gradational and the differences between chalk and marl facies are small. For the proposed research, the lithology will be defined as in Sonnenberg (2012), with "chalk" referring to carbonate content above 70%, and "marl" as 30-70% (Figure 2.5).

Changes in the thickness of the units that make up the Niobrara across Wattenberg are important to understanding the depositional history and to exploring for petroleum. One of the most pronounced trends in Wattenberg is a thin to missing east-west trend of the A chalk (Figure 2.6). While this has been correlated with a paleostructual high (Weimer and Sonnenberg, 1982), other its presence can be investigated further.

2.3 Niobrara Petroleum System

As defined by Magoon and Dow (1994), a petroleum system is made up of essential elements (source rock, reservoir rock, seal, overburden), processes (trap formation, generation-migration-accumulation of petroleum), and timing. From these components, the definition of a petroleum system has stratigraphic, geographic, and temporal controls. The Niobrara Petroleum System is an economic system due to the favorable descriptions of each of these constituents.

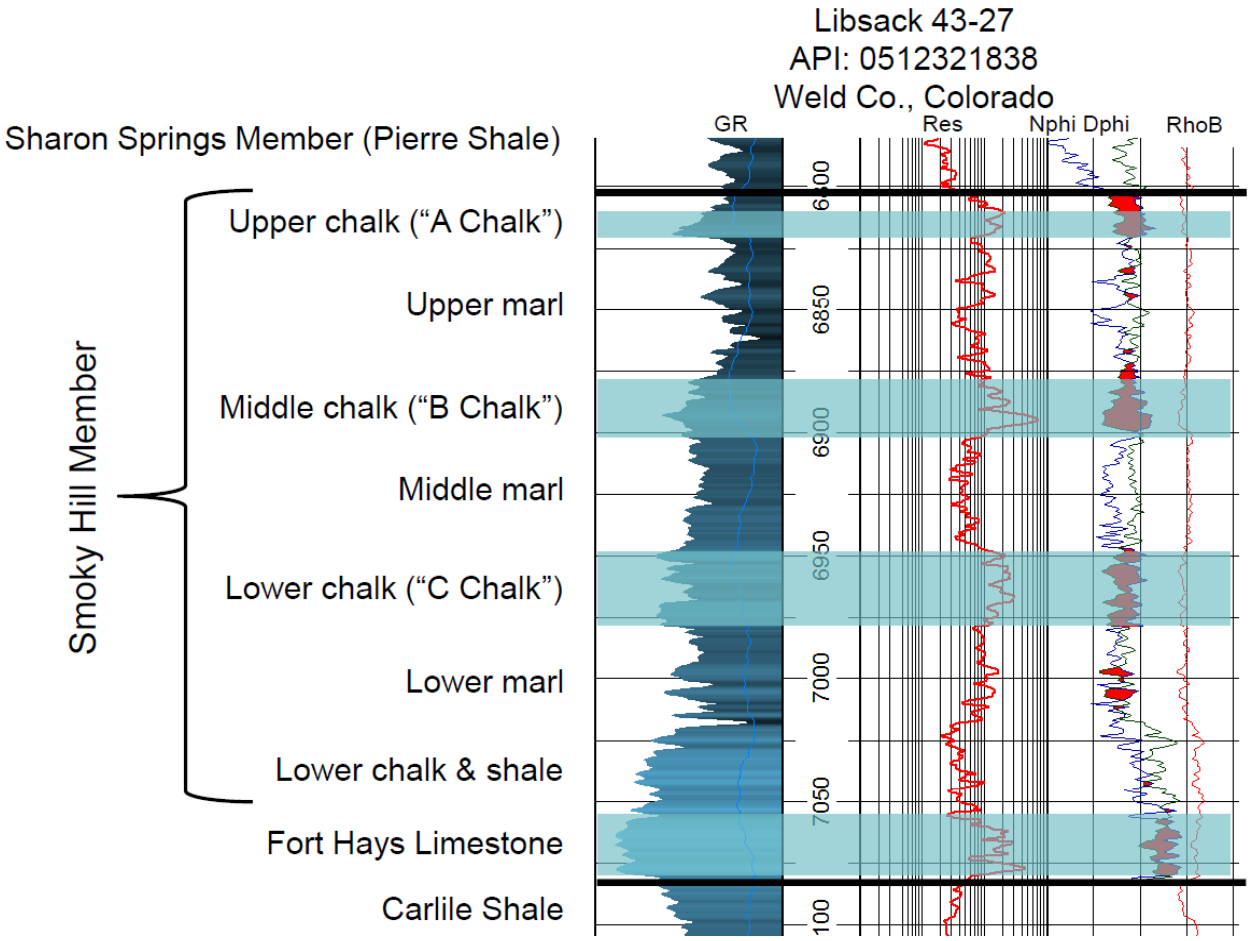

Figure 2.4. Niobrara type well log responses. Note the chalks have lower GR, higher resistivity, and neutron-density porosity crossover. In this well, the B Chalk only consists of the B2 interval, and the lower chalk and shale (between the C Marl and Fort Hays Limestone is present (after Drake and Hawkins, 2012).

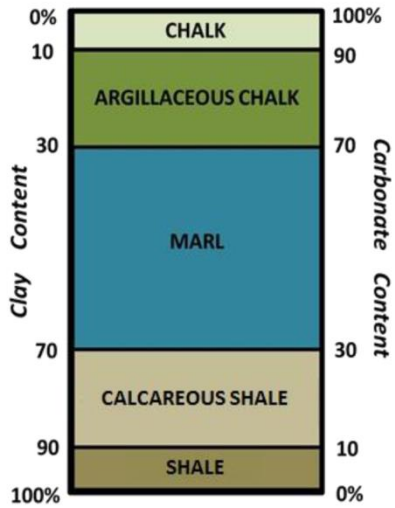

Figure 2.5. Naming convention for the shale-chalk continuum (after Sonnenberg, 2012).

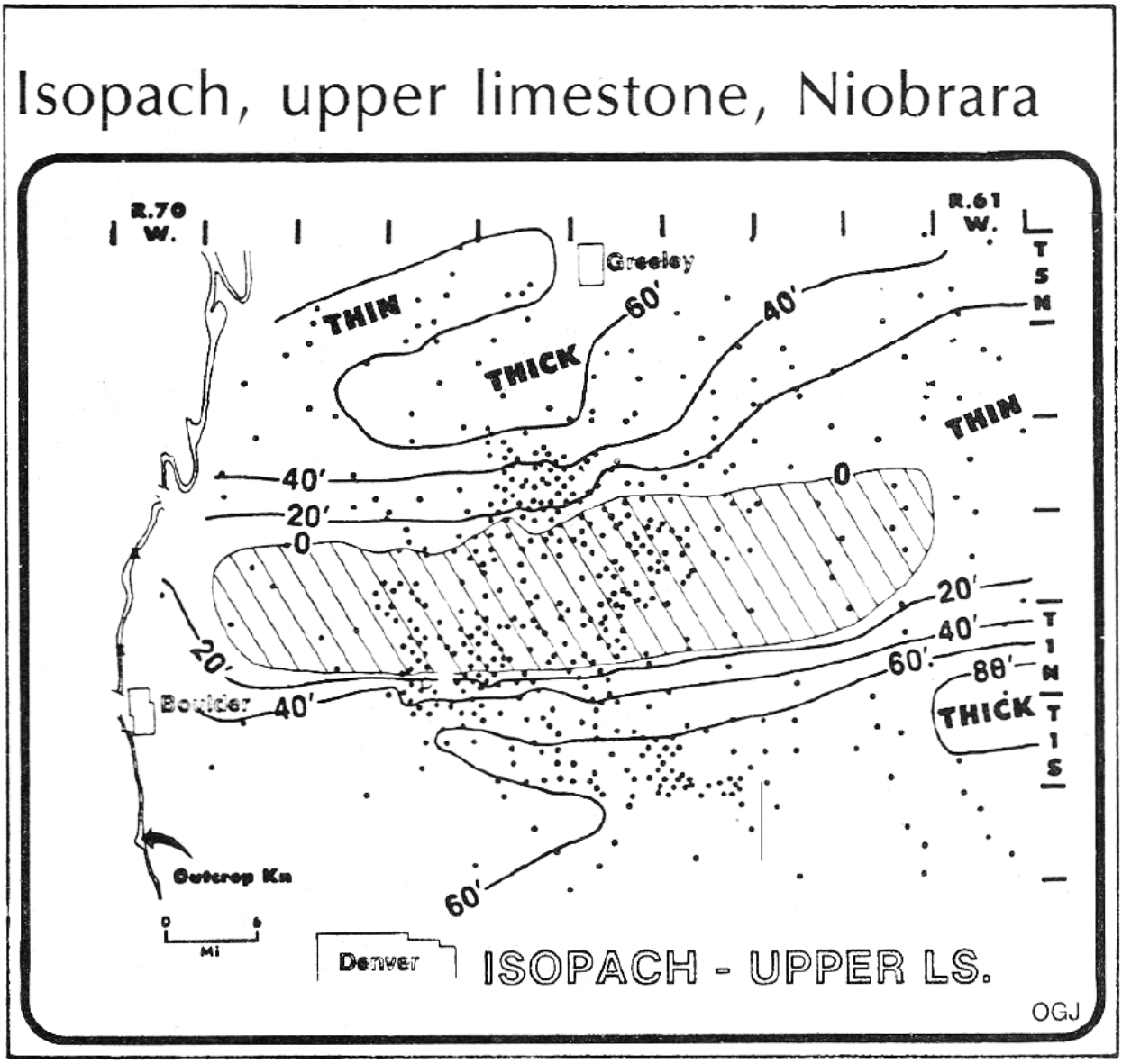

Figure 2.6. Isopach of the A Chalk of the Niobrara Formation showing its thin and absence over the center of Wattenberg Field. This thin has been attributed to submarine erosion over a paleo-high (after Weimer and Sonnenberg, 1982).

The essential elements of the Niobrara Petroleum System are part of the reason for the success of the play. The Niobrara is its own source rock, as TOC values have been shown to be high enough to be a source rock throughout its geographic range. In Wattenberg, the chalk benches have a slightly lower TOC (1-3%) than the marls (2-6%), and kerogen is dominantly Type II (oil-prone) (Weimer, 1996; Sonnenberg and Weimer, 1993; Jarvie, 2012; Sonnenberg, 2012).

While the marls are better source rocks, the chalks are better reservoirs. However, the porosity and permeability are low enough to be classified as tight and unconventional. Porosity is generally less than about 10% and permeability less than 0.1 md (Weimer, 1996; Luneau et al., 2011; Jarvie, 2012). With rocks this tight, fractures (both natural and induced) are critical to production. The Niobrara has relatively low clay content, especially in the chalk benches, which results in relatively brittle rocks. This property is essential to production. Early production from the Niobrara was centered on fields with high concentrations of natural fractures, such as Silo and Rangely fields. The presence of natural fractures in Wattenberg has been documented (Sonnenberg, 2012), but accurately modeling and predicting fracture patterns is still not feasible. Complex structures and debate over structural styles of the Denver Basin must be resolved prior to understanding natural fractures in Wattenberg.

Seal and overburden rocks are also present across Wattenberg. Directly above the Niobrara lies the Sharon Springs Member of the Pierre Shale. This is an organic-rich impermeable shale that acts as a seal to the Niobrara. The overlying Cretaceous rocks are the overburden, and are thick enough to have resulted in sufficient burial for petroleum generation. With the essential elements of a petroleum system defined, the processes that control the system can be discussed.

Since Wattenberg Field is an unconventional basin-centered petroleum accumulation, it does not have a classically-defined trapping mechanism. Instead, it is an inverted system, where the oil and gas are found where they were generated, with gas being deeper than oil, and oil deeper than water. The fluid types are separated by transition zones defined by maturity barriers and changes in pressure (Figure 2.7). However, traditional traps have been identified in Wattenberg. Weimer et al. (1986) describe Wattenberg as a series of stratigraphic-diagenetic traps with a minor structural influence. A structural high in the Cretaceous ran WSW-ENE across Wattenberg that may have some influence on trapping petroleum (Weimer and Sonnenberg, 1982; Longman et al., 1998). No matter how the trapping mechanism is described, the most important distinction is that the oil and gas are not trapped by forces of buoyancy, but rather by the tightness of the rock.

The processes of generation-migration-accumulation are inherently linked because the Niobrara is its own source rock. Gas in Wattenberg has been shown to be thermogenic (Smagala et al., 1984). Oil generation in the Niobrara began near the end of the Cretaceous and continued until significant uplift began about 5 million years ago (Figure 2.8) (Sonnenberg, 2012). The level of maturation varies significantly across Wattenberg. The center of the field has a vitrinite reflectance (Ro) of about 1.2%, and the outer edges of the field have Ro of about 0.9% (Figure 2.9) (Higley and Cox, 2005). This "hotspot" has been termed the Wattenberg Thermal Anomaly, and its cause has been attributed to intrusive igneous bodies in the basement rocks located at the northeastern extension of the Colorado Mineral Belt (Figure 2.10) (Higley, Gautier, and Pawlewicz, 1992; Sims and Finn, 2001; Higley, Cox, and Weimer, 2003; Higley and Cox, 2005).

The majority of petroleum found in the Niobrara in Wattenberg is the result of primary migration. Since this formation is both the source and reservoir, oil and gas have only been

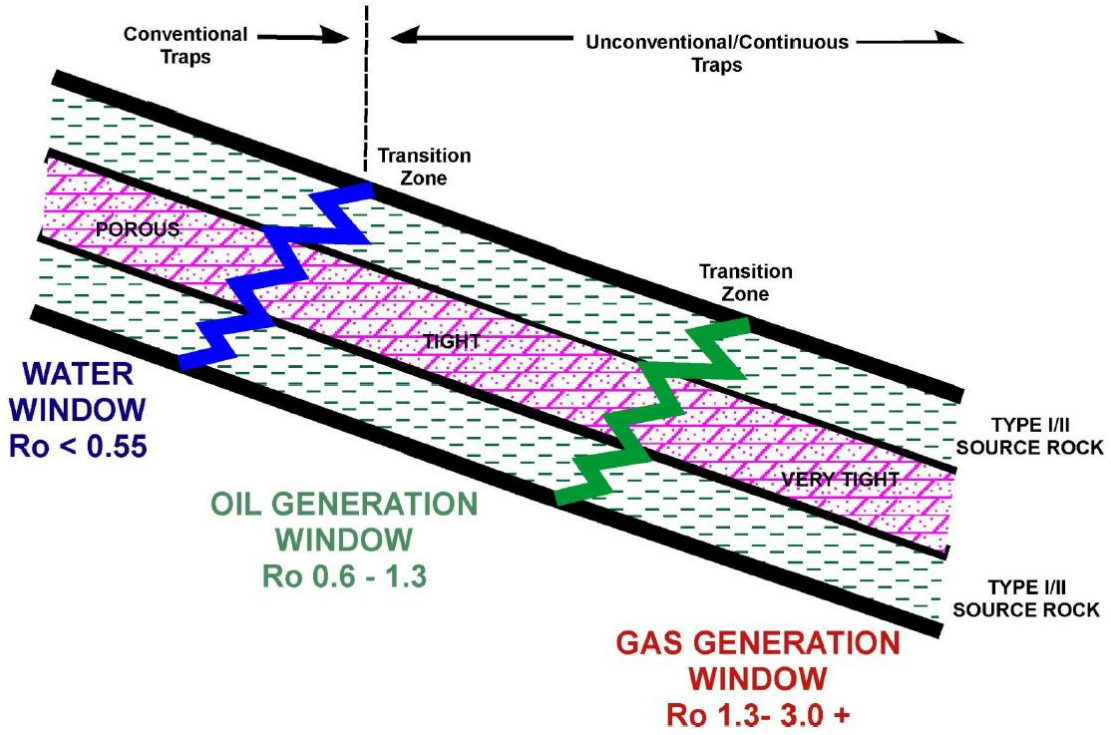

Figure 2.7. Diagram of an inverted petroleum system like the Niobrara in the Denver Basin. Note the transition zones between the different maturity windows and porosity differences (after Sonnenberg, 2012).

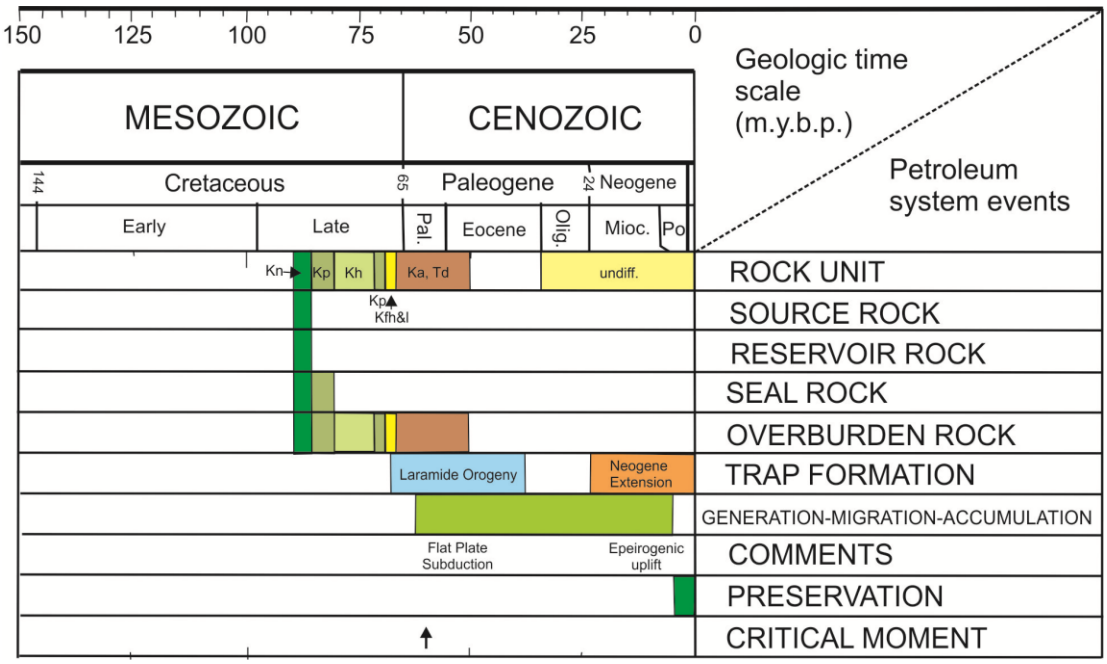

Figure 2.8. Niobrara Petroleum System Events Chart showing the timing of the various petroleum system events. Note the timing of the critical moment at the end of the Cretaceous and the end of generation-migration-accumulation about 5 Ma (after Sonnenberg, 2012).

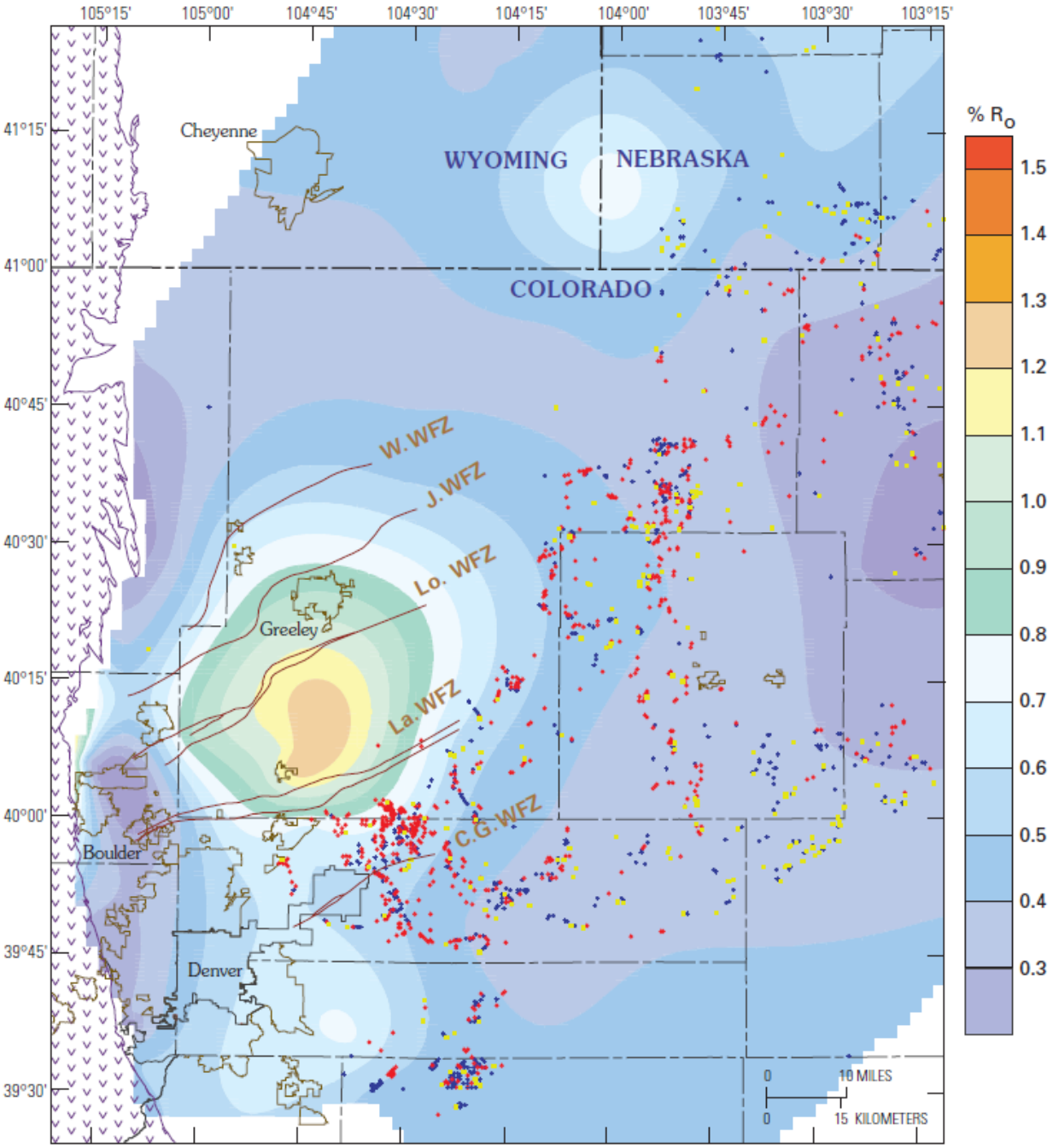

Figure 2.9. Contour map of vitrinite reflectance (percent Ro) from the Graneros, Huntsman, Mowry, and Skull Creek Shale source rocks. Other data on map includes wrench fault zones (WFZ) and producing D Sandstone wells as red (gas), yellow (oil), and oil and gas (blue) dots (after Higley and Cox, 2005).

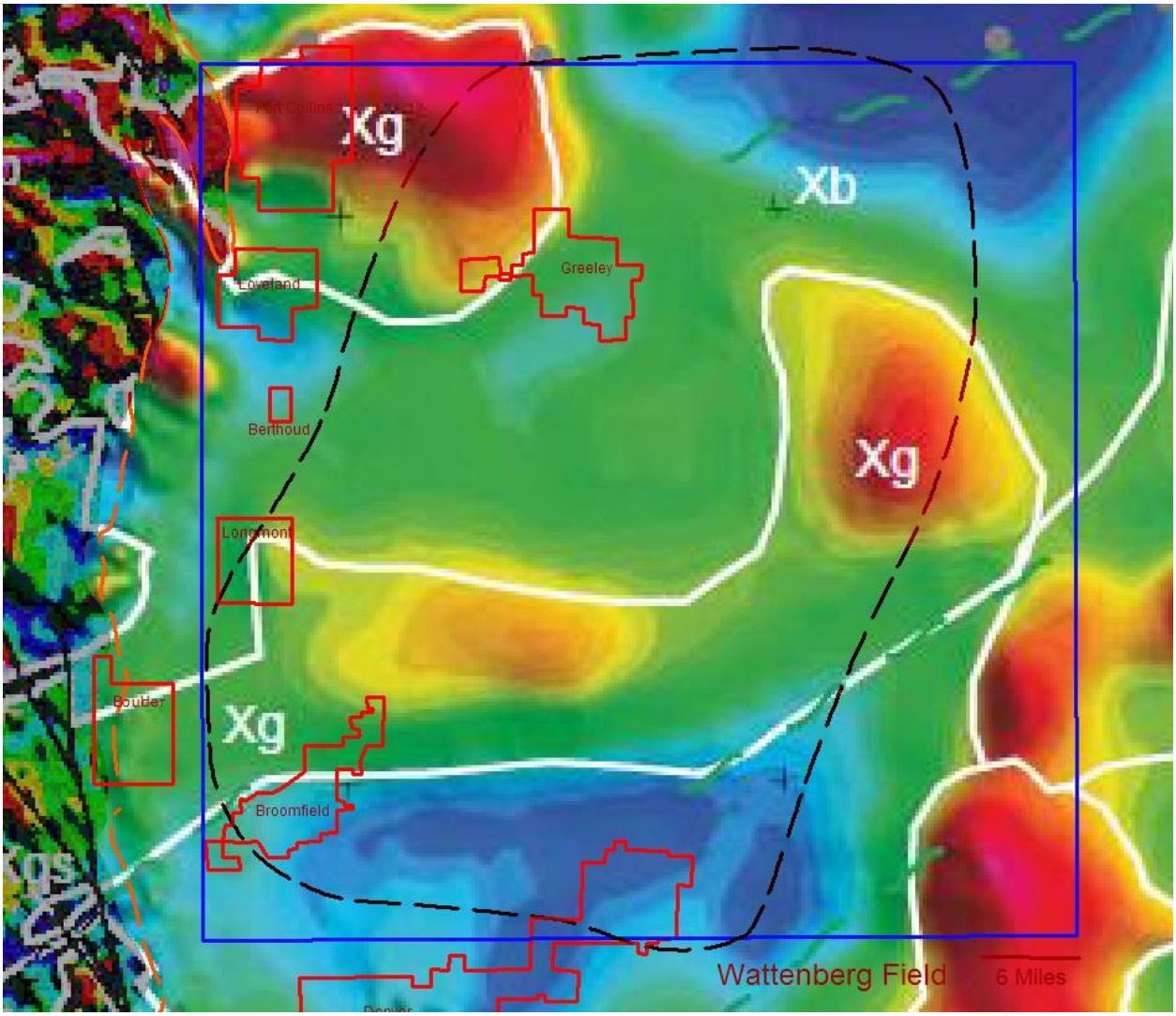

Figure 2.10. Aeromagnetic anomaly map showing anomalies in GWA (blue outline) attributed to igneous bodies in the basement rocks. High heat flow from these bodies may contribute to the Wattenberg Thermal Anomaly (modified from Sims and Finn, 2001).

expelled out of the organic matter and into the adjacent pore space. Secondary migration does take place as petroleum moves between formations and into traps in fields outside of Wattenberg. The most significant example of secondary migration in the GWA is into the Hygiene and Terry sands in Spindle Field (Pittman, 1989).

The accumulation of oil and gas within the Niobrara in Wattenberg is a direct result of the generation and migration of petroleum in the Niobrara Petroleum System. As evidenced by the overpressured cell that contains the Niobrara (Figure 2.11) (Weimer, 1996), much of the

petroleum generated in the Niobrara remains in place. This resource exists because of the combination and timing of all the elements and processes of the petroleum system.

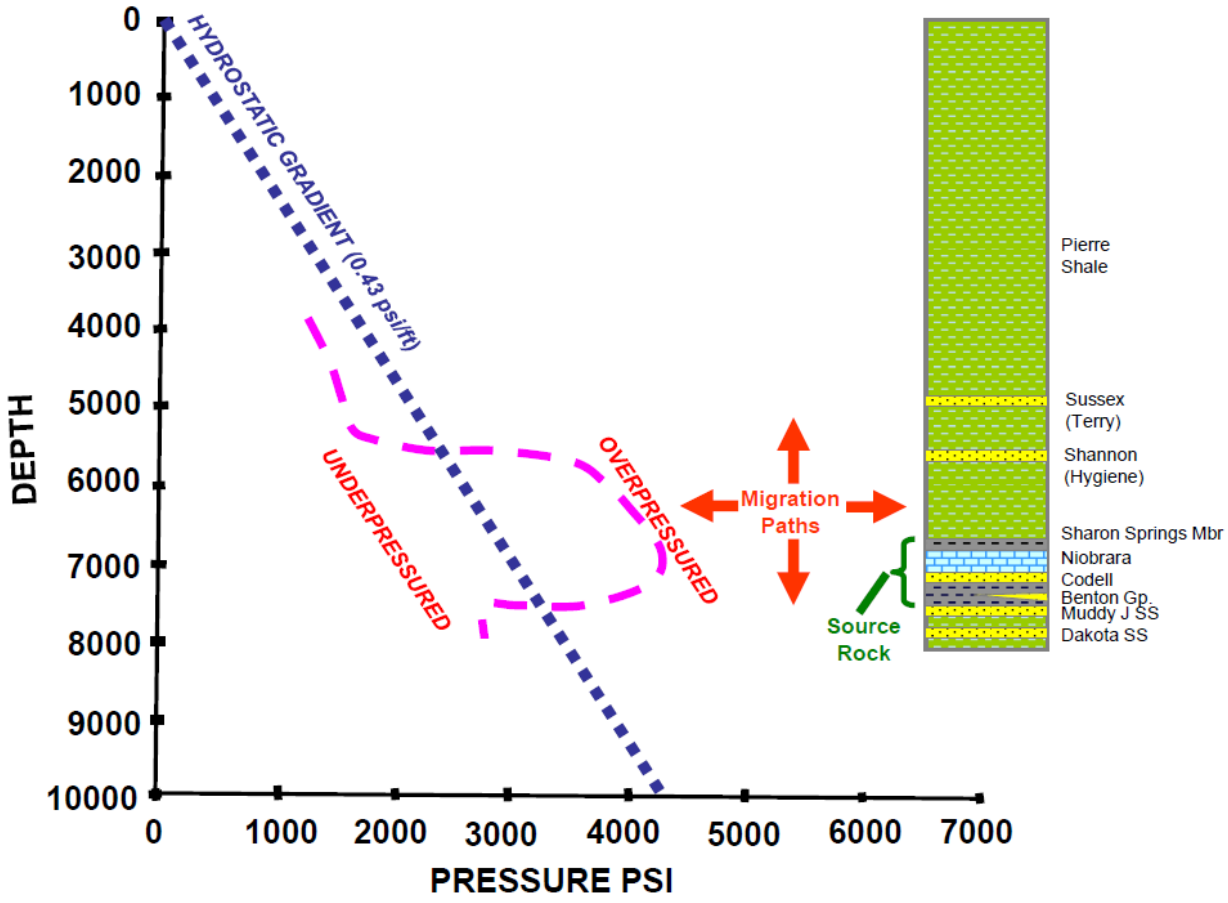

Figure 2.11. Depth-pressure graph of Denver Basin stratigraphy showing overpressuring in the Niobrara and related formations. However, note that the Dakota Group is underpressured, indicating flow barriers and changes in permeability (Sonnenberg, 2012 modified from Weimer, 1996).

2.4 Structural Complexities in Wattenberg Field

The tectonic history of the Denver Basin is important to understanding the structural complexities of the GWA. The basin began subsiding in the Late Pennsylvanian with the deposition of the Fountain Formation, but the majority of deformation took place during the Laramide Orogeny 67.5-50 Ma. It is now asymmetric, with the steep western side bounded by thrust faults along the Front Range of Colorado. The eastern side slopes gently (<0.5° dip) to

outcrop in Kansas. The basin is elongate roughly north-south, with the basin axis running through the center of Wattenberg. In the GWA, the greatest depth to basement is about 12,000 ft (Weimer, 1996; Higley and Cox, 2005; Nelson and Santus, 2011).

Aside from the asymmetrical syncline that defines the overall structure of the Denver Basin, the next most pronounced feature is a series of basement-involved wrench faults that run southwest-northeast across the basin (Weimer, 1996). These right-lateral wrench faults are named, from north to south, Windsor, Johnstown and Longmont, Lafayette, and Cherry Gulch (Figure 2.12). Weimer (1996) summarizes evidence for these wrench faults through subsurface mapping of faults and outcrop fracture, stylolite, and slickenside data. Movement along these faults has potential to compartmentalize reservoirs. Additionally, high concentrations of normal listric faults have been associated with the wrench fault zones and are proposed migrations paths for charging the Hygiene and Terry sands in Spindle Field (Weimer, 1996).

Recently, these normal listric faults have been reinterpreted as part of a polygonal fault system (PFS) present in at least two strata bound layers in the Denver Basin (Sonnenberg and Underwood, 2013). PFS are arrays of normal faults that are layer bound and have polygonal planform geometry (Cartwright, 2011). They have been recognized in many basins around the world, but have only recently been observed in the Denver Basin. This recent work has been possible through the use of 3D seismic data. Two tiers of polygonal faults have been recognized in the Niobrara and in the lower Pierre Shale (Figure 2.13).

The faults are generally too short (averaging about 4000 ft in length), discontinuous, and randomly oriented to map from well data, even on 20-acre spacing. These faults are further described as normal faults with about 45° dip and have about 20-90 ft of vertical displacement. The polygons created by these faults are somewhat discontinuous in the Niobrara, compared to

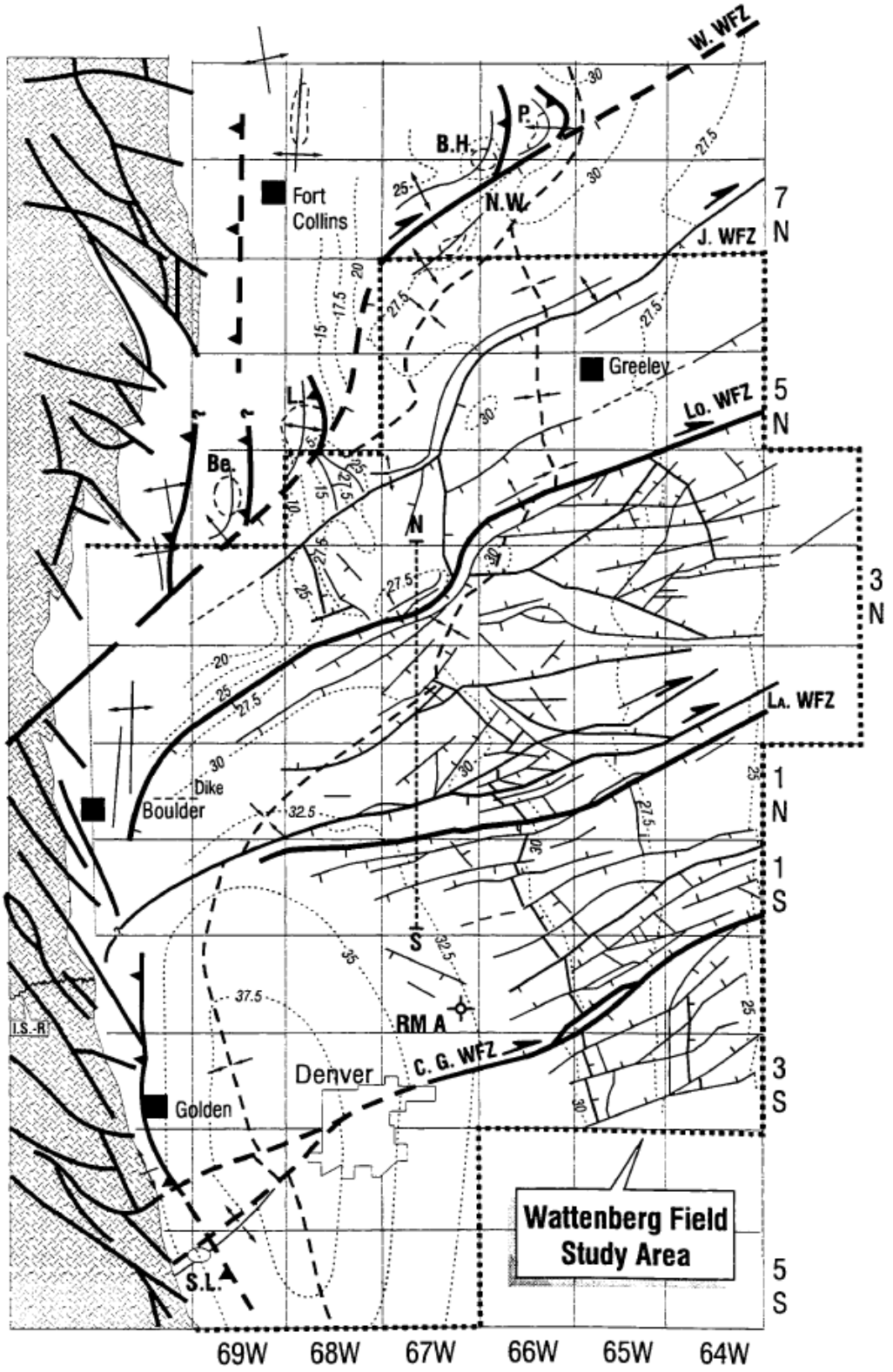

Figure 2.12. Wrench fault zones and related faults in the central Denver Basin. Arrows indicate direction of movement. Faults are near vertical and basement related. Dotted lines are subsea structure contours to top of Muddy (J) Sandstone in 100s ft (Weimer, 1996).

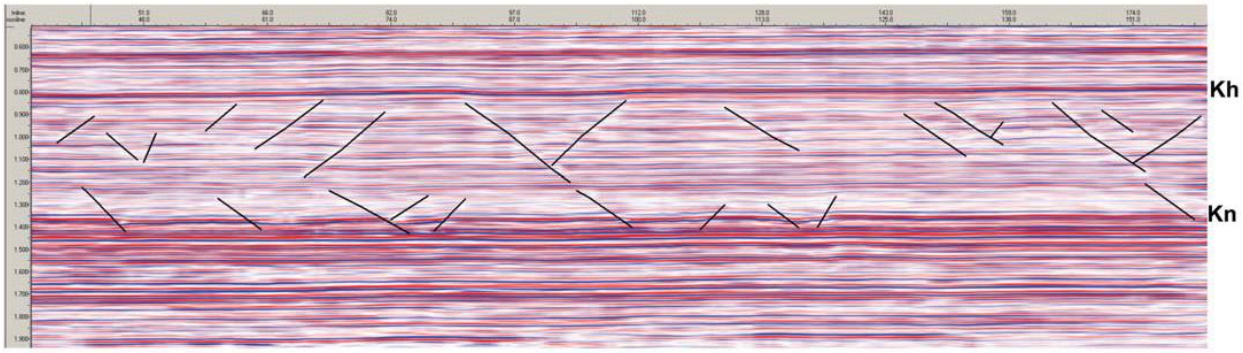

Figure 2.13. Arbitrary cross section through 3D seismic data with little vertical exaggeration showing two tiers of 45° normal faults in the Denver Basin identified as part of a polygonal fault system. Kh is Pierre Shale Hygiene Sandstone and Kn is Niobrara Formation (Sonnenberg and Underwood, 2013).

the tier in the lower Pierre Shale and other PFS. However, many fault intersections are at 120° (Figure 2.14) (Sonnenberg and Underwood, 2013).

The occurrence of natural fractures is of utmost importance to production out of the Niobrara. Since the formation is so tight, matrix permeability is too low to make the play economic. However, the presence of natural fractures in the Niobrara allows high enough fracture porosity and permeability to flow productive wells. The problem lies in predicting fracture patterns prior to drilling wells. There is currently a lack of published data that explains fracture patterns, but hypotheses have been proposed. Both Weimer (1996) and Sonnenberg and Underwood (2013) have suggested that extensional fractures may be associated with faults (from both tectonic and polygonal systems).

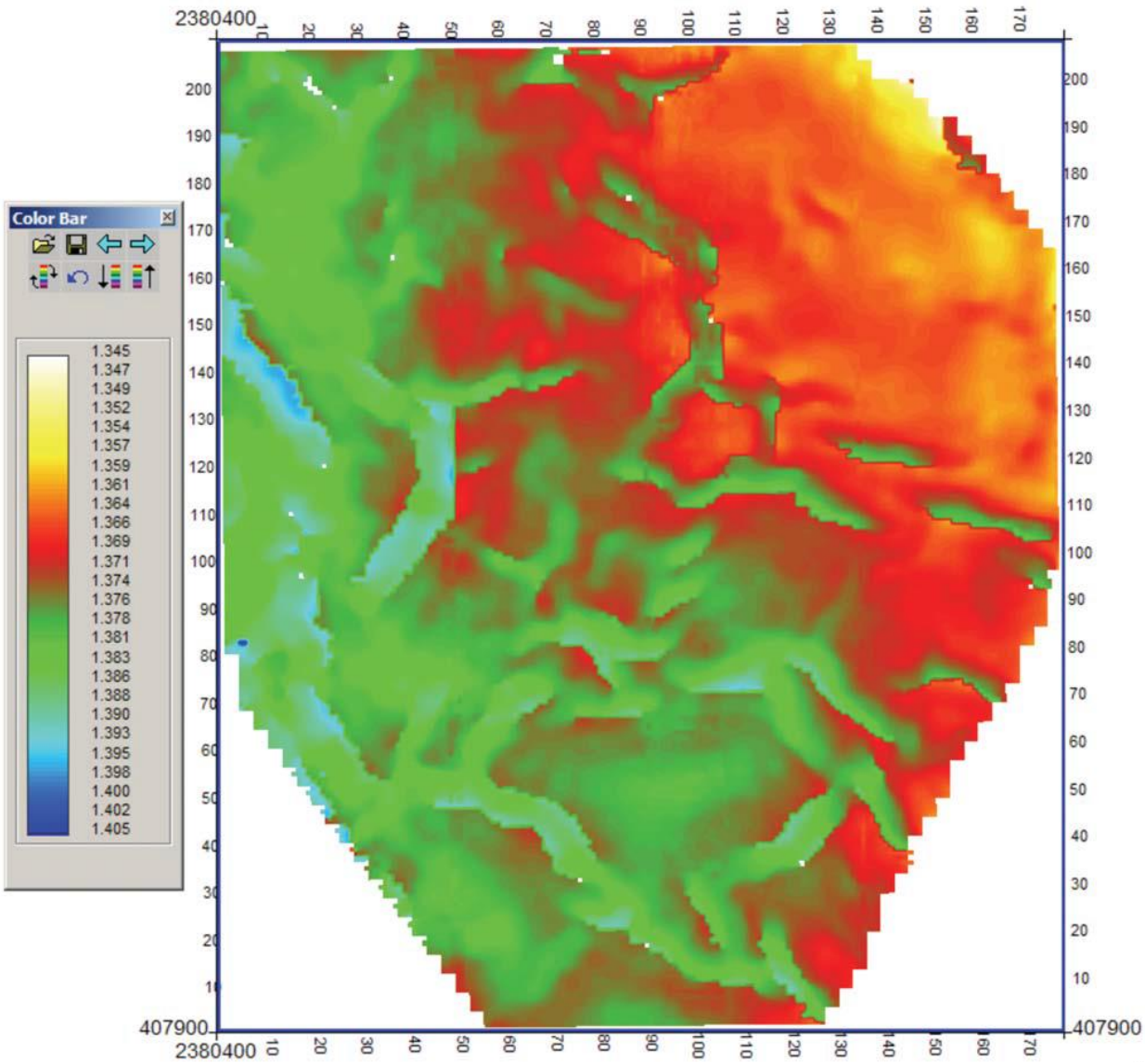

Figure 2.14. Niobrara Formation time structure map showing PFS. Red to yellow areas are higher and green to blue areas are lower. Note the polygonal to partial polygonal shapes formed by fault intersections, and the presence of randomly oriented grabens (Sonnenberg and Underwood, 2013).

CHAPTER 3

STRATIGRAPHIC AND STRUCTURAL TRENDS

While the individual chalk and marl benches within the Niobrara are generally continuous across the Denver Basin, there are variations within the GWA that are significant to the depositional history of the area. Additionally, structural trends observed in Wattenberg can be related to some of the stratigraphic features. The importance of these trends is in how they influence petroleum exploration and development. Faulting in the Niobrara is related to structure, but the complexities of these faults merit their own discussion is a separate chapter.

3.1 Niobrara Stratigraphy

The Niobrara Formation is made up of two members, the lower Fort Hays Limestone and the upper Smoky Hill Member. Directly beneath the Niobrara is the Codell Sandstone Member of the Carlile Shale, which is often included in discussions of the Niobrara due to its related petroleum production potential. The age of the Niobrara ranges from Upper Turonian (about 90 Ma) to Lower Campanian (About 82 Ma) (Drake and Hawkins, 2012).

The lithology of the Niobrara can be described in three components: carbonate sediment, siliciclastic sediment, and preserved organic carbon. The carbonate sediment is dominated by coccolith-rich fecal pellets. Siliciclastic sediment is generally shaley and originates from fluvial input from the Sevier highlands on the west side of the WIC Seaway. Organic carbon production was high in the WIC Seaway, but its preservation was controlled by bottom water anoxic conditions. The variation in these three lithologic components controls the variation within the Niobrara Formation (Dean and Arthur, 1998; Longman et al., 1998).

The cyclic compositional changes within the Niobrara can be attributed to sea level changes within the WIC Seaway. In general, the chalks were deposited during highstands and

the marls deposited during lowstands. During highstands, warm water moved further north into the WIC Seaway, which in turn increased carbonate production, lowered preservation of organic carbon, and lowered rates of deposition. During lowstands, warm water retreated southward, resulting in reduced carbonate production and increased siliciclastic input, higher preservation of organic carbon, and higher rates of deposition (Longman et al., 1998; Locklair and Sageman, 2008; Drake and Hawkins, 2012). These depositional cycles have been correlated to high-resolution orbital timescales (Locklair and Sageman, 2008). Due to differences in sedimentation rates, the lower abundance of carbonate in the marls has been attributed to dilution by increased siliciclastic deposition (Dean and Arthur, 1998; Locklair and Sageman, 2008; Drake and Hawkins, 2012). However, the cause of the changing sedimentation rates is unresolved, with Locklair and Sageman (2008) citing orbital timescale correlations, and Dean and Arthur (1998) suggesting tectonic processes changing sediment supply from the Sevier highlands.

The units within the Niobrara are described, mapped (when appropriate), and discussed to establish the stratigraphic trends and relationships in the GWA. This discussion helps facilitate an interpretation of the depositional history of the area. Lithology data is from XRD analysis from a well near the seismic data. Formation and bed tops were picked from digital logs across Wattenberg and mapped in IHS PETRA using the gridding method minimum curvature. A feature present in the following isopach maps is various "potholes" where one well in any given area has an anomalously low value. This is interpreted to be the presence of a normal fault removing part of the section. It should be noted, however, that the digital contouring process draws circular depressions around these wells, which do not accurately represent true geological conditions. In reality, these depressions are elongate along normal faults, but since their orientation cannot be determined, they cannot be contoured any more accurately than the circular

"potholes." The same color scale and contour interval are used for all isopach maps to allow for the direct visual comparison of the relative differences between units of the Niobrara.

3.1.1 Codell

The Codell Sandstone Member of the Carlile Shale underlies the Niobrara in the GWA. It is a quartz rich sandstone with XRD data from 12 samples showing an average of 60.0% quartz, 20.9% clays, 2.3% carbonates, 0.6% TOC, and 16.2% other minerals. A typical log response of the Codell in the GWA has a gamma ray of about 80-110 API units, low resistivity (8-12 Ω-m), jump in neutron porosity compared to the Fort Hays (10-30%) and large spike in density porosity (10-13%). The spike in density porosity is due to the log calibrated to limestone matrix and the Codell's siliciclastic nature.

The Codell isopach in Figure 3.1 shows how this unit thins to the southeast. It pinches out within the borders of the GWA, and reflects the trend in siliciclastic deposition described by Kauffman (1977) and Longman et al. (1998) and shown in Figure 2.2. Aside from this wedge-shaped geometry, the Codell is very consistent across Wattenberg, with few anomalous data points and typical thicknesses between 10 and 25 ft where the majority of Wattenberg wells are located.

3.1.2 Fort Hays

Whether the contact between the Codell and Fort Hays Limestone is conformable or not (Longman et al., 1998; Locklair and Sageman, 2008), it is known that a major change in the depositional environment occurred. For the first time since the Greenhorn Formation was deposited, the carbonate factory in the WIC Seaway was turned on. The result is a clean chalk with XRD data from 9 samples averaging 72.1% carbonates, 13.5% quartz, 8.8% clays, 0.2% TOC, and 5.4% other minerals. Other analyses of the Fort Hays generally show even higher

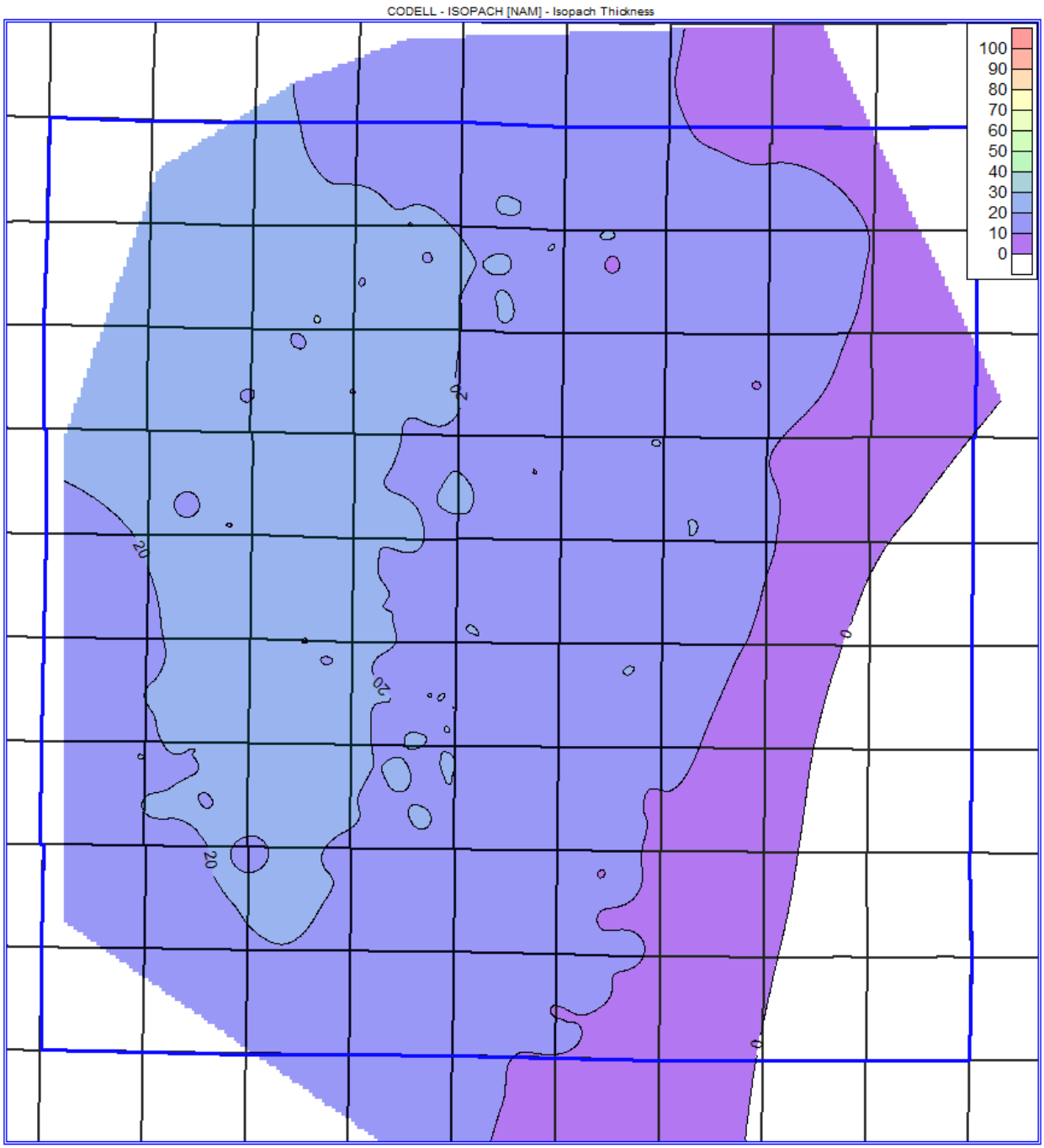

Figure 3.1. Isopach of Codell Sandstone Member of the Carlile Shale. This unit is thickest in the northwest corner of the GWA and thins to the southeast, pinching out within the GWA. The color-filled contour interval (10 ft) is the same for this series of figures showing the isopachs of the various units considered in this study to allow for the visual comparison of relative differences.

proportion of carbonates, and seven of the nine samples do have an average of 89.3% carbonate. The other two samples are from the margins of the unit and have a greater input of siliciclastics. As it is a clean chalk, the typical log response is as expected: very low gamma ray (20-40 API units), low resistivity compared to other chalks in the Niobrara (10-25 Ω-m), very low porosity (about 5% neutron and density porosity).

An isopach of the Fort Hays shows relatively consistent thickness with an overall trend of thinning to the northwest (Figure 3.2). This trend is the inverse of the Codell and may be the result of differential compaction and compensational sedimentation or the result of the depositional trend described by Longman et al. (1998) of more carbonates to the southeast.

3.1.3 Basal Chalk/Marl

The Basal Chalk/Marl, or D Chalk/Marl, is the first of the informally named units within the Smoky Hill Member of the Niobrara Formation. It is made up of cyclical, interbedded chalk and marl beds, but overall shares a similar lithology to the other chalk benches of the Niobrara than the marls. Data from 9 XRD samples reveal an average of 48.1% carbonates, 25.1% clays, 19.8% quartz, 0.5% TOC, and 6.5% other minerals. The Niobrara is known for its high organic content and as an effective source rock, but these data show that the lower 75 ft of the formation is organic poor. Oxic conditions prevailed in the Niobrara through the deposition of this Basal Chalk/Marl unit. As a chalk that is less clean than the Fort Hays, the gamma ray is higher (60-80 API units), resistivity lower (<10 Ω-m), and higher neutron porosity (7-20%), and similar density porosity (about 5%). Its lithology is not considered as distinctively different as the other chalk benches in the Niobrara, and it is commonly described as being a chalk-rich bed at the base of the C Marl. The following section describes the C Marl and an isopach map of both units together.

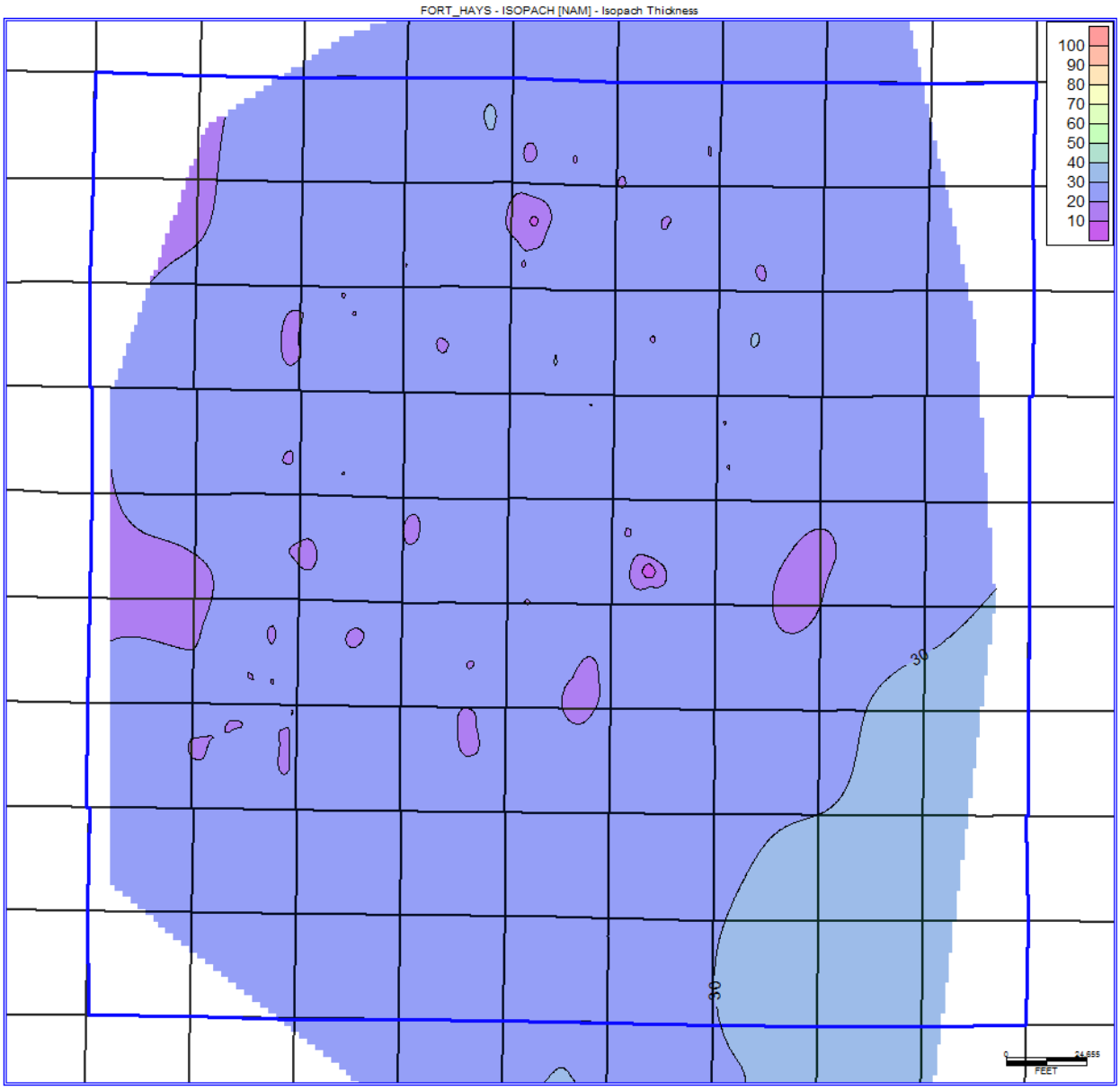

Figure 3.2. Isopach of the Fort Hays Limestone Member of the Niobrara Formation. This unit displays a relatively consistent thickness, but thins to the northwest. This is an inverse of the Codell Sandstone and may represent differential compaction and compensational sedimentation or regional siliciclastic and carbonate depositional trends. Color-filled contour interval is 10 ft.

The thickness of the Basal Chalk/Marl varies across Wattenberg, with a general trend of thickening to the south (Figure 3.3). This trend reflects the depositional patterns of the WIC Seaway, where more carbonate sediment was deposited to the south.

3.1.4 C Marl

The C Marl is the first of the organic rich marls in the Niobrara. It is made up of interbedded hot shales and chalk-bearing beds in its lower portion. It is often grouped with the Basal Chalk/Marl due to their similar characteristics in the Denver Basin. Data from 9 XRD samples gives average mineralogies of 55.4% carbonates, 16.1% clays, 12.3% quartz, 3.9% TOC, and 12.3% other minerals. The C Marl has some of the highest TOC values of the Niobrara, and is one of the most important source rock intervals. Its log response is characteristic of the Niobrara marl benches with a variable gamma ray (80-220 API units), low to moderate resistivity (5-30 Ω-m), high porosity (15-25% neutron porosity and 5-10% density porosity).

The isopach of the C Marl (including the Basal Chalk/Marl) increases in thickness dramatically to the south (Figure 3.4). This represents a southern shift of the depocenter of the WIC Seaway. The majority of this trend is within the Basal Chalk/Marl, but the C Marl also increases in thickness to the south. This isopach map differs from the Codell and Fort Hays by the presence of potholes of faulted out sections.

3.1.5 C Chalk

The C Chalk is the first of the main chalk beds of the Niobrara that is a common drilling target. Like much of the rest of the Niobrara, it is cyclical in nature, with alternating chalk-rich and chalk-poor beds. Data from 10 XRD samples gives a mineralogical makeup of 79.2% carbonate, 7.8% clays, 4.9% quartz, 2.3% TOC, and 5.8% other minerals. Its typical log

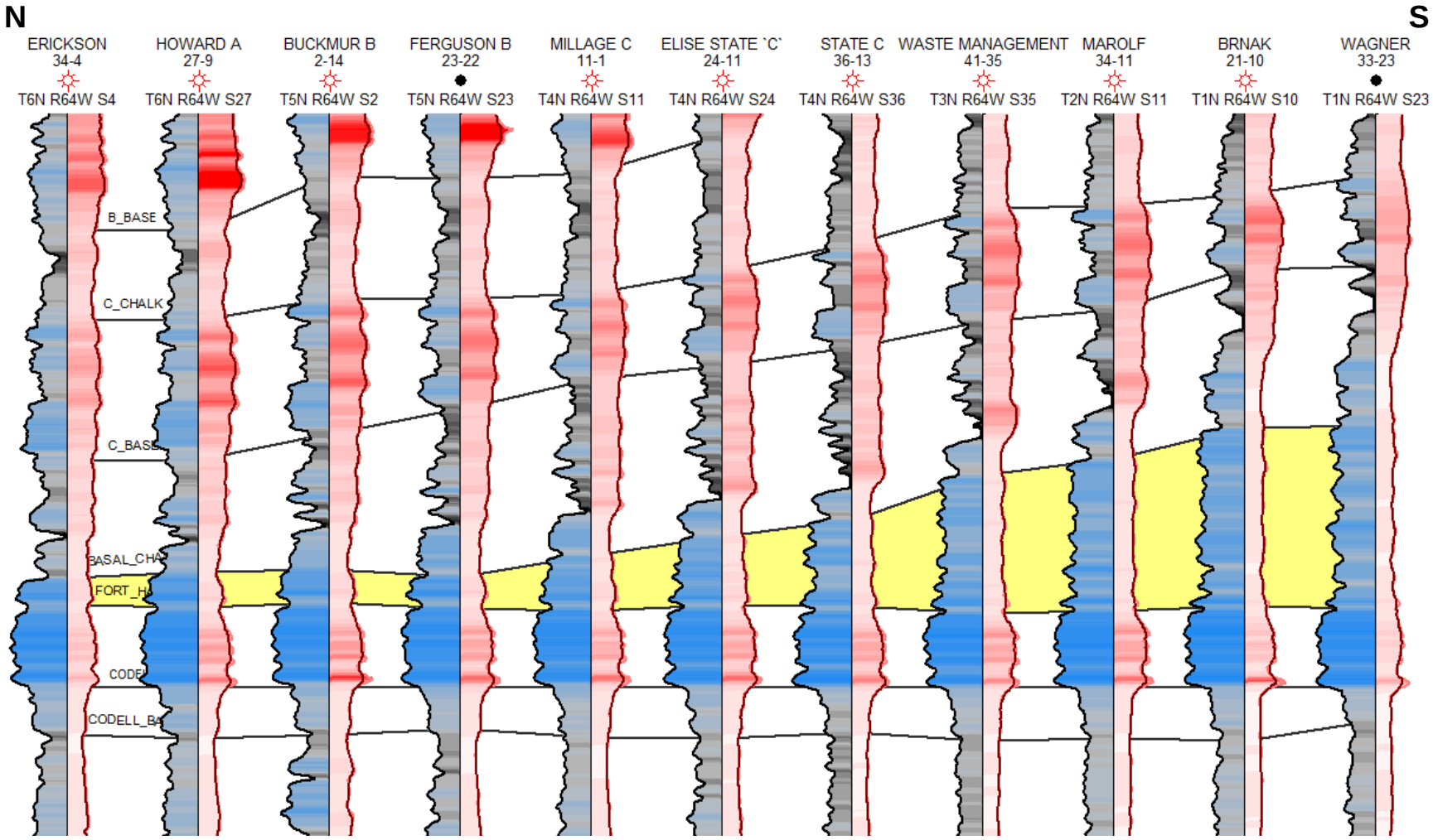

Figure 3.3. North-south cross section across Wattenberg showing the changes in the Basal Chalk/Marl (yellow). Track 1 is color-filled gamma ray and Track 2 is color-filled resistivity. Thickness increases from 10 ft to the north to 70 ft to the south end of the field. This stratigraphic cross section is hung on the top of the Codell.

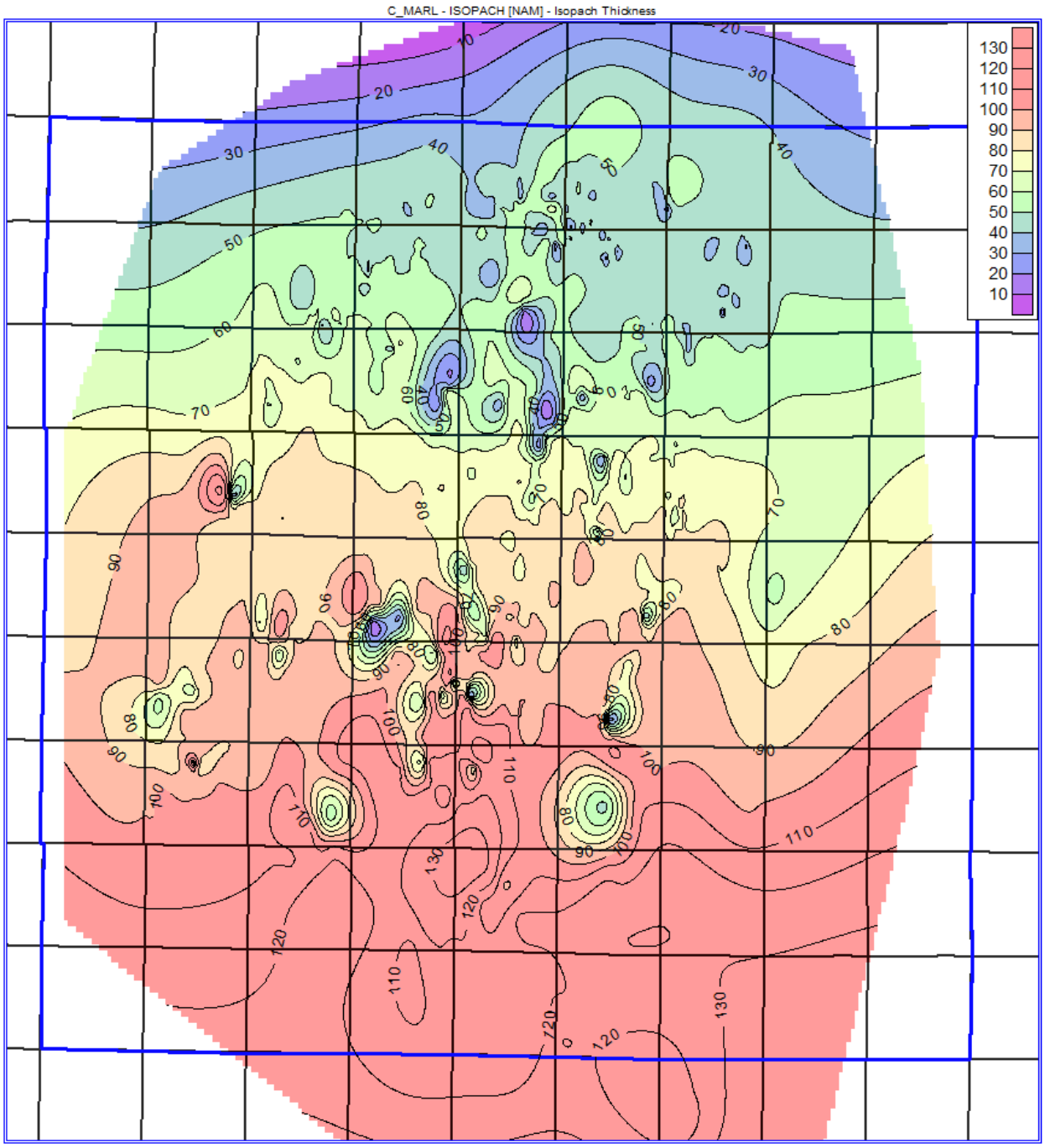

Figure 3.4. Isopach of the C Marl (including the Basal Chalk/Marl interval). This isopach shows a dramatically thickening trend to the south, representing a southern shift in the depocenter of the WIC Seaway. Note the increase in potholes of faulted out section compared to the Codell and Fort Hays.

response shows three low gamma ray beds (75-100 API units) with two interbedded high gamma ray beds (125-200 API units). This gamma ray trend is remarkably consistent across the field and makes the C Chalk one of the more easily recognizable units of the Smoky Hill Member. The resistivity follows suit, with three small spikes aligning with the gamma ray spikes, and is typically elevated at 20-50 Ω-m. Neutron and density porosity logs are both 10-15%, commonly with minor amounts of crossover, indicating the presence of gas.

The C Chalk isopach is 20-50 ft across most of Wattenberg Field (Figure 3.5). A thick trend exists in a northwest-southeast direction in the west half of the field, with a parallel thin trend directly to its north. The cause for these trends may be due to variable sedimentation rates controlled by currents and/or bathymetry of the WIC Seaway. These trends are important to oil and gas development, as they reflect changes in pay thickness.

3.1.6 B Marl

The B Marl is the middle marl unit of the Niobrara, lying between the B Chalk and the C Chalk. Mineralogy data from 9 XRD samples give an average composition of 58.4% carbonate, 20.9% clay, 11.1% quartz, 2.7% TOC, and 6.9% other minerals. It has similar composition to the C Marl, but not as high TOC. However, the TOC is still high enough to be considered a source rock. The log response is also similar to other marls of the Niobrara. Gamma ray is highest in the middle of the unit, and decreases towards the B Chalk and C Chalk (120-200 API units). Resistivity is lower than the surrounding chalks (10-25 Ω-m), neutron porosity is higher than the surrounding chalks (15-30%), and density porosity is a generally constant in this part of the Smoky Hill (8-11%).

The B Marl isopach is 10-60 ft for the majority of the field, reaching its thickest in the southwest corner in T1N R69W at 90 ft (Figure 3.6). Thickness trends are present, and show an

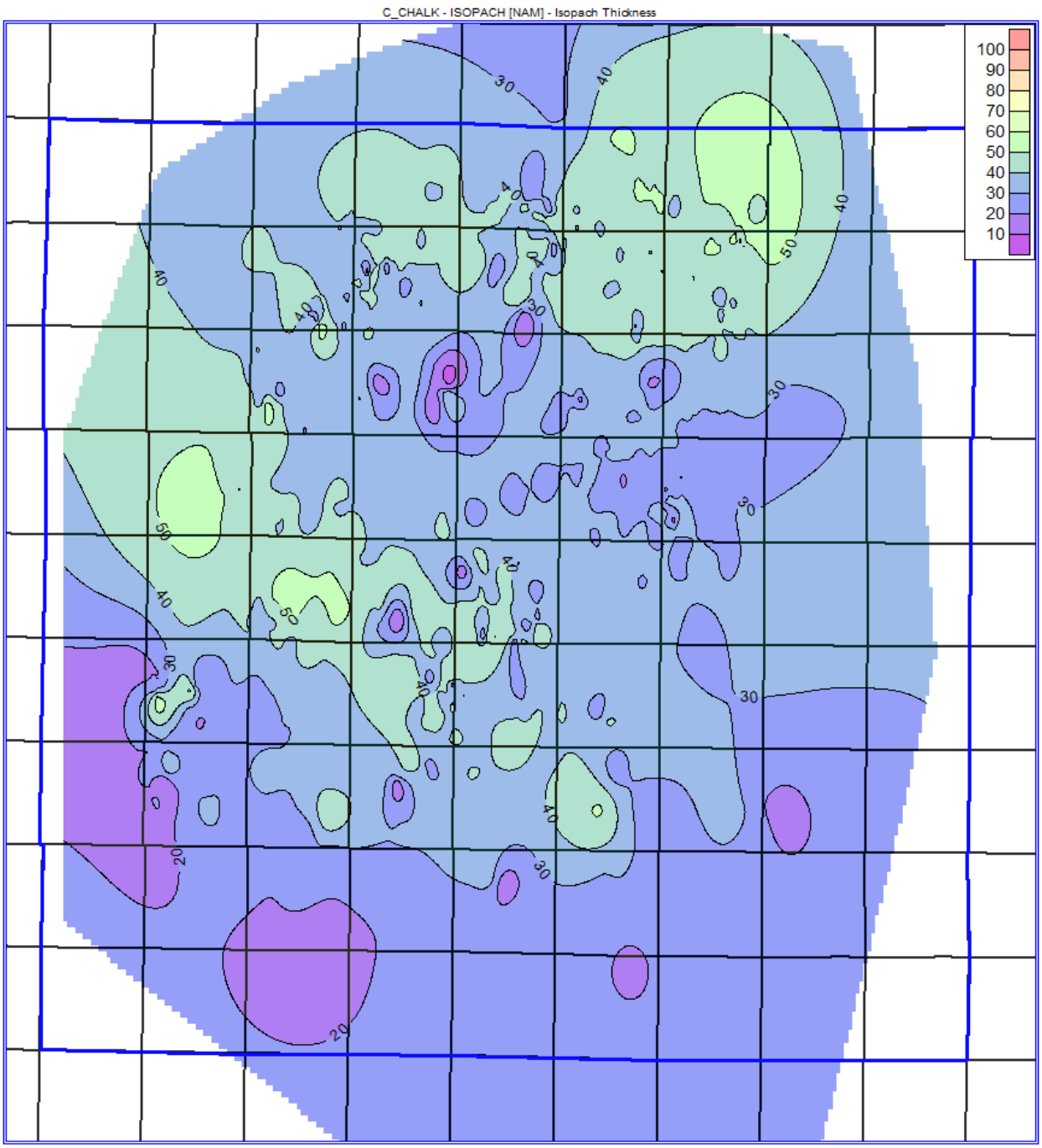

Figure 3.5. Isopach of the C Chalk. This unit has two trends oriented northwest-southeast. A thick trend (>40 ft) extends from the northwest corner to the center of the field, and a thin trend (<40 ft) parallel to the thick trend lies just to its north.

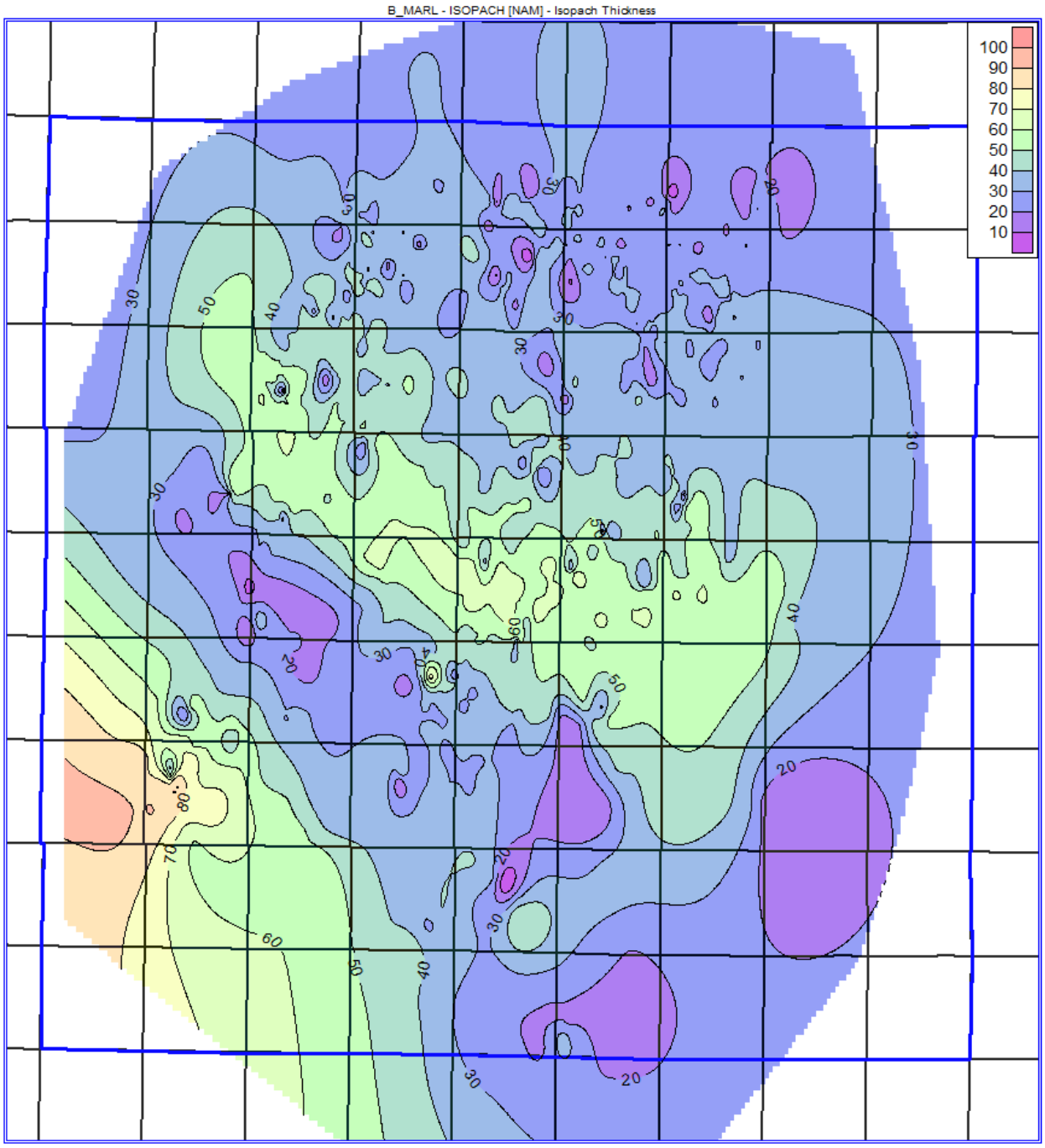

Figure 3.6. Isopach of the B Marl. This unit shows an inverse of the thickness trends of the underlying C Chalk, and a thickening in the southwest corner of the GWA centered on T1N R69W. The cause for the relationship between this isopach and the C Chalk isopach is likely due to differential compaction and compensational sedimentation.

inverse of the C Chalk isopach map. There is a thin directly over the C Chalk thick and a thick over the C Chalk thin. This relationship is likely due to differential compaction and compensational sedimentation.

3.1.7 B Chalk

The B Chalk is a very important reservoir unit within the Niobrara. It has long been an exploration target due to its characteristic high resistivity. Unlike the C Chalk, the B Chalk changes dramatically across the field. At the north and south parts of the field, the B Chalk can be separated into two chalks (termed B1 and B2) with a thin interlaying marl, and in the middle, the B1 chalk becomes more like the overlaying A Marl. Six XRD data samples from the B Chalk (only the B2 in this well) give average mineralogical composition of 71.8% carbonate, 10.7% clays, 7.2% quartz, 2.2% TOC, and 8.1% other minerals. Log response varies across the field and is affected by the thickness of the main B Chalk interval (B2). Where present, the B1 interval had a more subdued log response than the B2. Therefore, in most cases, the B1 is grouped in with the A Marl. For the B Chalk across the majority of the field, gamma ray is 75-125 API units, and both porosity logs are 10-15% with some crossover. Resistivity trends in Wattenberg are complex and most pronounced in the B Chalk and are discussed in a later chapter, but typically is the highest of the whole Niobrara (20-100+ Ω-m).

The B Chalk isopach shows trends that correlate with the underlying units (Figure 3.7). It shows a similar pattern of thick and thin trends as the C Chalk and an inverse of the trends in the B Marl. In this unit, the thin centered in T4N R66W and the thick is centered in T2N R67W, with both trends showing northwest-southeast elongation. As with the underlying trends, these are likely due to differential compaction and compensational sedimentation.

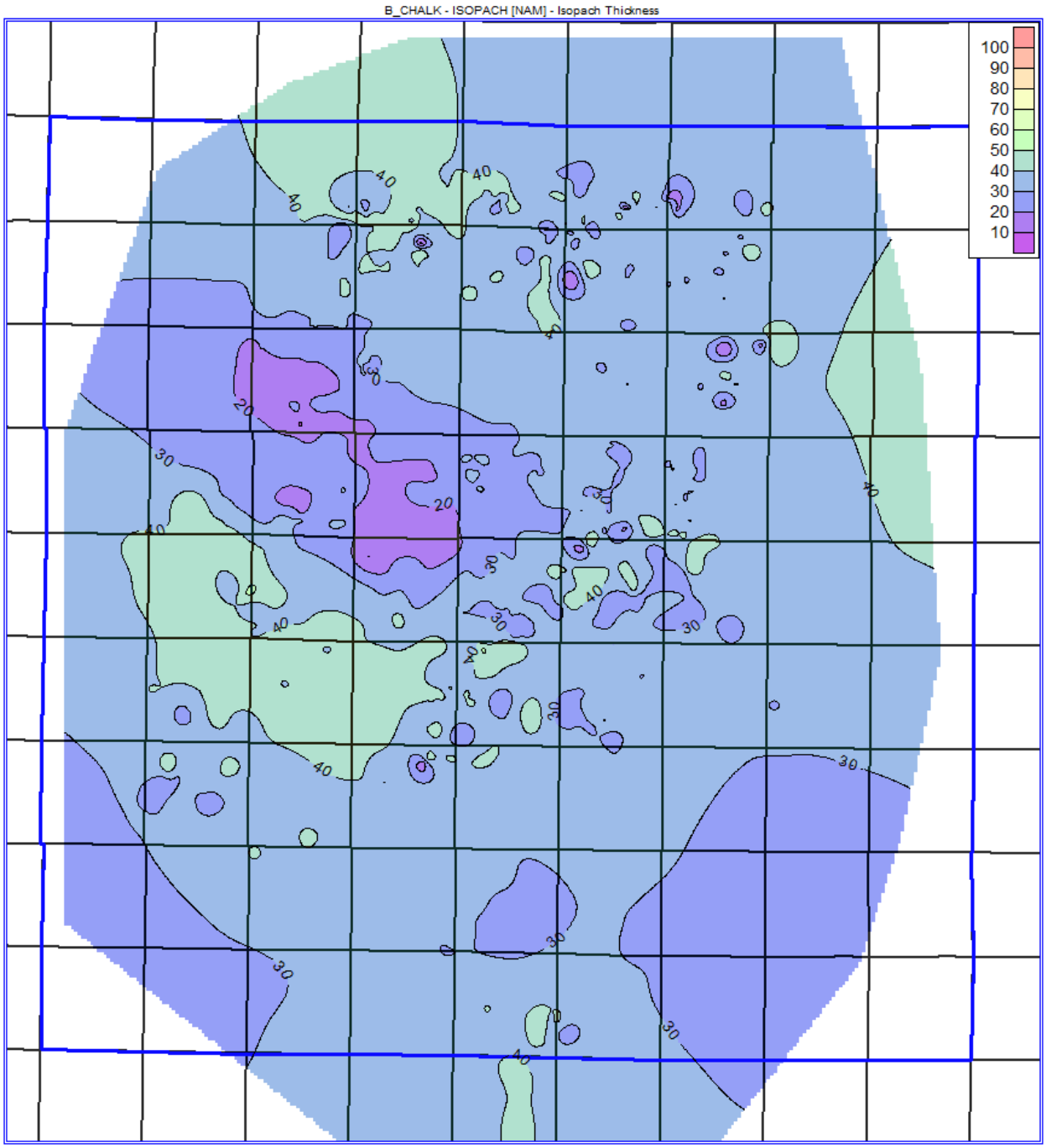

Figure 3.7. Isopach of the B Chalk. This map includes only the B2 interval where the B Chalk can be divided into two. The B Chalk isopach shows similar trends to the C Chalk and an inverse of the B Marl trends. This is due to differential compaction and compensational sedimentation.

3.1.8 A Marl

The A Marl is the uppermost organic-rich marl of the Niobrara. It lies between the A and B Chalks and marks the top of the Niobrara in the middle of the field. Its lithology is comparable to other Niobrara marls, with nine XRD samples giving average mineralogical composition of 50.9% carbonate, 21.8% clays, 13.0% quartz, 2.6% TOC, and 11.7% other minerals. The log response of the A Marl is characterized by the highest gamma ray signature of the whole Niobrara (100-250 API units), resistivity similar to the B Marl (10-30 Ω-m), high and variable neutron porosity (12-30%), and comparatively lower density porosity (7-10%).

The A Marl isopach shows a dramatic east-west thin across the GWA (Figure 3.8). This trend is large enough to be related to structure, and this relationship is discussed in detail in section 3.2. The feature's size is also influenced by the inclusion of the B1 Chalk in this mapped interval (bottom of A Chalk to top of B Chalk). Since the B1 Chalk is absent in the middle of the field, there is a stratigraphic input to the size of the isopach trend.

3.1.9 A Chalk

The A Chalk is the uppermost unit within the Smoky Hill Member of the Niobrara Formation and the thinnest of the chalk benches. It is also notably absent across much of the middle part of the GWA. The core with XRD sampling available for this research is located in this area where the A Chalk is absent, so no mineralogical characterization is possible for this unit. Typical A Chalk log response shows gamma ray decreasing with depth (100-180 API units), resistivity much higher than the overlying Sharon Springs and somewhat higher than the underlying A Marl (15-40 Ω-m), lower neutron porosity than the surrounding strata (12-22%), and similar density porosity as the underlying A Marl (8-11%). There is less porosity crossover in the A Chalk than the B Chalk and C Chalk.

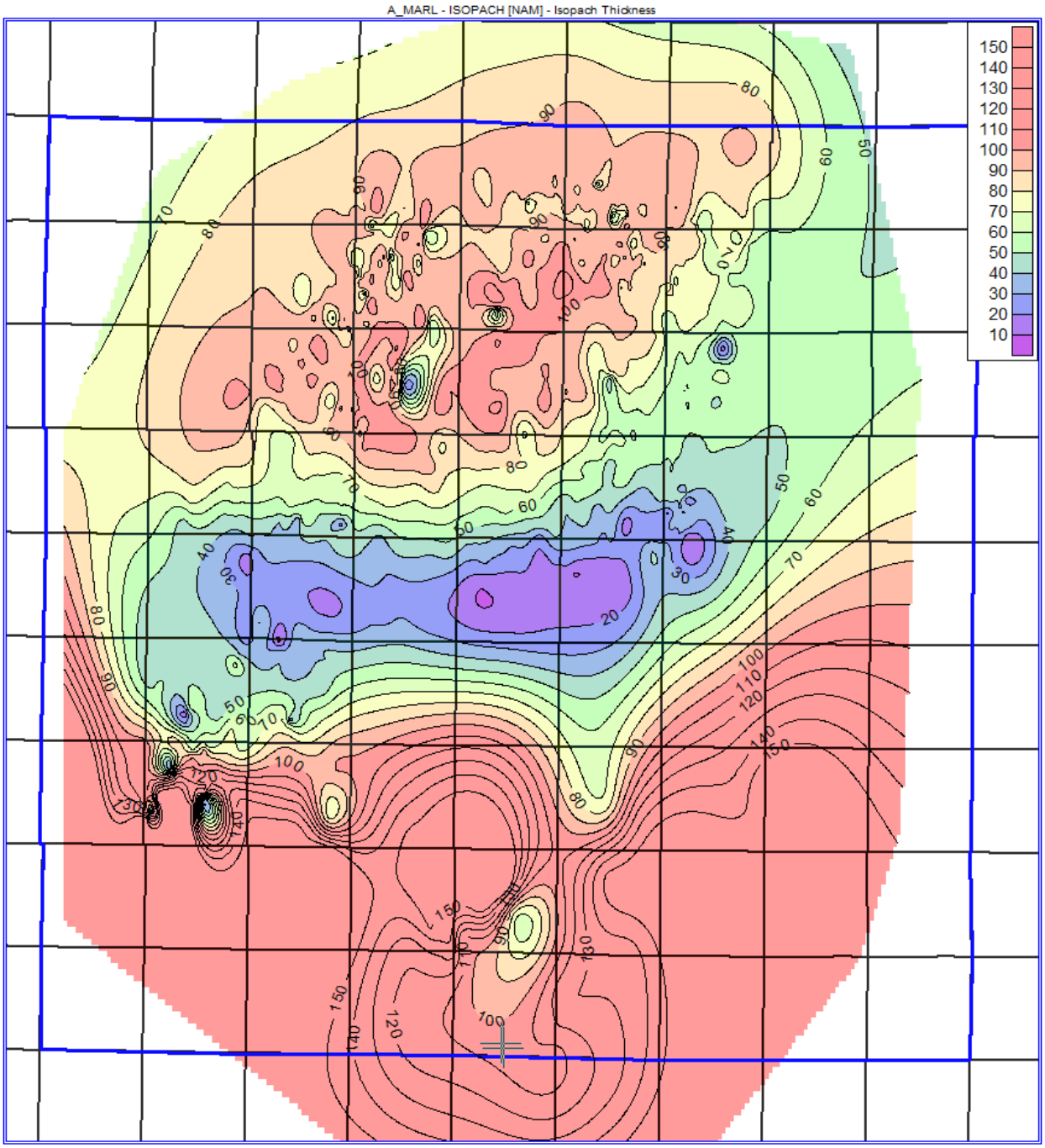

Figure 3.8. Isopach of the A Marl (including the B1 Chalk where present). The most significant feature in this map is the thin running east-west across the middle of the field and turning northeast-southwest in the east side of the field. This feature is likely related to structure and the absence of the B1 Chalk in the center of the field.

The A Chalk isopach shows the relatively thin chalk present in the north and south parts of the field, but absent in the middle in an east-west trend (Figure 3.9). This east-west trend is similar and related to the east-west thin of the A Marl. However, the A Chalk thin is located further south and lacks the northeast-southwest feature on the east side. The change in thickness of the A Chalk from a typical thickness of >20 ft to absent is abrupt, and occurs over a distance of about one to four mi. In this transition, the upper part of the A Chalk is missing, until the last remaining part of the unit is the low gamma ray spike at the base of the A Chalk.

3.2 Wattenberg Structural Trends

Deformation of the Cretaceous strata in the Denver Basin has been ongoing since its deposition. Most notably, the Laramide Orogeny had the greatest influence on the shape of the basin, and controlled the size, shape, and nature of Wattenberg Field. Besides the basin axis syncline, other smaller structural features are observed in Wattenberg and affect the reservoir quality.

3.2.1 Basin Axis Syncline

As it currently lies, the Denver Basin is a section of the larger foreland basin that made up the WIC Seaway. The Laramide Orogeny split this larger basin into the smaller basins of the Rocky Mountains and gave the Denver Basin its shape. The shape of the Denver Basin is paramount to the presence of Wattenberg Field. The higher thermal maturity of Cretaceous source rocks buried in the deepest part of the basin is the cause of the petroleum generation. While the Wattenberg Thermal Anomaly complicates this relationship, burial depth does play an important role in thermal maturity. Since the field was originally discovered and developed as a basin-centered gas accumulation in the J Sandstone, the correlation between structure and petroleum goes back to Wattenberg's discovery.

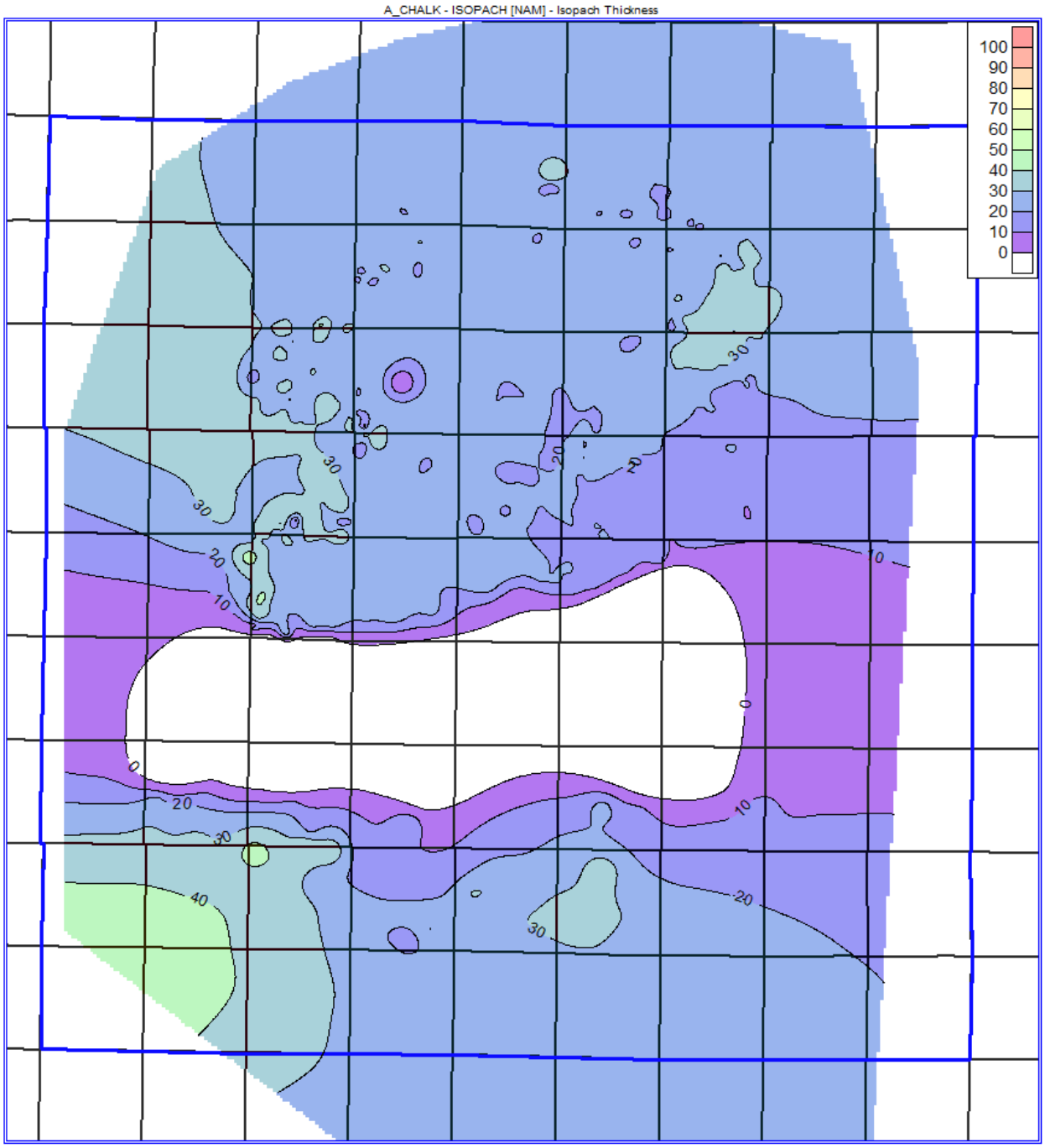

Figure 3.9. Isopach of the A Chalk. The most significant feature of the A Chalk isopach is the thin and absence of the unit in the middle of the field in an east-west oriented elongate body. This feature is similar and related to the thin of the A Marl, but centered about one township to the south and lacks the northeast-southwest feature on the east side. Aside from this trend, the thickness of the A Chalk is relatively constant.

The basin axis syncline strikes about 15° from north through Wattenberg Field. On the top of the Niobrara Formation, the dip is steeper to the west of the axis and gentler to the east in the GWA, reflecting the asymmetry of the whole basin (Figure 3.10). The structure map on the top of the Codell reflects the changes in the structure due to the thickness of the Niobrara (Figure 3.11).

3.2.2 Wattenberg Paleo-high

An ancient structural high crossing the Wattenberg field in an east-west orientation has been hypothesized (Weimer and Sonnenberg, 1982; Drake and Hawkins, 2012) primarily based on the thin in the A Chalk. In addition to the Wattenberg paleo-high, other paleo-highs have been recognized elsewhere in the Denver Basin. However, evidence from the dataset used in this research suggests that the presence and history of this paleo-high is more complicated.

A structure map on the top of the B Chalk is similar to the other structure maps of the Niobrara, with one important difference (Figure 3.12). There is a structural high running east-west through the middle of the field due to the thinning and absence of the A Chalk and A Marl. When the isopachs of the A Chalk and A Marl are added together, the total size of this thin trend can be seen as up to 100 ft and about 20 mi wide. Additionally, this structure correlates with an intrusive igneous body of granitic rocks 1.7 Ga mapped by Sims and Finn (2001) (Figure 3.13). These two features have a very similar geometry, but the intrusive body is centered about 10 mi south of the center of the stratigraphic thin. The crest of this paleo-high was not stationary during its active period. The thinnest part of the A Marl is 6-10 mi to the north of the center of the A Chalk absence. This suggests the crest moved south during this time.

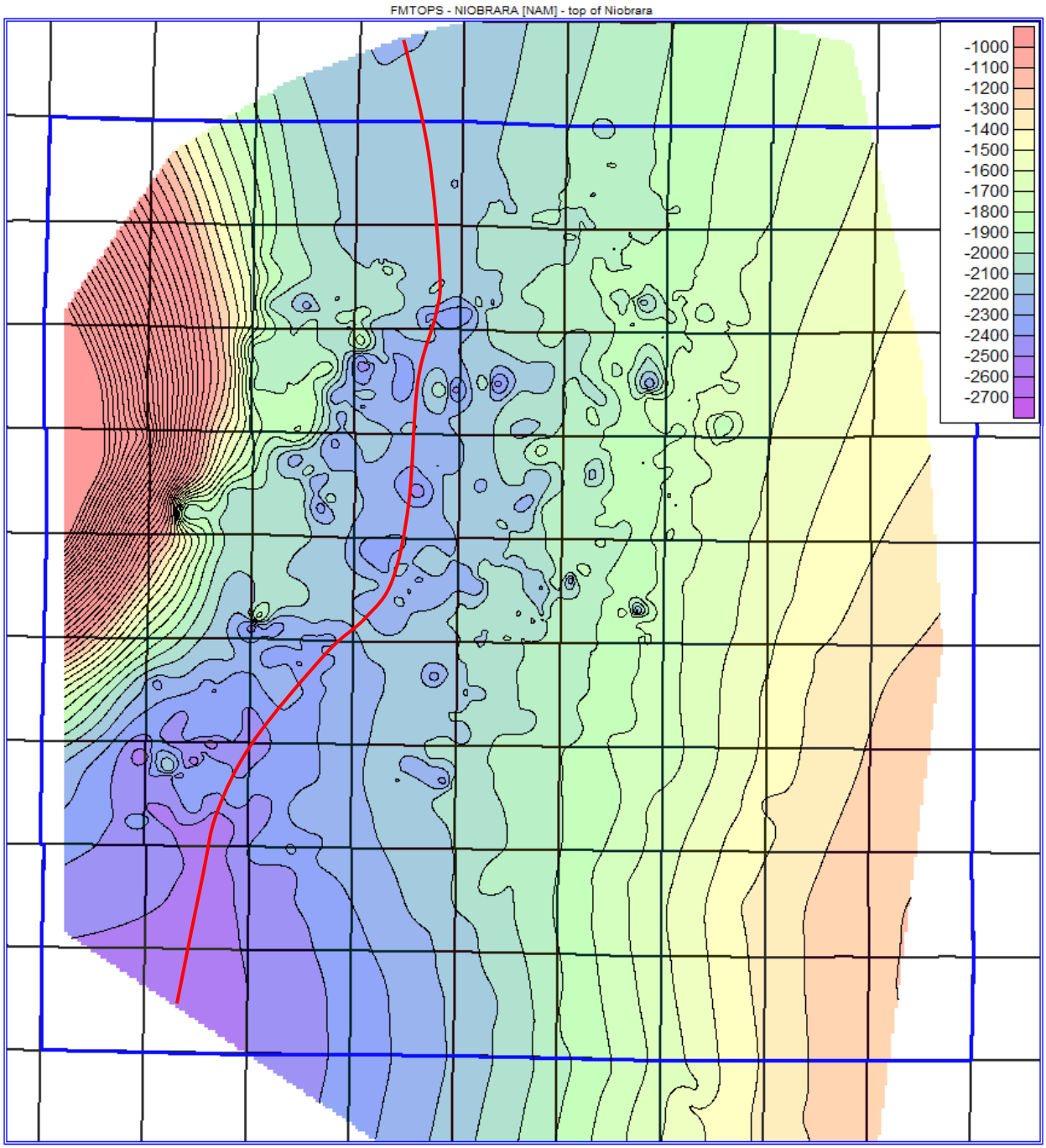

Figure 3.10. Structure map on the top of the Niobrara Formation. Red line shows the basin axis. Note the differences in dip between the west edge of the field and the east flank and the presence of "potholes" showing the faulted nature of the Niobrara top.

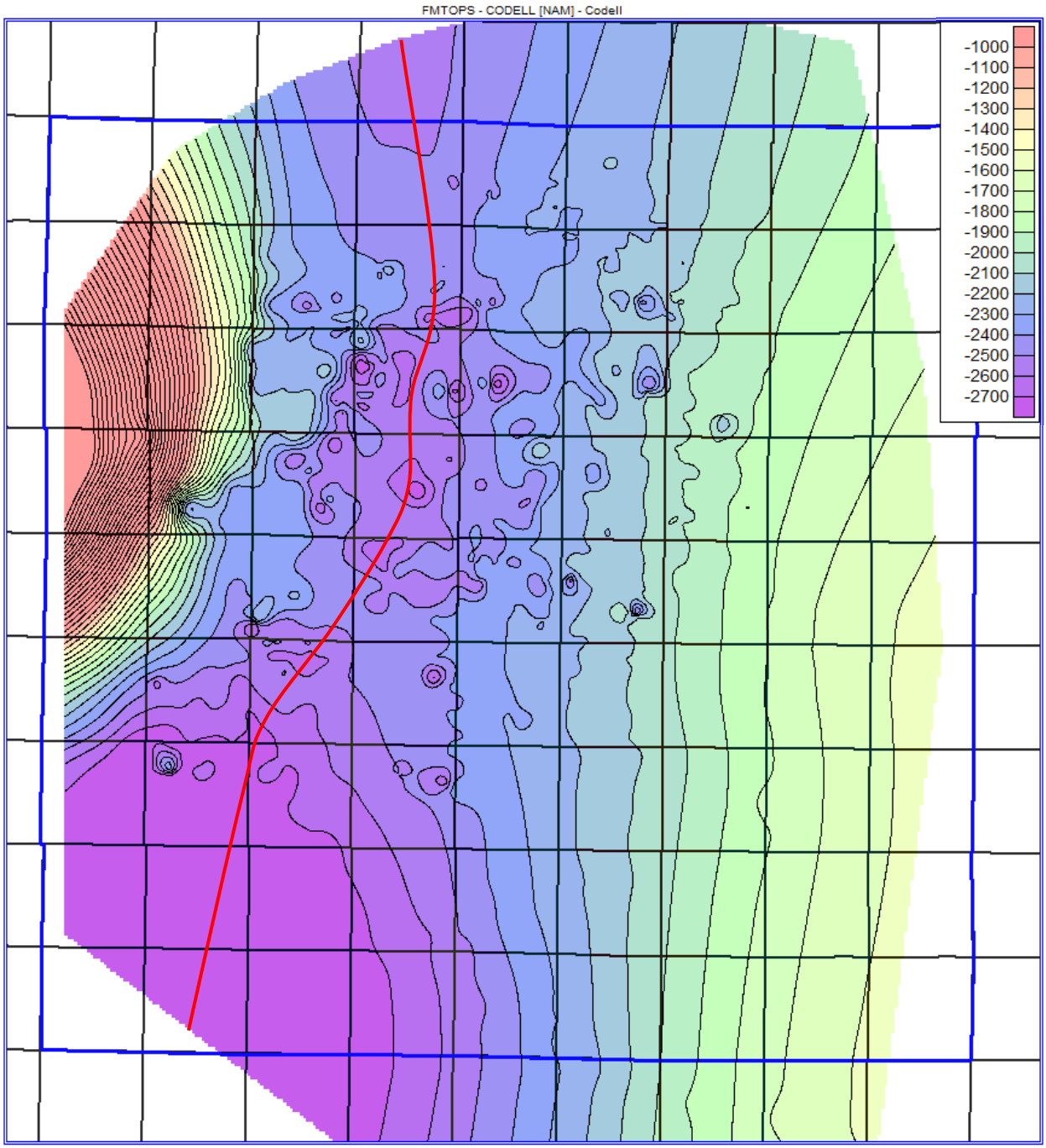

Figure 3.11. Structure map on the top of the Codell Sandstone. Red line shows the basin axis, and the color-filled contour scale is the same as the Niobrara structure map. The most significant change between the Niobrara structure and the Codell structure is the Codell shows more deepening in the southern part of the field.

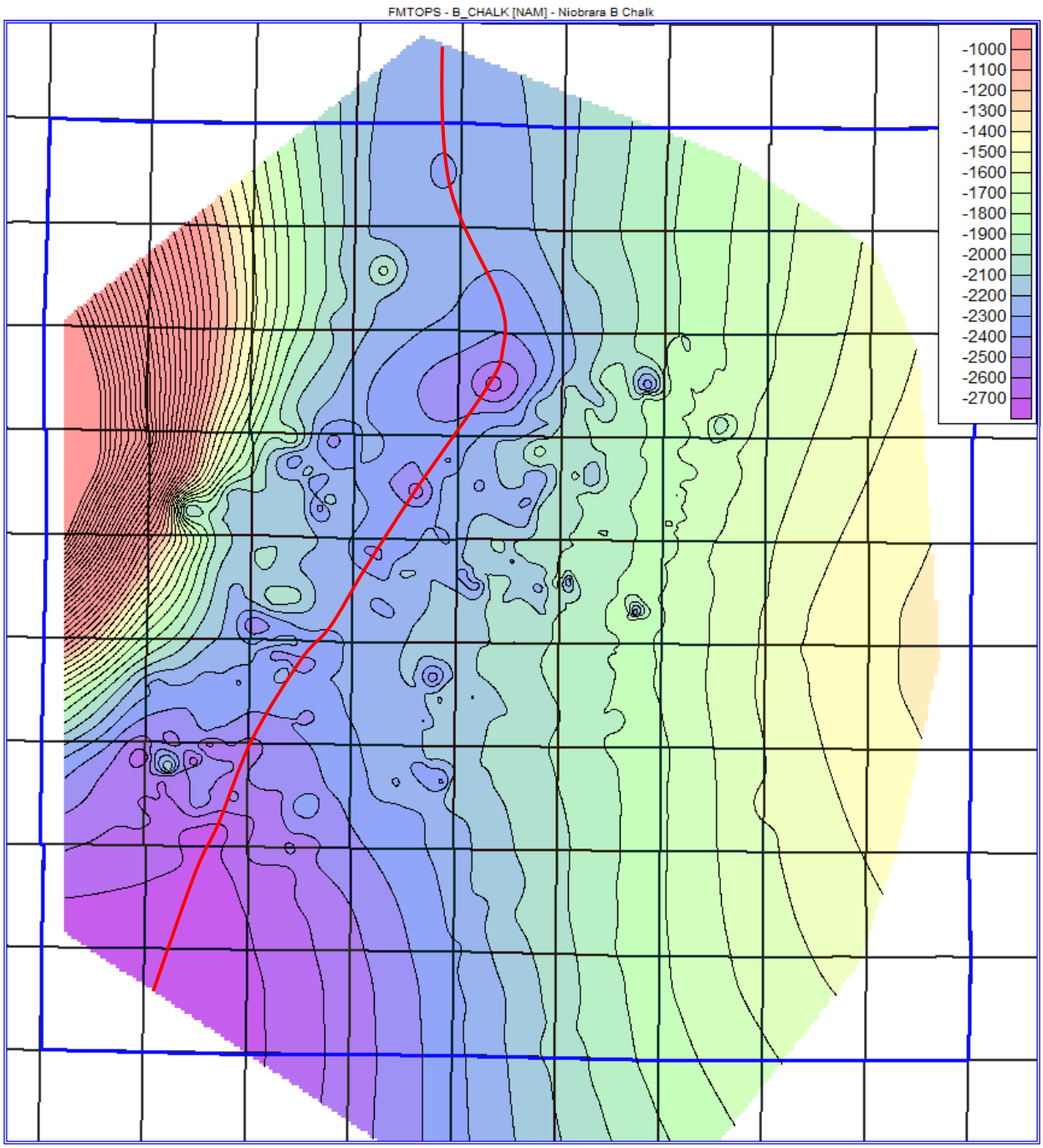

Figure 3.12. Structure map on the top of the B Chalk. Red line shows the basin axis, and the color-filled contour scale is the same as the Niobrara structure map. The most significant feature of this map is the evidence of Wattenberg paleo-high that runs perpendicular to the basin axis.

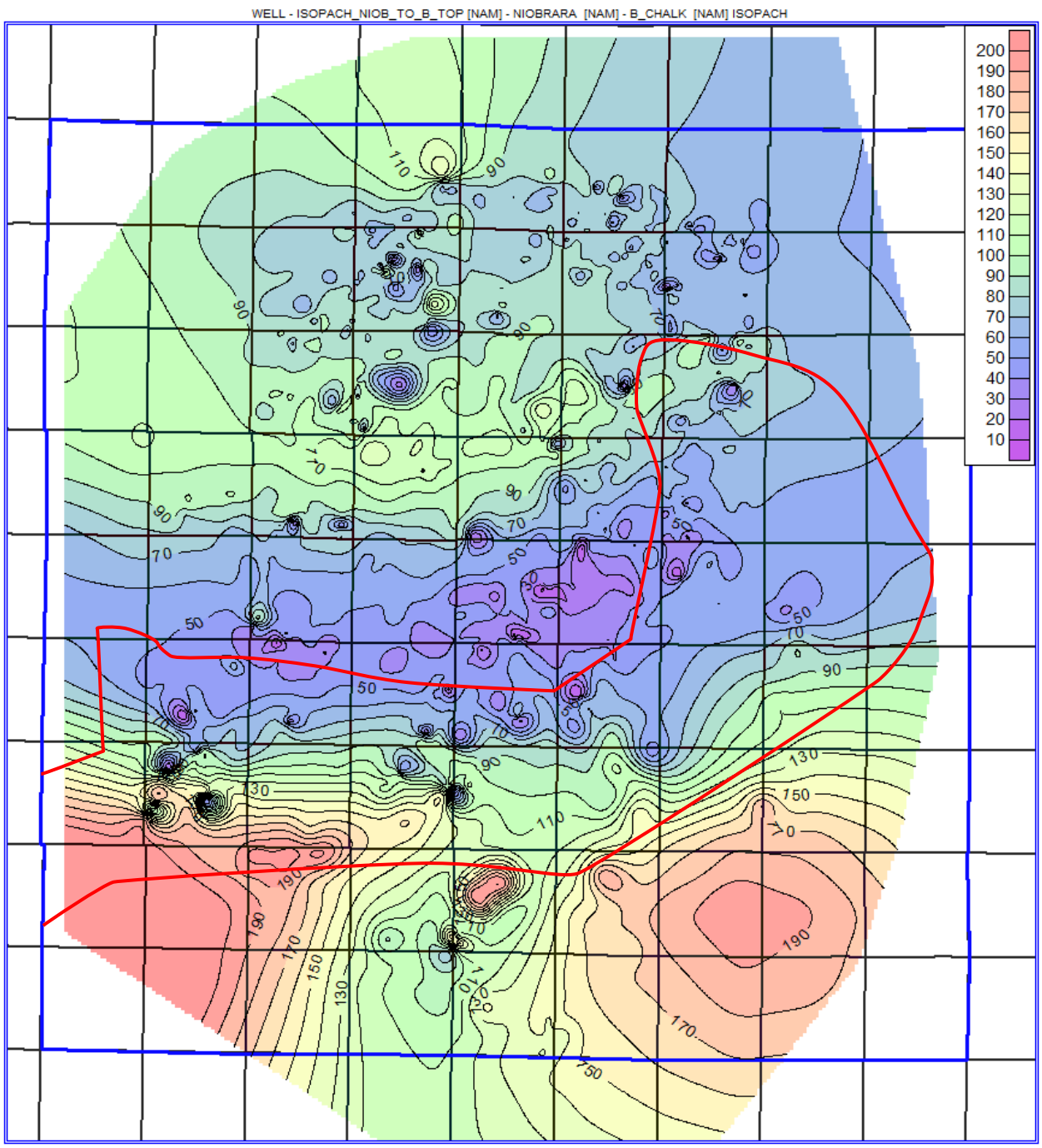

Figure 3.13. Isopach of the A Chalk and A Marl (or top of the Niobrara to the top of the B Chalk). This thin trend has about 100 ft of relief and is about 20 mi wide. The red line is the outline of the basement intrusive body identified and mapped through aeromagnetic data (Sims and Finn, 2001). Although there is some offset, the geometry of the thin and the intrusion are very similar.

CHAPTER 4

FAULTING STYLES AND CHARACTERISTICS

Of the three styles of faulting that have been recognized in the Niobrara formation (wrench, salt dissolution, and polygonal), polygonal is most relevant to horizontal well development of the Niobrara in Wattenberg. Wrench faults have been interpreted throughout the Denver Basin, including the GWA, but their scale is of limited concern to horizontal well placement. Faults related to dissolution of Permian salt are critical to the success of Silo Field in Wyoming, but their presence has not been observed in the GWA. However, the Polygonal Fault System recognized in the Niobrara is pervasive throughout the GWA and is at a scale that is of concern to the drilling of horizontal wells. These PFS faults have been recognized by previous research (Sonnenberg and Underwood, 2013; Underwood, 2013), and are observable in the dataset for this thesis. The geometry, distribution, and timing of polygonal faults in Wattenberg are discussed in this chapter.

4.1 Fault Geometry and Distribution

Previous work from 3D seismic data has described these faults as 500-4500 ft in length, having vertical displacement of 20-90 ft, and dips of about 45°. Additionally, the Niobrara tier faults have random orientations, with a weak trend of northeast-southwest strikes. The polygons formed by the Niobrara tier tend to be incomplete, and faults are found both as pairs creating a graben and as single faults (Sonnenberg and Underwood, 2013).

Analysis of the current 3D seismic survey shows these related faults as 1000-10,000 ft in length, 30-150 ft of vertical displacement, and dips of about 45° (Figure 4.1-1.3). Unlike the faults described by Sonnenberg and Underwood (2013), these faults are less randomly oriented, with a strong northeast-southwest trend in their strike. Also, the faults in this survey are more

commonly seen as parallel faults creating grabens. The grabens are as long as the faults and 200-1000 ft wide and are commonly seen en echelon. The faults themselves are typically limited to the Niobrara Formation, and occasionally the lower Pierre Shale or Carlile. Since few faults penetrate the Carlile Formation, the Codell Sandstone exhibits less deformation than the top of the Niobrara, and the isopach of the Niobrara accommodates the bulk of the thinning. Wells in grabens typically have faulted out section equal to the vertical displacement on Niobrara top.

Similar to Sonnenberg and Underwood (2013), a second tier of normal faults are recognized in the Pierre Shale beneath the Hygiene Sandstone (Figure 4.2). The faults in the upper tier have a larger vertical extent and wider spacing, but less vertical displacement. Additionally, a zone of minimal deformation separates the two tiers of faulting. This seismic section shares many similarities with Figure 2.13.

4.2 Growth Strata

As normal faults create and reduce accommodation space, thicker successions can develop over downthrown areas. The timing of the deposition of these thicker strata is congruent with fault growth, giving rise to the term growth strata. Since the majority of normal faults under consideration are within a tier, examining the growth strata for these faults is limited to the lower Pierre Shale directly above the Niobrara. Specifically, gamma ray log traces of the Sharon Springs and lower Pierre Shale allow for the correlation of growth strata across normal faults.

The tight well spacing within the 3D seismic survey is ideal for understanding changes across a fault. Figure 4.4 shows the distribution of growth strata over a graben. The deformation from the faulting is compensated for by about 400 ft above the Niobrara in the wells on the horsts and 550 ft over the graben. From the multiple horizons picked in the lower Pierre Shale, the increase in accommodation space was distributed throughout this time (i.e., movement on the

fault occurred throughout the time these strata were deposited). The growth strata in this example are typical of the other grabens in the 3D seismic survey area.

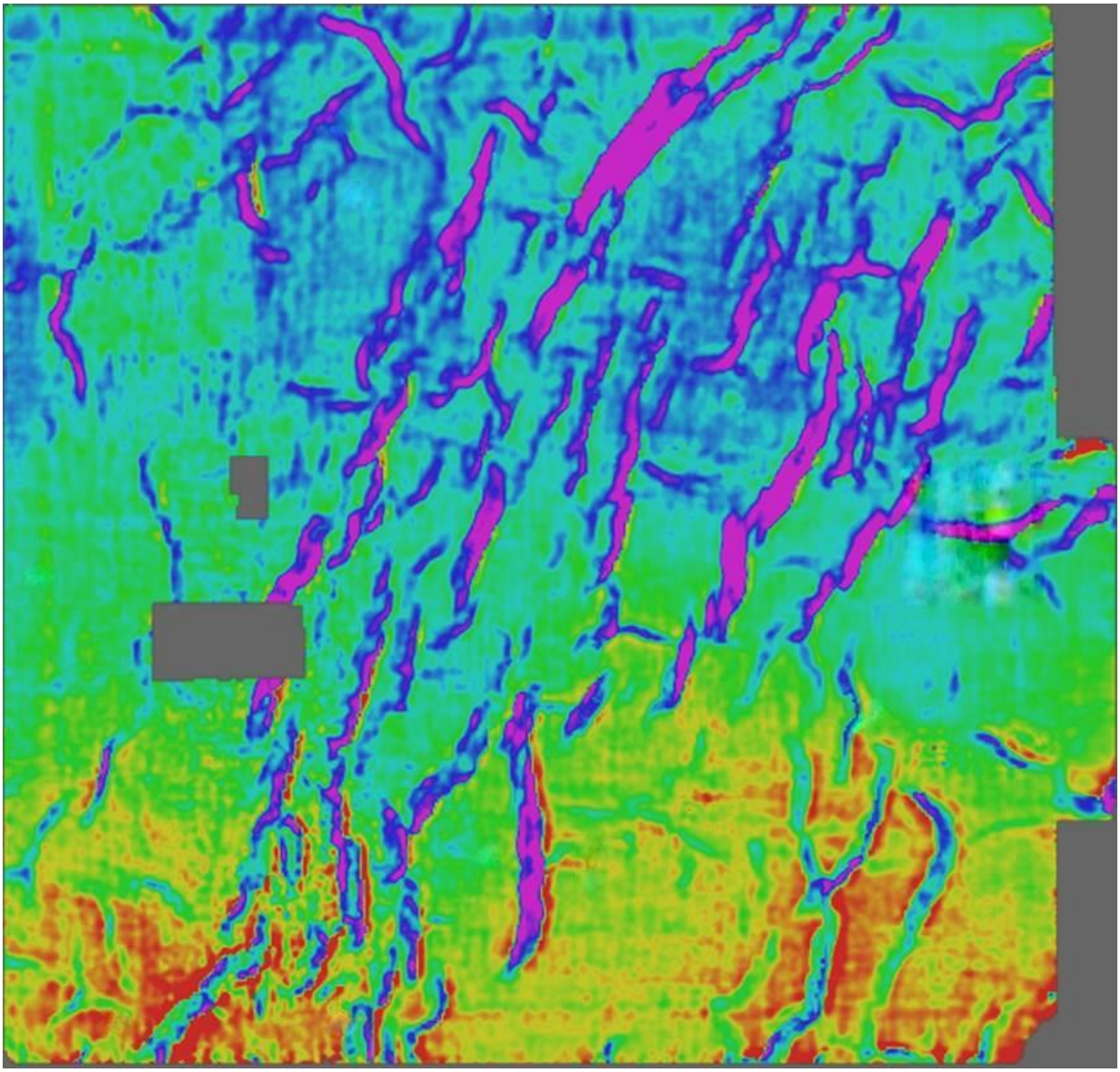

Figure 4.1. Isopach of the Niobrara from the 50 mi^2 3D seismic survey (M. White, 2014, personal communication). Cool colors indicate thin areas and warm colors indicate thick areas. Note the presence of northeast-southwest grabens, en echelon geometry of the grabens, overall thickening to the south, and partial polygons formed by the faults. Faults generally do not penetrate the Codell, resulting in the Niobrara isopach and structure having the same spatial pattern.

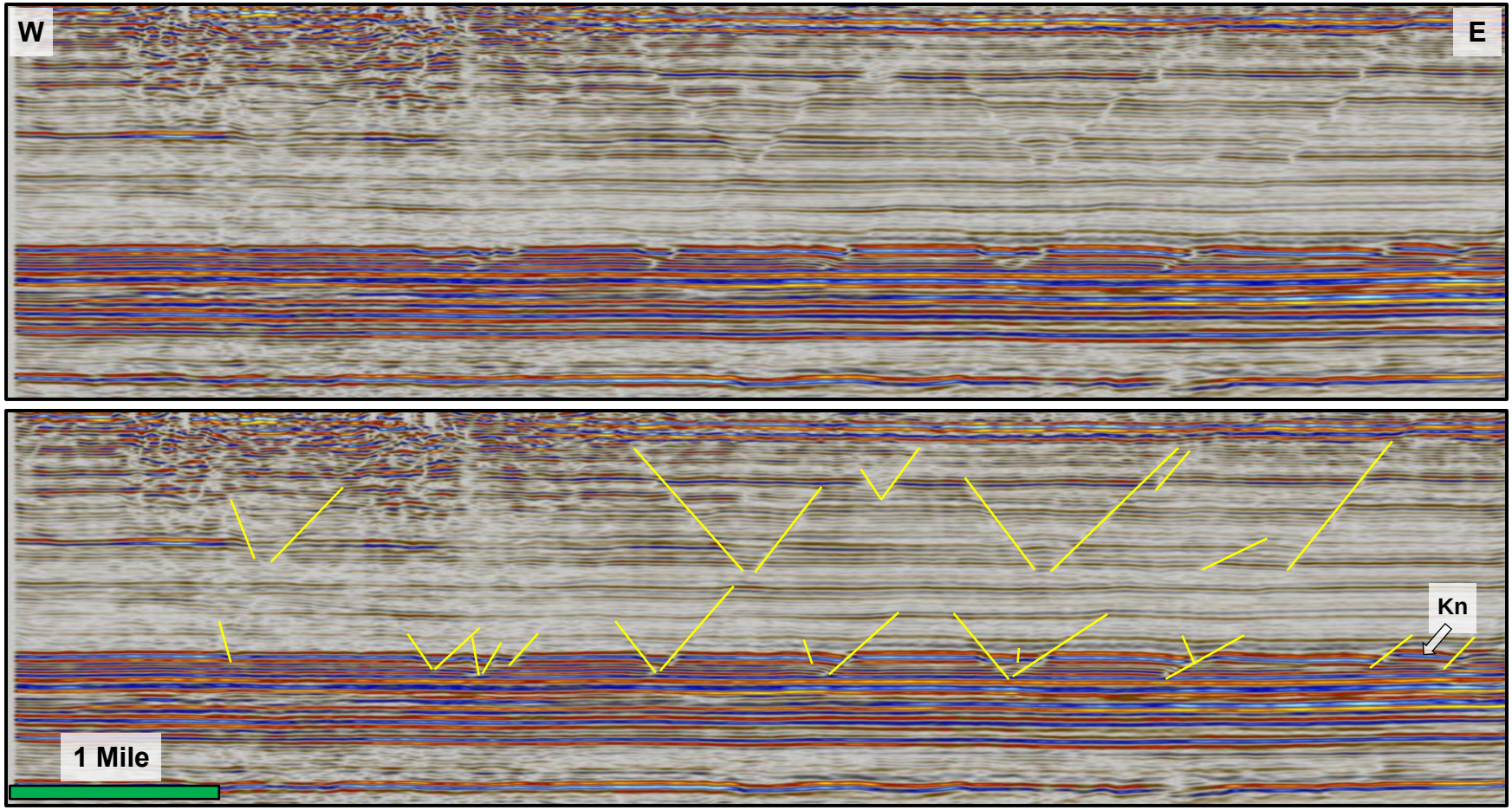

Figure 4.2. West-east cross section of the 3D survey showing the faulting in the Niobrara (A. Grechishnikova, 2014, personal communication). Although the vertical axis is in time, the section has minimal vertical exaggeration. Faults are shown in yellow, Kh is the Pierre Shale Hygiene Sandstone, and Kn is the Niobrara Formation. Note the presence of two separate tiers of faulting; one in the Pierre Shale and one in the Niobrara, separated by a relatively undeformed interval. Faults typically have dips of about 45°.

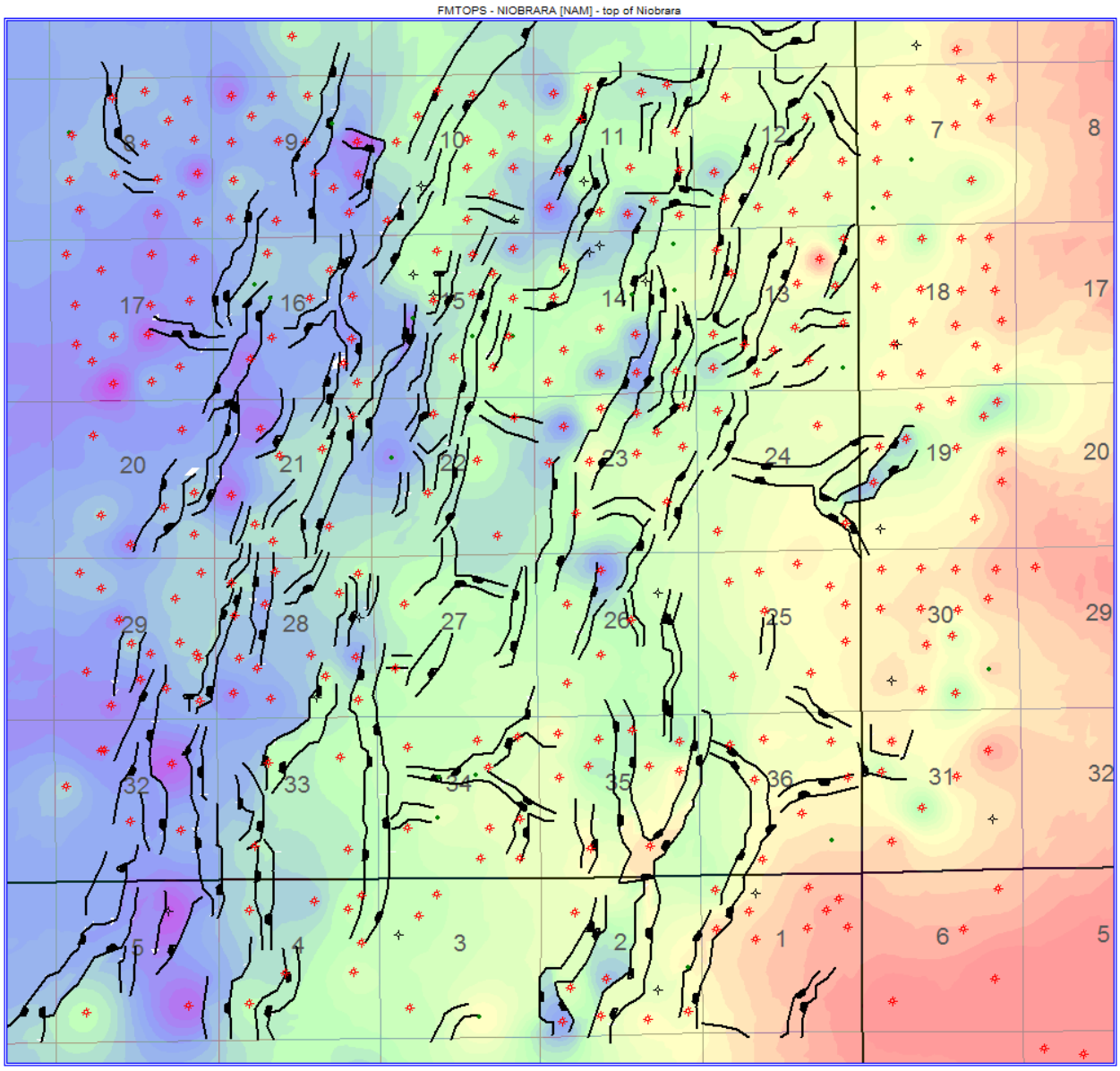

Figure 4.3. Structure map of the top of the Niobrara over the southeast portion of the 3D seismic survey. Fault traces are taken from the seismic data and incorporated into the contour map of well tops. Note the commonly paired nature of the faults and their predominately northeast-southwest orientation. Additionally, faults show en echelon orientation (e.g., Section 23).

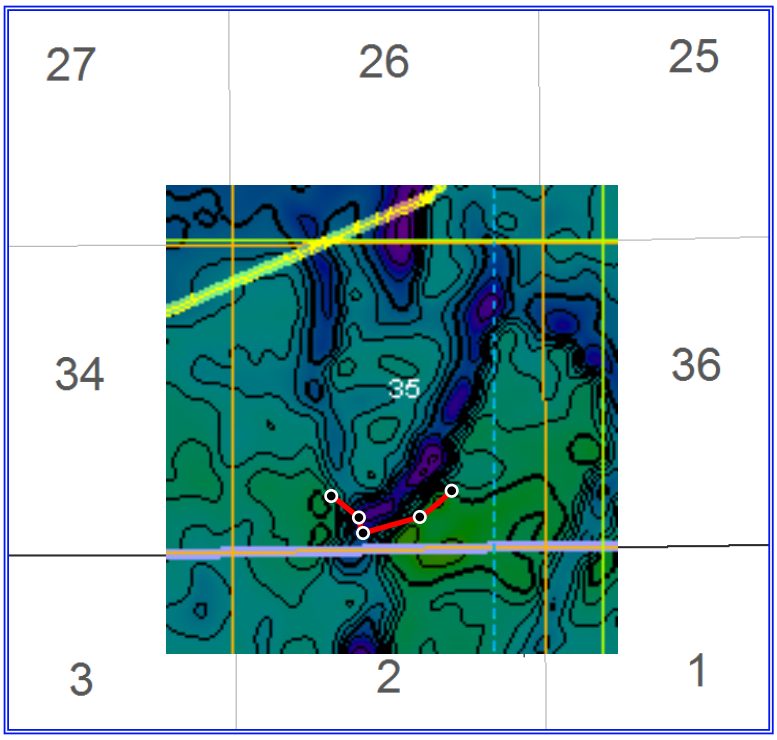

Figure 4.4. Time structure map of the Niobrara over Section 35 of the 3D survey. Note the northeast-southwest trending graben and the location of the cross section in Figure 4.5 (M. White, 2014, personal communication).

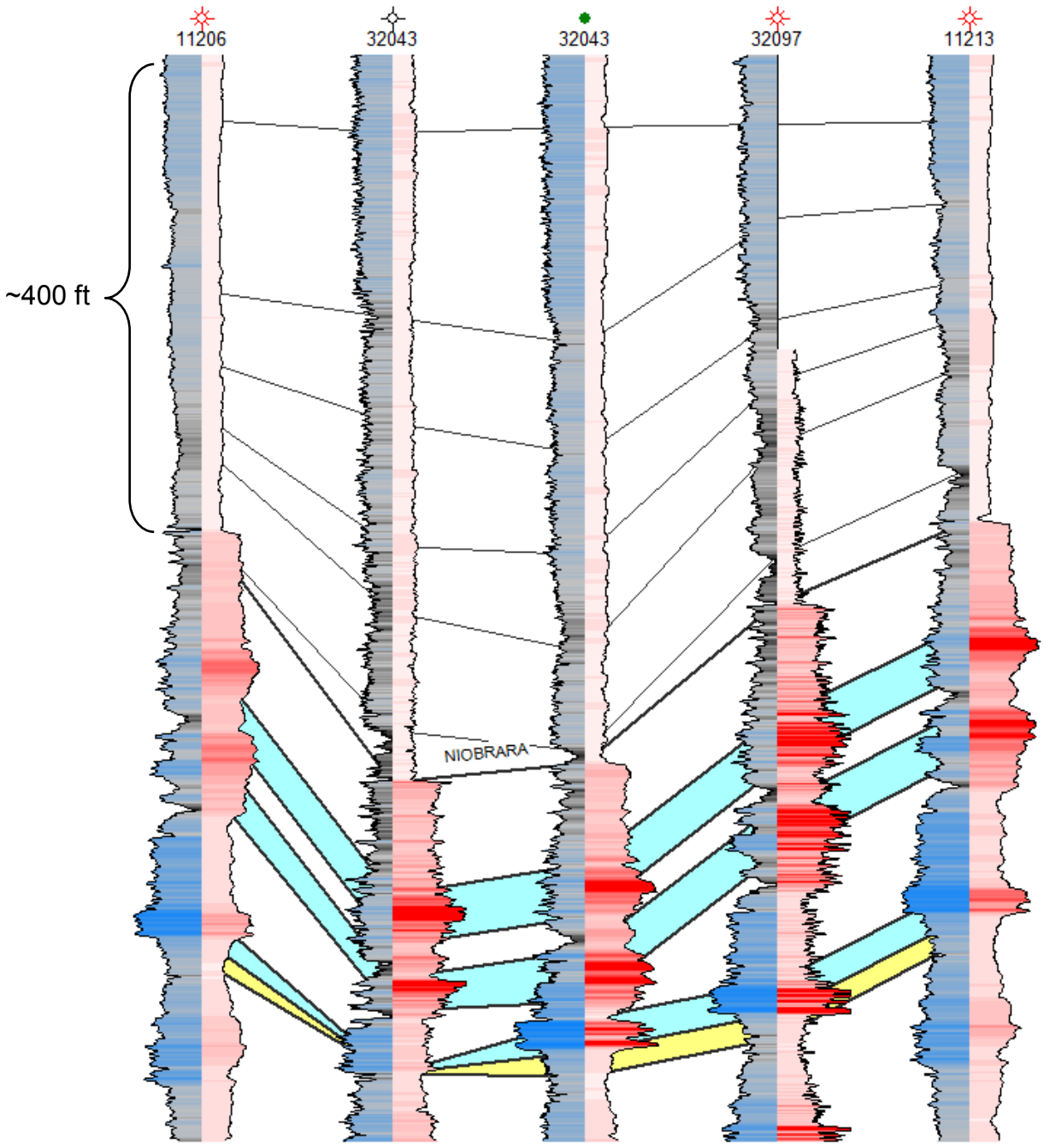

Figure 4.5. Structural cross section over a graben showing the faulting within the Niobrara and related growth strata. The two wells at the bottom of the graben have faulted out section from the C Marl to Codell, resulting in the majority of the deformation in the top of the Niobrara taken up by changes in the Niobrara isopach. Growth strata are limited to about 400 ft above the Niobrara in wells outside the graben. Vertical displacement of this graben is about 150 ft.

CHAPTER 5

LOG DATA TRENDS

The set of digital logs used in this research has sufficient spatial distribution to map various log properties. Those properties that relate to an increased understanding of the Niobrara Petroleum System are included in this analysis. Specifically, a log-derived TOC calculation and resistivity trends are presented in this chapter.

5.1 Log-Derived Total Organic Carbon

A common and widely accepted method for using well logs to calculate organic richness is the Δ log R technique (Passey et al., 1990). Also known as the Passey Method, this technique uses relative changes in resistivity and porosity in combination with maturity to calculate a TOC approximation in weight percent. When resistivity and a porosity log are overlain and properly scaled, they track each other in water-saturated organic-lean rocks. However, in the presence of organic-rich source rocks or petroleum-bearing reservoir rocks, the logs separate. This separation is complicated by the presence of generated petroleum increasing resistivity in mature source rocks. As a result, maturity must be factored into the equation to compensate for the increased resistivity values (Passey et al., 1990).

Beitz et al. (2013) completed a study of the B Chalk of the Niobrara in the Denver Basin using this method. While their work provided a regional-level look at the B Chalk, it ignored the organic-rich marls of the Niobrara and failed to accurately account for the Wattenberg Thermal Anomaly. These two shortcomings can be addressed using the set of logs available for this thesis work.

The Δ log R technique was adapted to fit the logs available and to improve accuracy and resolution of TOC maps. Deep induction resistivity (ILD) and bulk density (RHOB) logs were

chosen as the two logs as inputs to the Δ log R equation. The Passey Method recommends using sonic logs as the porosity log, but 2737 wells have RHOB and only 43 wells have sonic logs. Prior to calculating TOC, the separation between the resistivity and porosity must be calculated, resulting in variable called Δ log R using Equation 5.1 where R is the resistivity value, $R_{baseline}$ is the resistivity of non-source clay-rich rocks (4 Ω-m), RHOB is the bulk density value, and $RHOB_{baseline}$ is the bulk density of non-source clay-rich rocks (2.58 g/cm^3).

$$\Delta \log R = \log_{10}(R/R_{baseline}) - 2.50 * (RHOB - RHOB_{baseline}) \quad (5.1)$$

The result of this equation was turned into a digital log, and used in Equation 5.2 to calculate TOC. The other variable in this equation is level of organic metamorphism (LOM), which uses a continuous scale that can be related to maturity data such as vitrinite reflectance or the rock evaluation parameter Tmax (Passey et al., 1990). The vitrinite reflectance map from Higley and Cox (2005) (Figure 2.9) was digitized, gridded, and had the values sampled to the wells so each well had a unique LOM based on its location within the GWA. This TOC log was then compared to two wells with core TOC data for calibration (Figure 5.1). The two sources of TOC data track each other well in the marls for both wells. However, the well with lower maturity has much higher calculated TOC than core-derived TOC in the chalks. Since maturity is the only other variable in the calculation, it is presumably the source of the variation.

$$TOC = \Delta \log R * 10^{2.297 - 0.1688 * LOM} \quad (5.2)$$

With 1565 wells having the correct logs to perform the TOC calculation, a sufficient dataset of log-derived TOC was created to map the spatial distribution of TOC in Wattenberg Field. TOC summary statistics were calculated for each chalk and marl of the Smoky Hill, Fort Hays, and Codell. All maps of log-derived TOC are dominated by maturity. The Wattenberg Thermal Anomaly gives such a large range of LOM from the center of the field to the edge, that

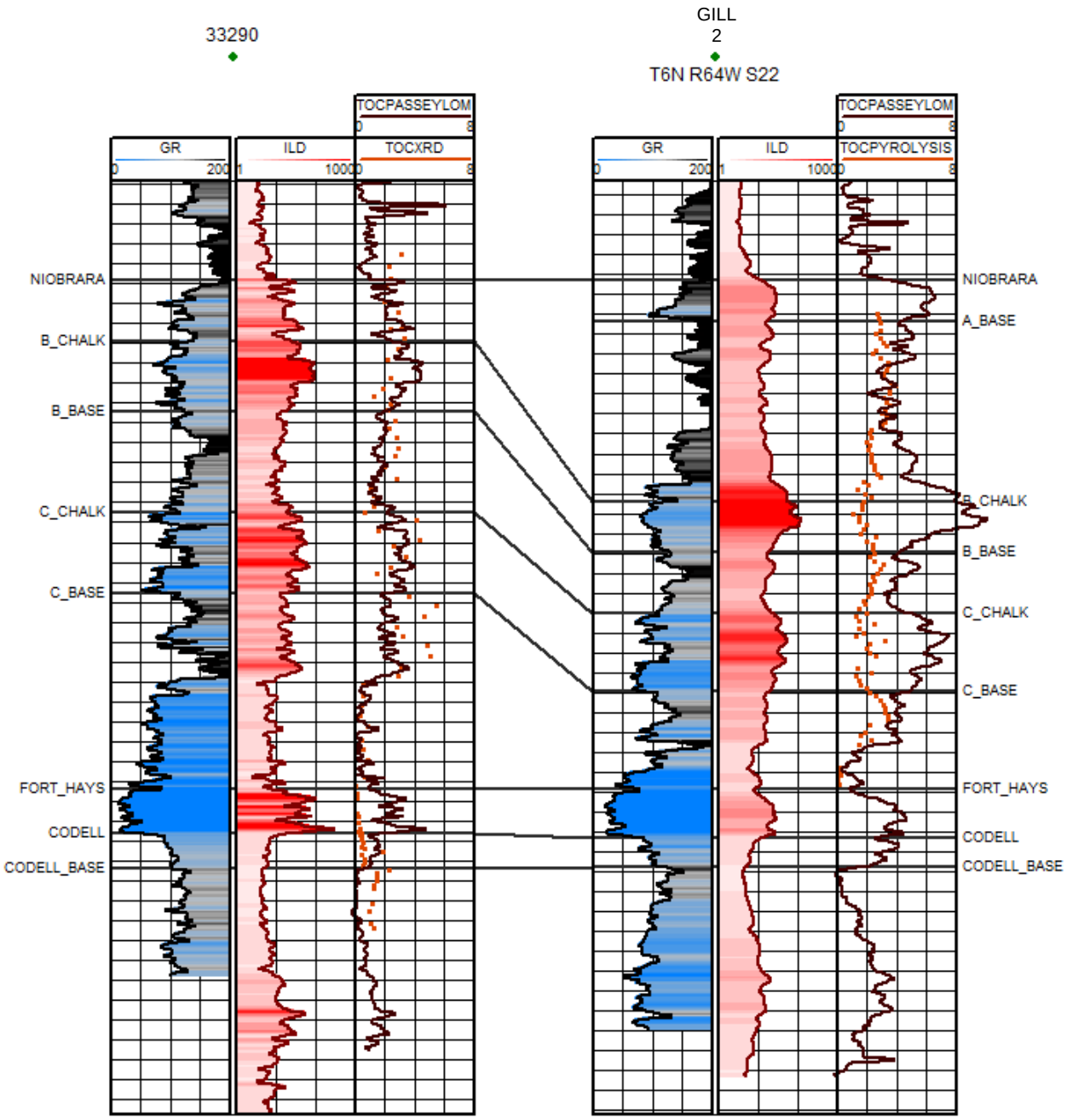

Figure 5.1. Log-derived TOC compared to core TOC data. Shown in Track 3, these two wells have TOC data from core (orange points; XRD on well 33290 and pyrolysis on well Gill 2 [USGS, 2013]) to compare to the log-derived TOC (brown curve). Well 33290 has a LOM of 11.3 (located near the center of the Wattenberg Thermal Anomaly), and the two sets of TOC data track each other closely. There is some breakdown of the calculated TOC in the Fort Hays and Carlile due to significant changes in lithology affecting both the resistivity and bulk density logs. Well Gill 2 has a LOM of 9.1 (located on the flank of the Wattenberg Thermal Anomaly), and the two sets of TOC data track each other only in the marls. The log-derived TOC may be significantly higher than the core TOC in the chalks due to the effect of maturity on the TOC calculation.

the TOC calculation is dominated by this input variable. That is, the range in LOM is much greater than the range in Δ log R. The A Marl shows an average TOC of 1-2% near the center of the GWA, and up to about 6% near the edge of sufficient well control (about 4 townships away from the center of the GWA) (Figure 5.2). The B Marl shows a similar pattern, but TOC is about 1% lower (Figure 5.3). The C Marl shows a unique trend in TOC. Where the Basal Chalk/Marl is present, the TOC is near zero. To exclude this and map the source rock portion of the C Marl, the average TOC of upper C Marl excluding the Basal Chalk/Marl was computed and mapped (Figure 5.4). This is the richest source rock interval of the Niobrara in the GWA.

The spatial scale of these maps limits any interpretation beyond the presence of the Wattenberg Thermal Anomaly, so applying the Passey Method to other spatial scales may provide more insight. Beitz et al. (2013) have studied changes across the Denver Basin at a regional level, and the dataset of digital logs from the large-scale study area within Wattenberg Field provides an opportunity to examine TOC distribution at a higher resolution. For example, the upper, organic-rich part of the C Marl shows a small range in TOC compared to the small-scale study area (Figure 5.5). However, trends do emerge, such as the modest high over Section 25.

5.2 Resistivity

Resistivity trends in the Niobrara have been studied in the past (Smagala et al., 1984), but only recently has an anomalous resistivity low been observed in the middle of Wattenberg Field (Cumella and Sheevel, 2012). This anomaly is thought to be a result of the complex relationship between resistivity and maturity. Initial findings show that as maturity (vitrinite reflectance) increases, resistivity increases to a point. Then at the higher maturities, resistivity values come back down. However, hypotheses for its cause have not been shown to fully explain the feature.

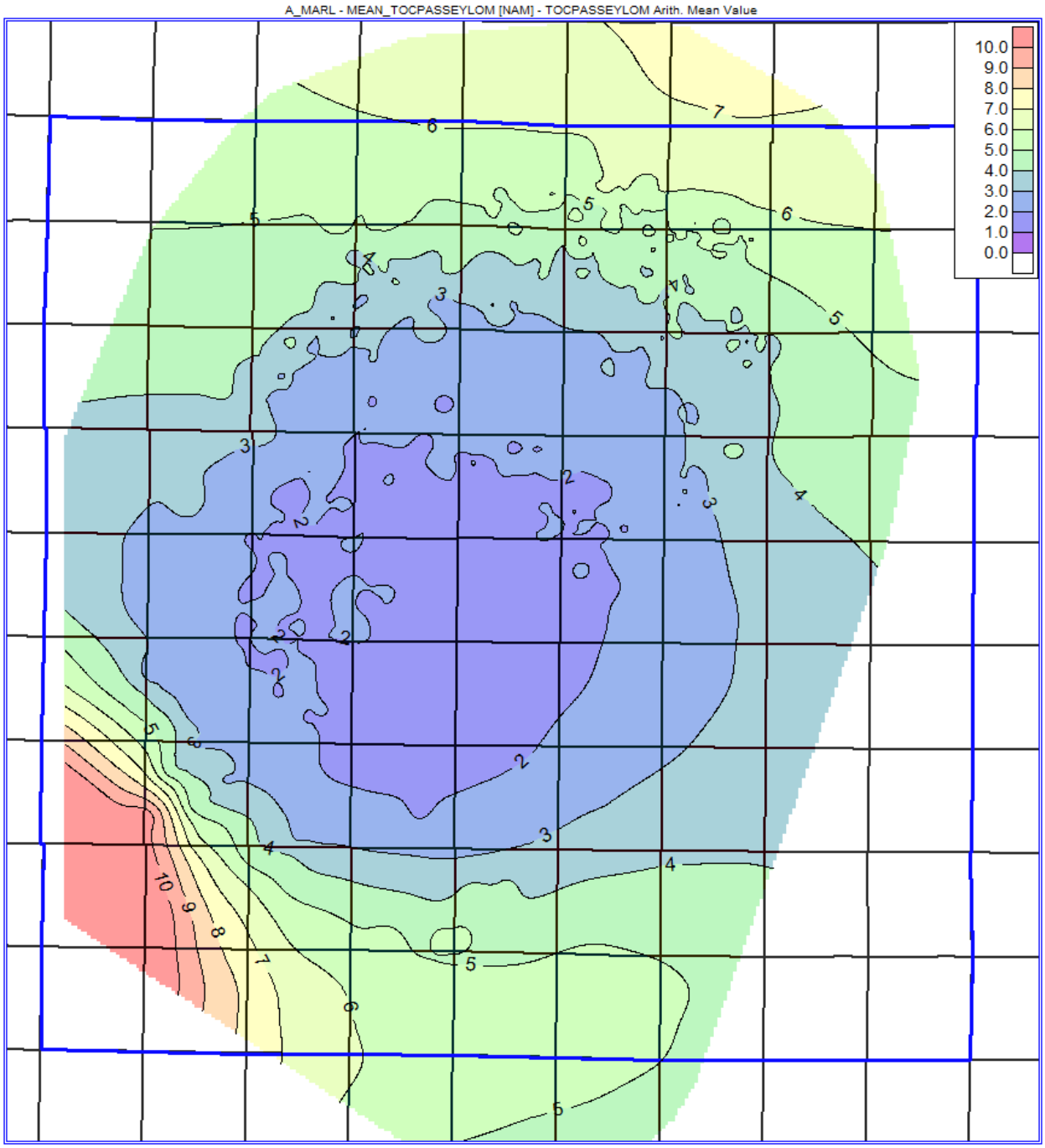

Figure 5.2. Mean log-derived TOC of the A Marl. The decrease in TOC towards the center of the field reflects the increase in maturity towards the center of the Wattenberg Thermal Anomaly.

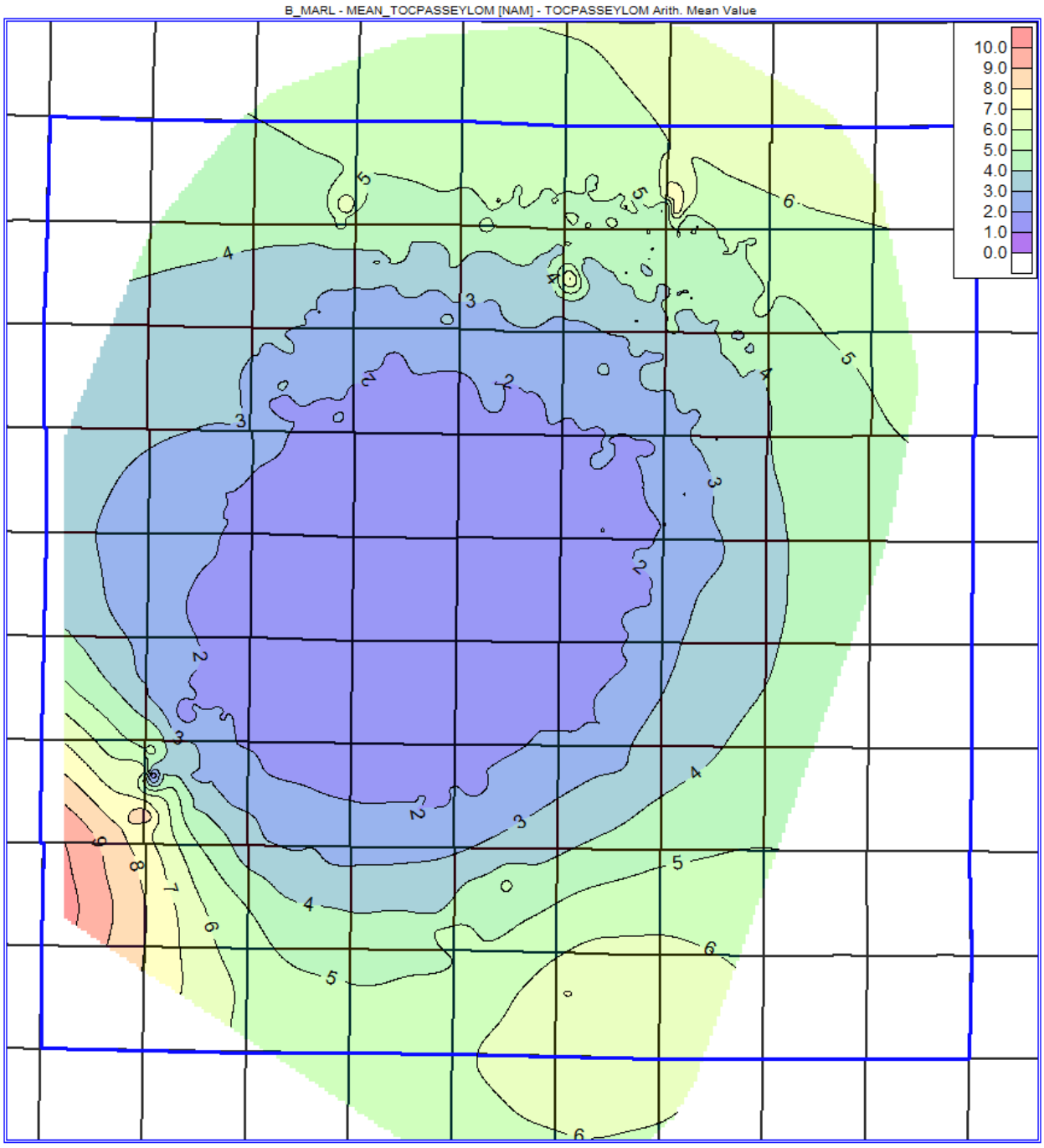

Figure 5.3. Mean log-derived TOC of the B Marl. This map is similar to the average TOC map of the A Marl, but about 1-2% lower in most places.

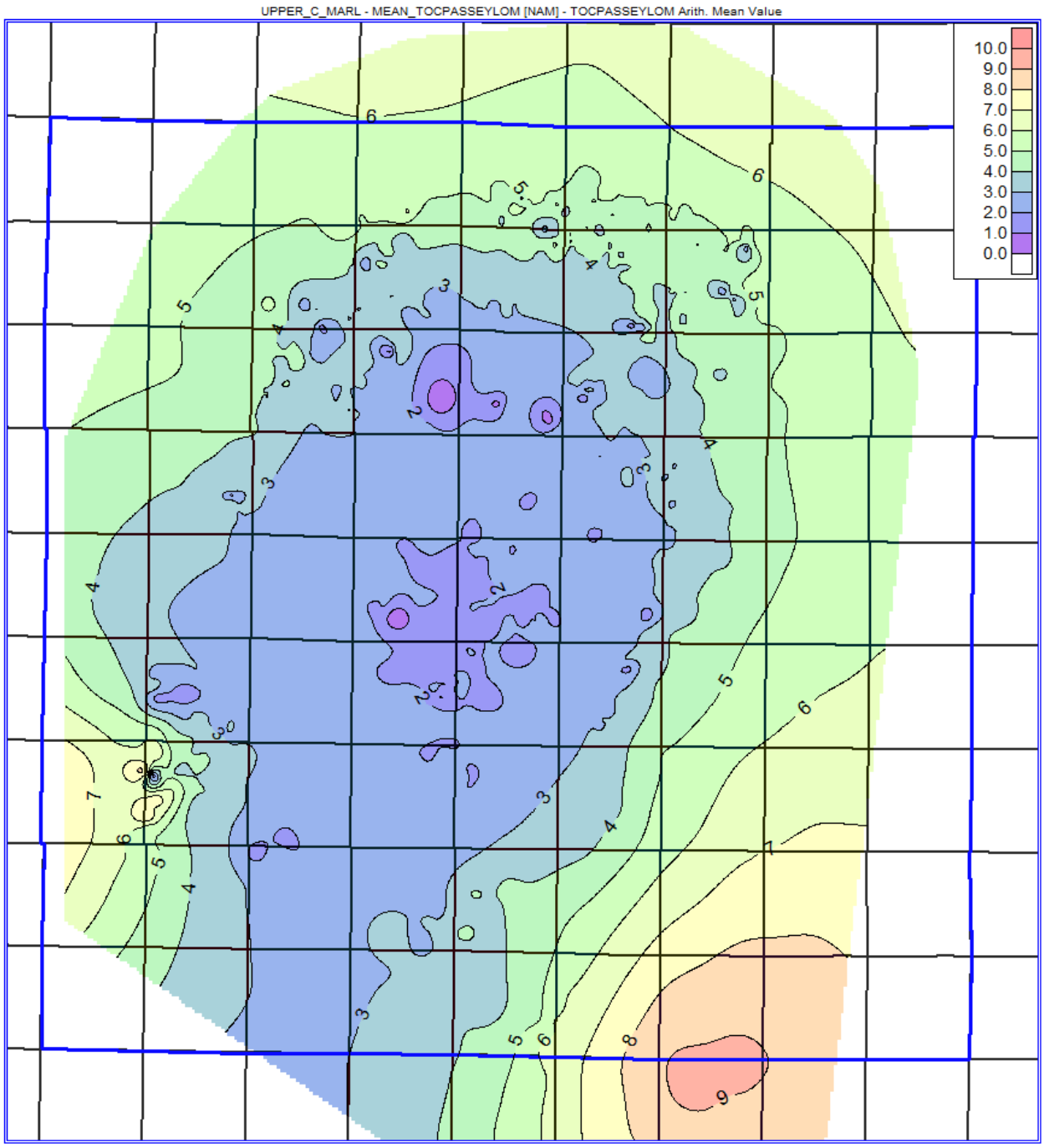

Figure 5.4. Mean log-derived TOC of the upper 20 ft of the C Marl. Since the lower part of the C Marl and Basal Chalk/Marl have minimal TOC values, only the upper, source-rock portion of the C Marl is mapped in this figure. This map shows slightly higher TOC in the center of the field, and slightly lower TOC in the southern part of the field compared to the other marls.

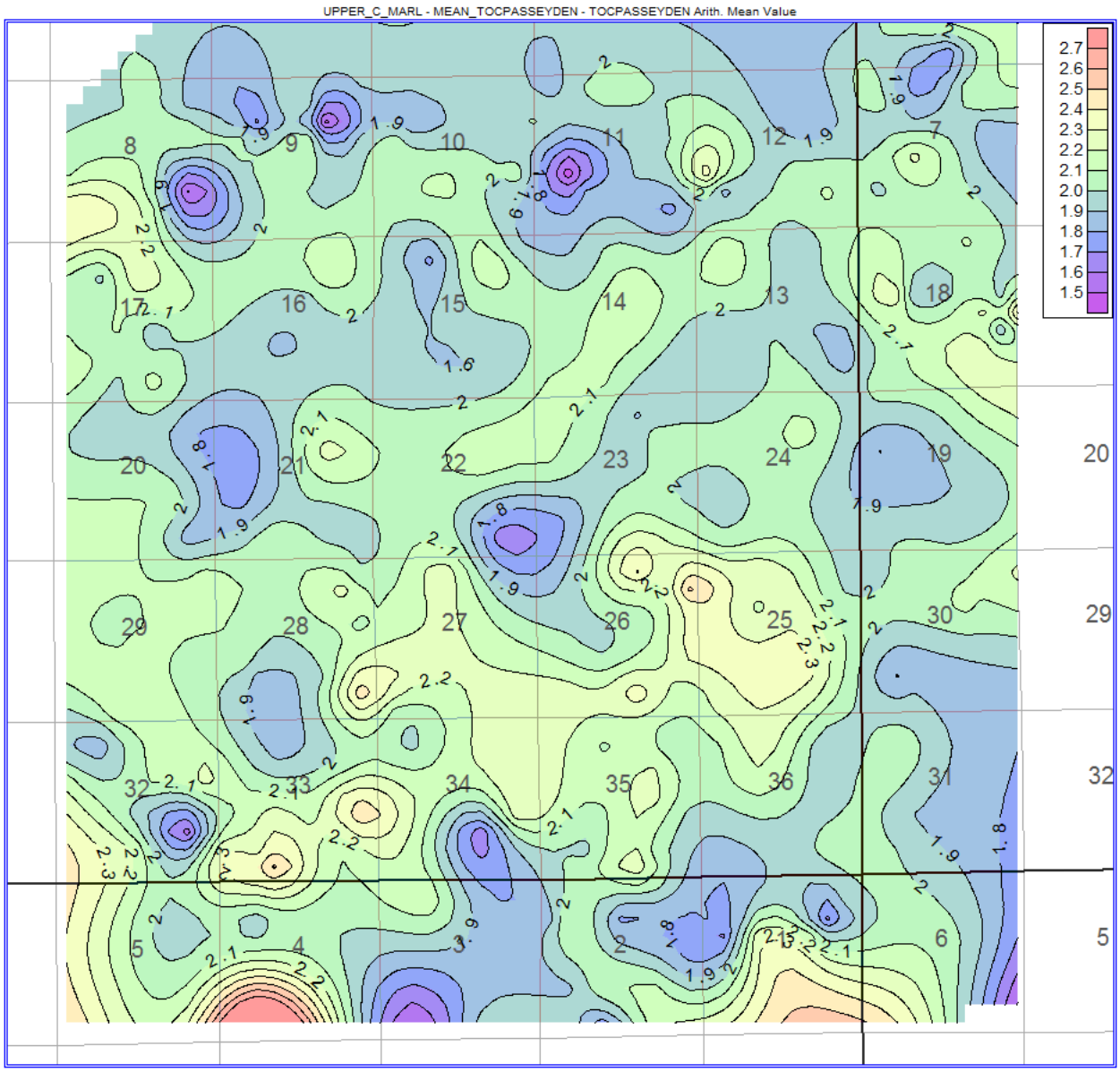

Figure 5.5. Mean log-derived TOC of the upper, organic-rich C Marl over the large-scale study area. Note the small range in TOC, but a small high over Section 25.

Typically, resistivity increases with maturity, as generated petroleum is more resistive than formation water. Smagala et al. (1984) were able to show this relationship in the K Zone of the Niobrara (a high resistivity bed within the C Chalk) in the Denver Basin (Figure 5.6A) to create a map of resistivity-derived maturity. Since this data is on a log-log plot, the shape of the data trend may be warped, especially away from the origin. Johnson and Bartshe (1991)

replotted the data on a linear scale (Figure 5.6B), allowing for a reinterpretation of the trend and the recognition of anomalous high resistivity values with higher maturity. This still may not be the best representation of the K Zone resistivity and maturity data, as the scales of the data are best suited for a semi-log plot (M. Al Duhailan, 2013, personal communication). This plot allows for the data with a large range (resistivity) to be plotted on a log scale and the data with a small range (vitrinite reflectance) to be plotted on a linear scale (Figure 5.6C). This final plot shows how the resistivity levels off (and may begin to come back down) at the highest maturities.

The drop in resistivity at high maturity can be seen clearly spatially. Cumella and Sheevel (2012) observed this in resistivity maps and cross sections of the Piceance Basin, Sand Wash Basin, and Denver Basin. Moving from the basin margin to the deepest, most mature area, resistivity increases and then decreases. Around Wattenberg Field, this leads to a ring of higher resistivity (Figures 5.7-5.8). The anomalous resistivities are limited to the B Chalk, B Marl, and C Chalk.

Trying to understand the possible causes of this resistivity anomaly begins with correlating the anomaly with other trends in the GWA. First, the resistivity aligns with vitrinite reflectance data from Higley and Cox (2005) (Figure 5.9). Second, it aligns with GOR and oil gravity (Figure 5.10). The resistivity anomaly also aligns with overpressuring in the Codell (Figure 5.11). While the Niobrara is known to be overpressured (Weimer 1996, Figure 2.11), this figure shows the spatial distribution of the overpressuring. Additionally, the resistivity low correlates with stratigraphic thins in the B Chalk and C Chalk, but no thin is present in the B Marl.

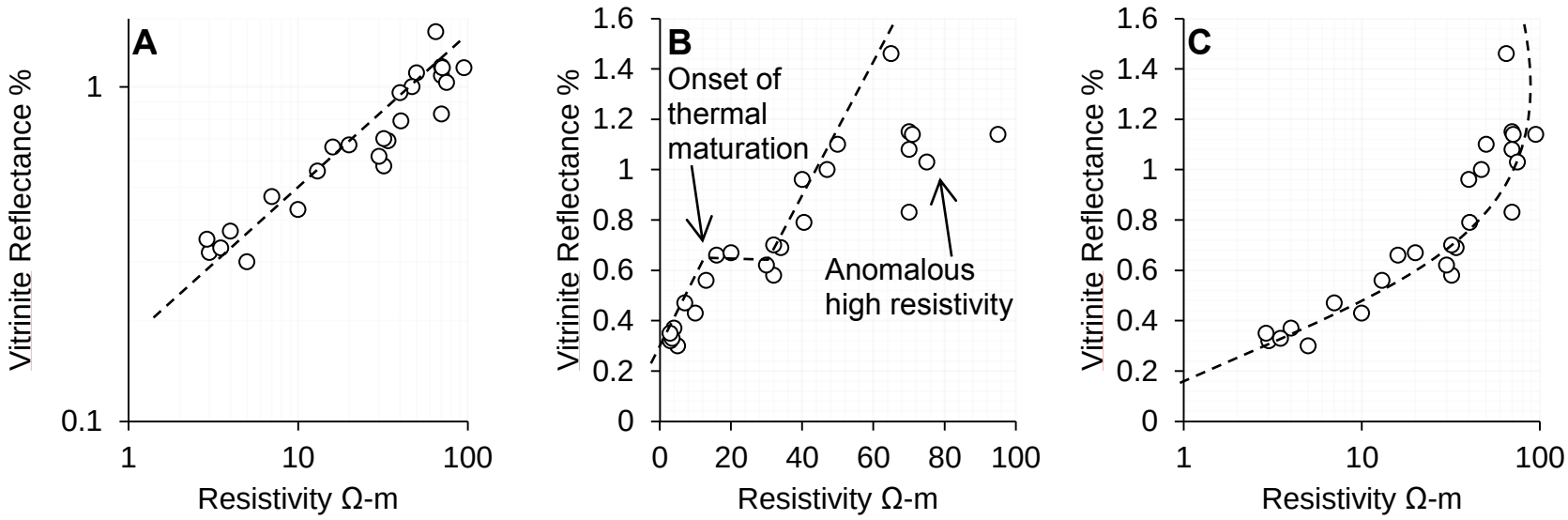

Figure 5.6. Plots of resistivity and vitrinite reflectance of the Niobrara K Zone marker bed in the Denver Basin. (A) The data as originally plotted by Smagala et al. (1984) on a log-log plot showing a strong correlation. (B) The same data replotted and reinterpreted on a linear scale by Johnson and Bartshe (1991). (C) The same data plotted on a semi-log plot after M. Al Duhailan (2013, personal communication) showing the resistivity leveling off and possibly coming down with increasing maturity.

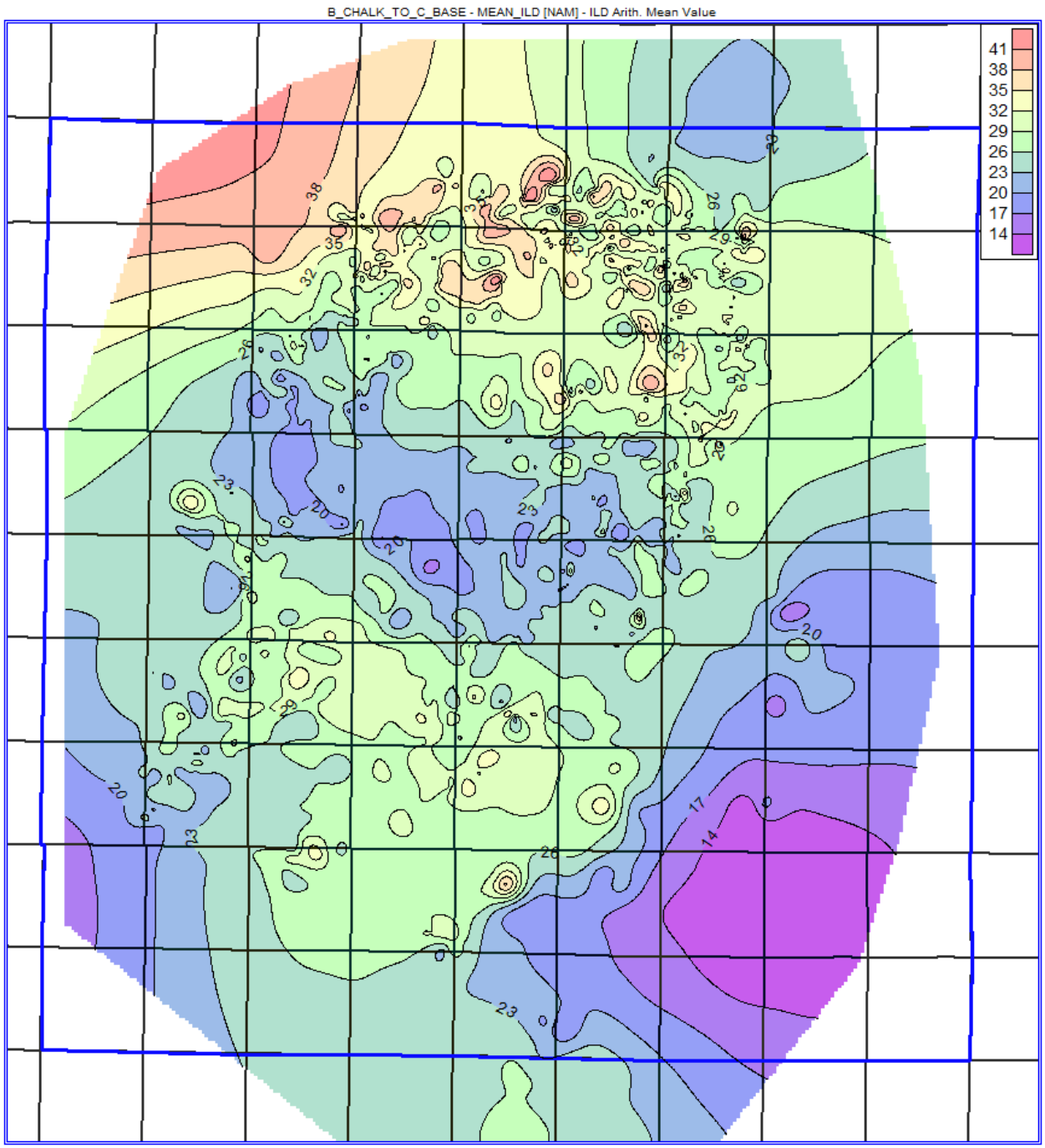

Figure 5.7. Mean resistivity map of the B Chalk, B Marl, and C Chalk interval of the Niobrara. The resistivity low in the center of the field (<23 Ω-m) is limited to these three units. Note the ring of higher resistivity surrounding the low (>26 Ω-m) and the lower resistivities at the margins of the field. Limited well control results in the anomalous high values in the northwest corner of the field.

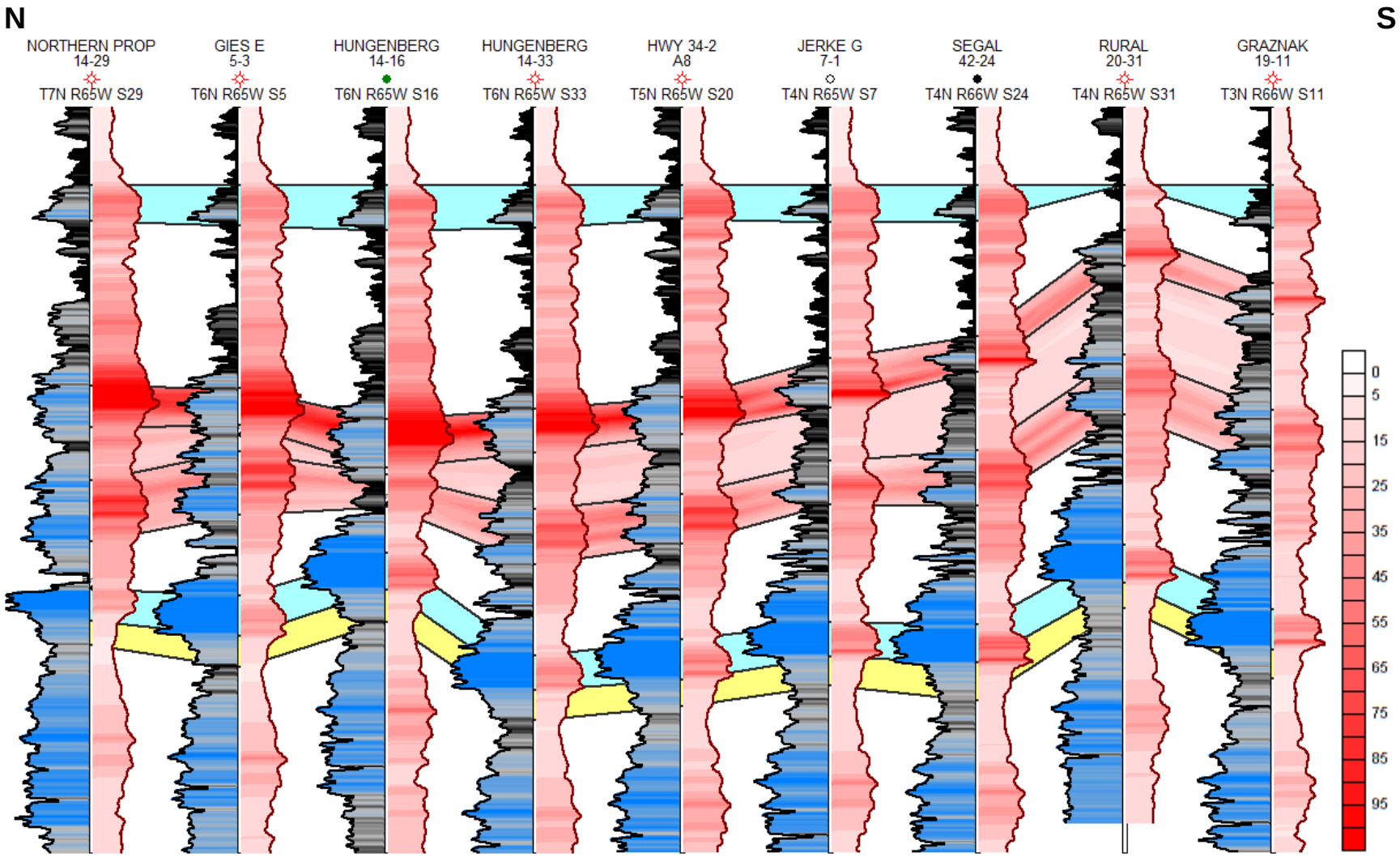

Figure 5.8. North-south cross section across the northern part of Wattenberg Field showing the decreasing in resistivity. These wells represent the areas with the highest resistivity to the areas with the lowest resistivity. The red interpretive color fill is the resistivity of the B Chalk, B Marl, and C Chalk (scale on right is in Ω-m), the A Chalk and Fort Hays are blue, and the Codell is yellow.

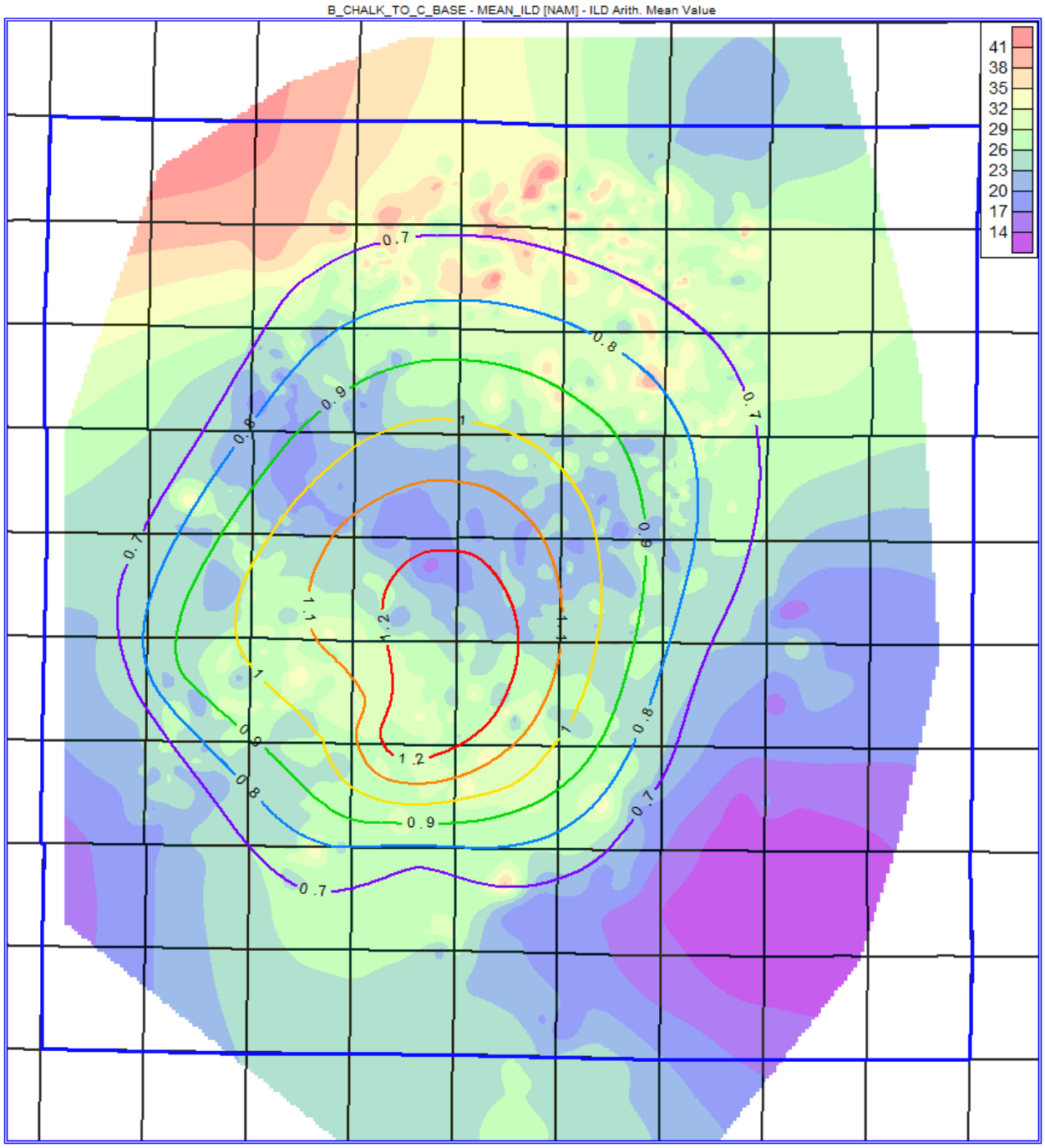

Figure 5.9. Niobrara resistivity low with vitrinite reflectance contours. The same resistivity map from the previous figure correlates to the Wattenberg Thermal Anomaly (after Higley and Cox, 2005).

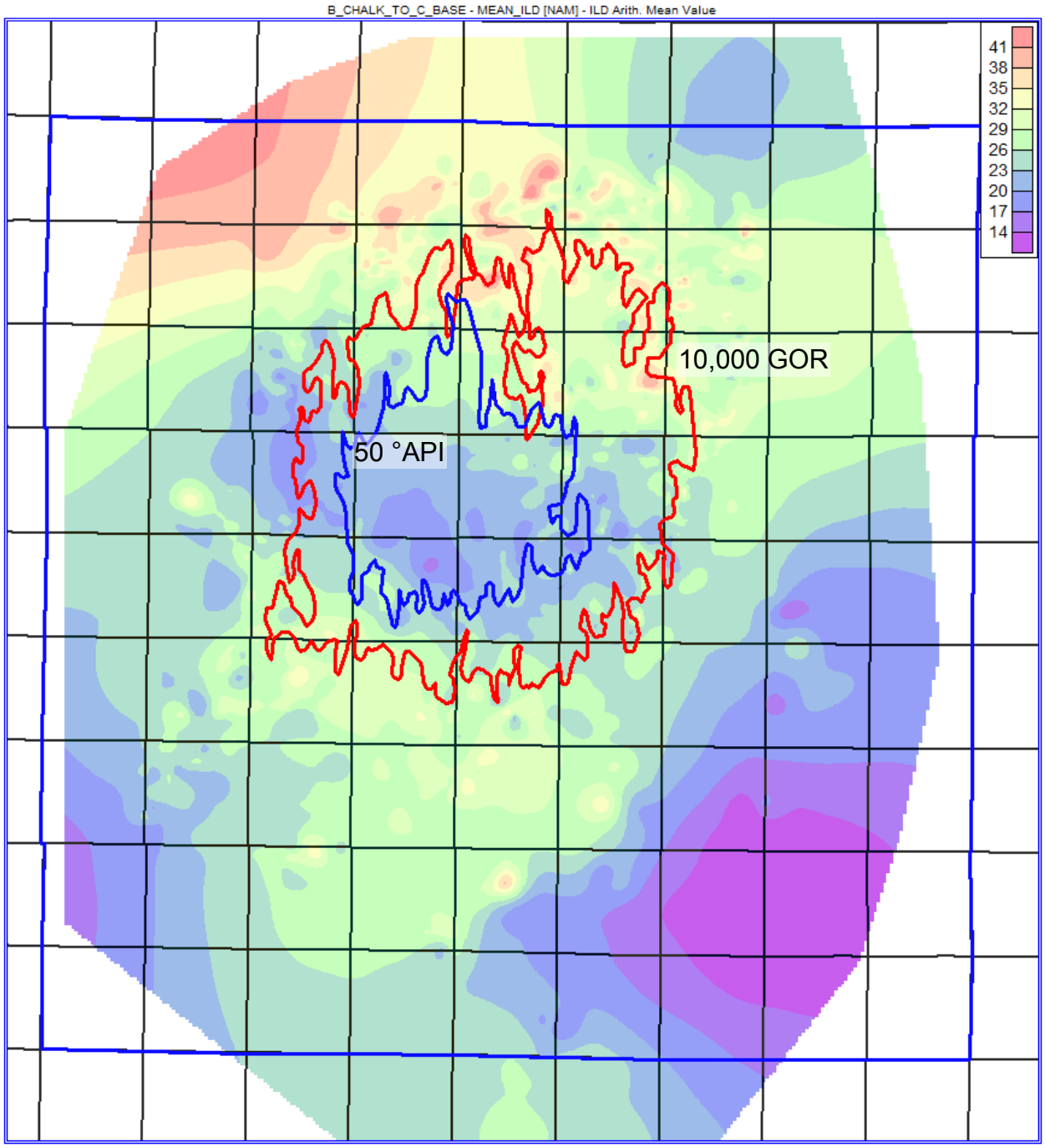

Figure 5.10. Niobrara resistivity low with 50 °API oil gravity (blue) and 10,000 GOR (red). Oil gravity and GOR data from IHS Energy (2013).

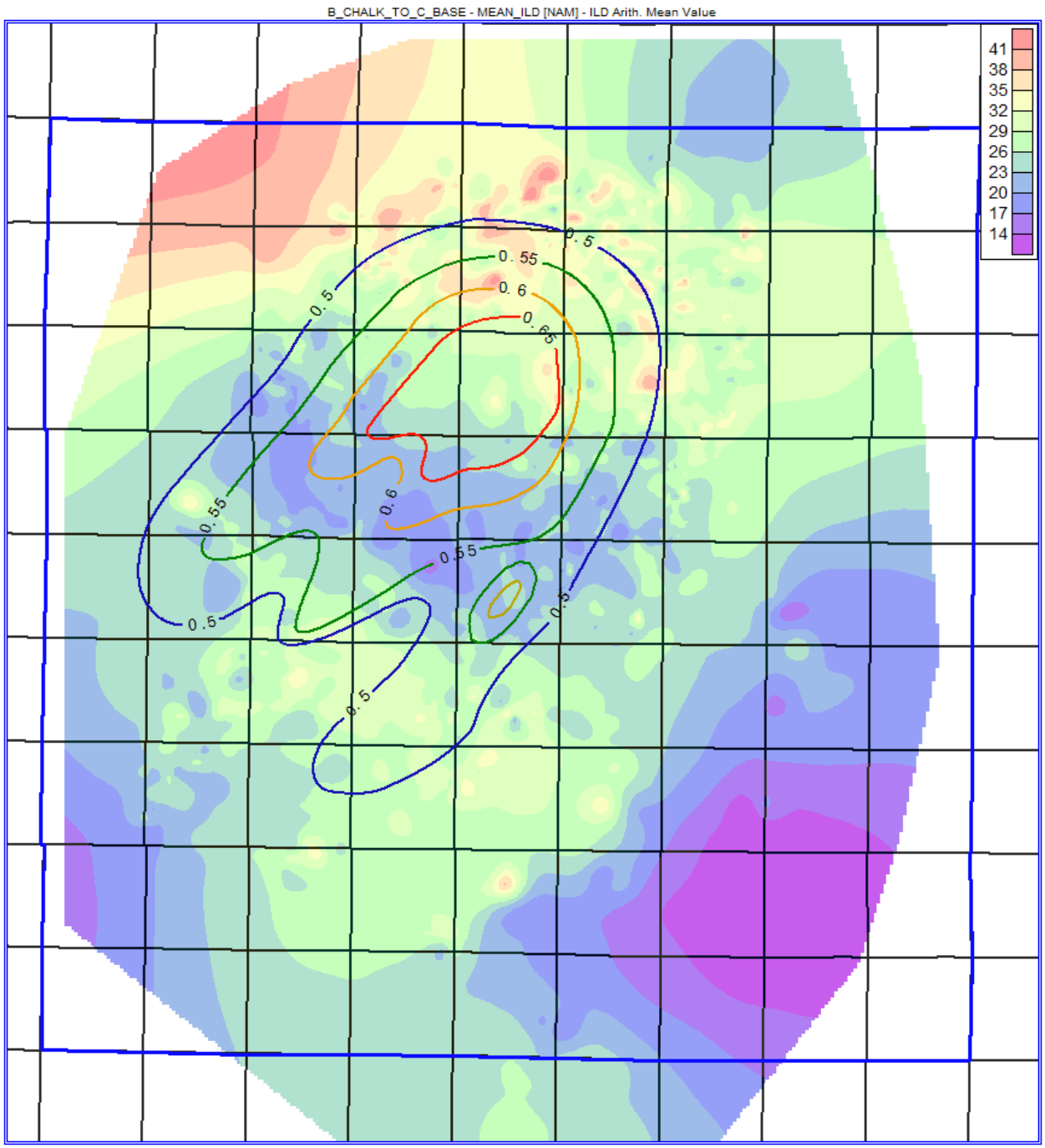

Figure 5.11. Niobrara resistivity low with Codell overpressuring contours (psi/ft). Overpressuring contours from Birmingham et al. (2001).

CHAPTER 6

DISCUSSION

The results presented in Chapters 3-5 give insight into the characteristics of the Niobrara Formation in Wattenberg Field. In particular, the spatial data provides a foundation for the understanding of stratigraphic, structural, and other trends in the field. This chapter gives space for a discussion of these results.

6.1 Relationship between Structure and Stratigraphy

Structural features in Wattenberg Field that affect the Niobrara are primarily interpreted through changes in stratigraphy. This is most pronounced in the east-west thin at the top of the Niobrara. However, alternative hypotheses for the changes in stratigraphy must be considered before a structural interpretation is accepted. The strongest alternative hypothesis is lack of deposition over the thin trend as a result of bypass or variable sedimentation. For example, the B1 Chalk in the northern part of the field thins to the south as it approaches the east-west thin trend (Figure 6.1). As it thins, the gamma ray response of this unit shows the individual spikes becoming closer together, suggesting different locations experienced different rates of sedimentation. Additionally, the gamma ray response becomes higher to the south, indicating a compositional change as well. However, evidence for compositional changes is not present in all units on both sides of the feature. Based on gamma ray log trace of the A Chalk and the B1 Chalk on the south side of the thin trend, as the units thins, the gamma ray log spikes are not being compressed, but instead are missing from the top down. The absence of pervasive condensed section is strong evidence against the hypothesis of bypass or variable sedimentation.

Instead, the interpretation with the strongest evidence is that the thin was created by erosion. The way gamma ray spikes disappear from the top down toward the axis of the thin is

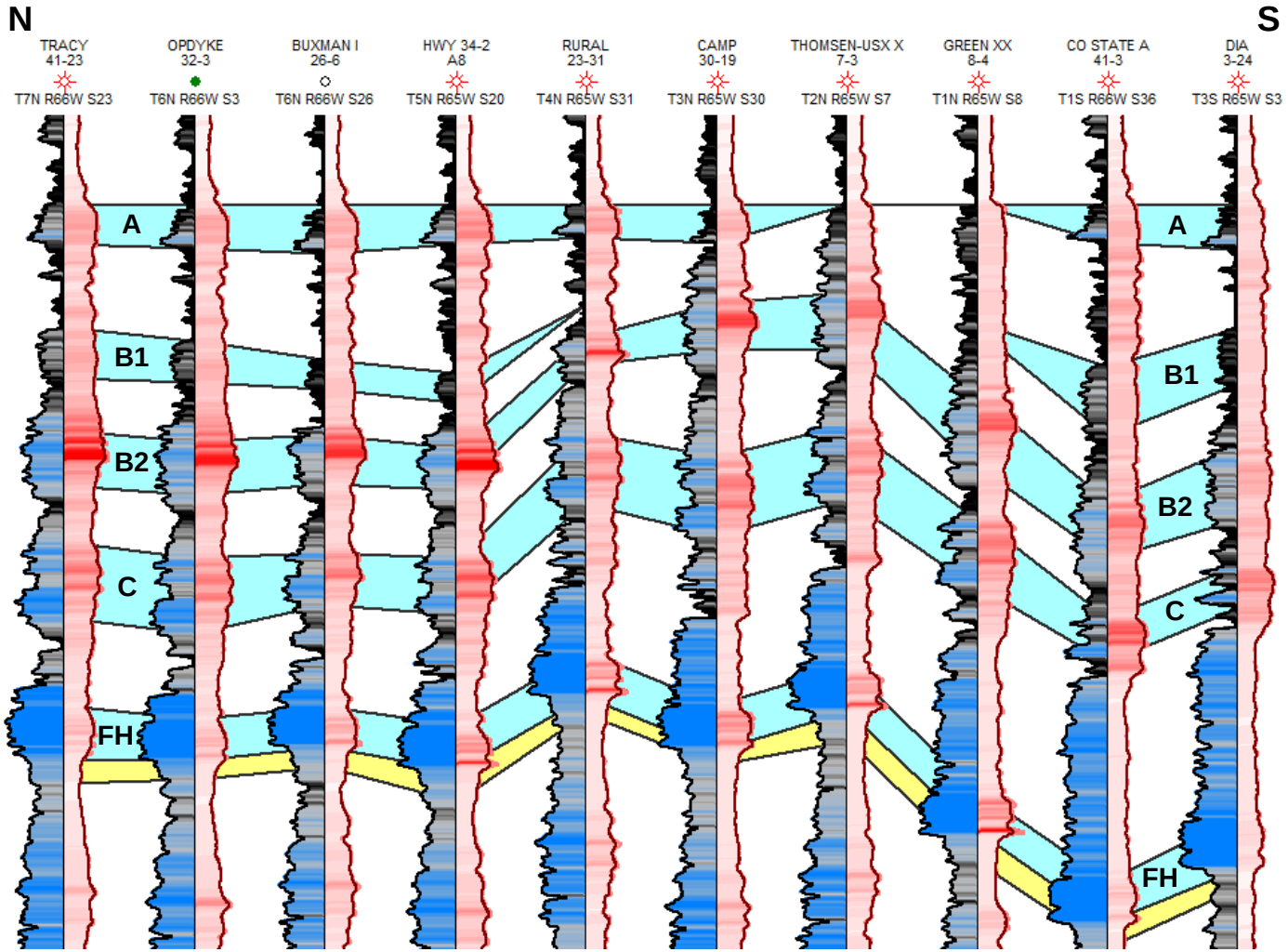

Figure 6.1. North-south cross section of the Niobrara across Wattenberg Field. This stratigraphic cross section is hung on the top of the Niobrara. Chalk benches (A, B1, B2, C, and Fort Hays) are shown in blue, and the Codell Sandstone is shown in yellow. This cross section shows the thinning and absence of the A Chalk, A Marl, and B1 Chalk. Note how the gamma ray traces of the B1 chalk north of the thin trend condense and how this differs from the truncating gamma ray traces off the top of the A Chalk and B1 Chalk south of the thin trend.

most likely created by erosion. Additionally, since no evidence of subaerial exposure has been reported in the Niobrara, this was likely submarine erosion. The WIC Seaway had sufficient currents for this to occur (Longman et al., 1998; Drake and Hawkins, 2012).

6.2 Faulting Styles and Characteristics

While other faulting styles are present in the Cretaceous section of the Denver Basin (i.e., wrench faulting, salt dissolution faulting), layer-bound normal faulting in the Niobrara is the most relevant to this study area. Evidence from well logs and 3D seismic data supports the recent interpretation of a polygonal fault system (PFS) (Sonnenberg and Underwood, 2013). Faults recognized in this study match many characteristics of PFS. Their length, throw, vertical extent, and paired nature are all similar to the fault system recognized by Sonnenberg and Underwood (2013) and fall within the range of typical for PFS (Cartwright, 2011).

What makes the faults in this study unique is that they do not display random orientations, but have a strong northeast-southwest orientation. This orientation was recognized as a weak trend by Underwood (2013) and can be a normal arrangement of faults in PFS (Cartwright, 2011). Additionally, the grabens recognized in this study show an en echelon arrangement, suggesting a left-lateral component of transtension during their formation (Figure 6.2). The direction of shear is opposite of the right-lateral basement-involved wrench faults interpreted in the Denver Basin despite a similar shear orientation.

The timing of faults can be related to the analysis of growth strata above the faulted interval. Since growth strata above the Niobrara tier of faulting is limited to the lower ~400 ft of the Pierre Shale, movement on these faults stopped by the time deposition of the sediment at this level. This shows the faults occurred early after deposition and at relatively shallow depths. Additionally, the since the faults are at a lower angle (about 45°) than typical normal faults, they

may have undergone compactional flattening; a hypothesis suggested by others to explain this phenomenon of PFS (Cartwright, 1996; Sonnenberg and Underwood, 2013). If this is the case, it would be further evidence for early timing of the faults. With this timing, the faults are unlikely related to later tectonic events such as the Laramide Orogeny.

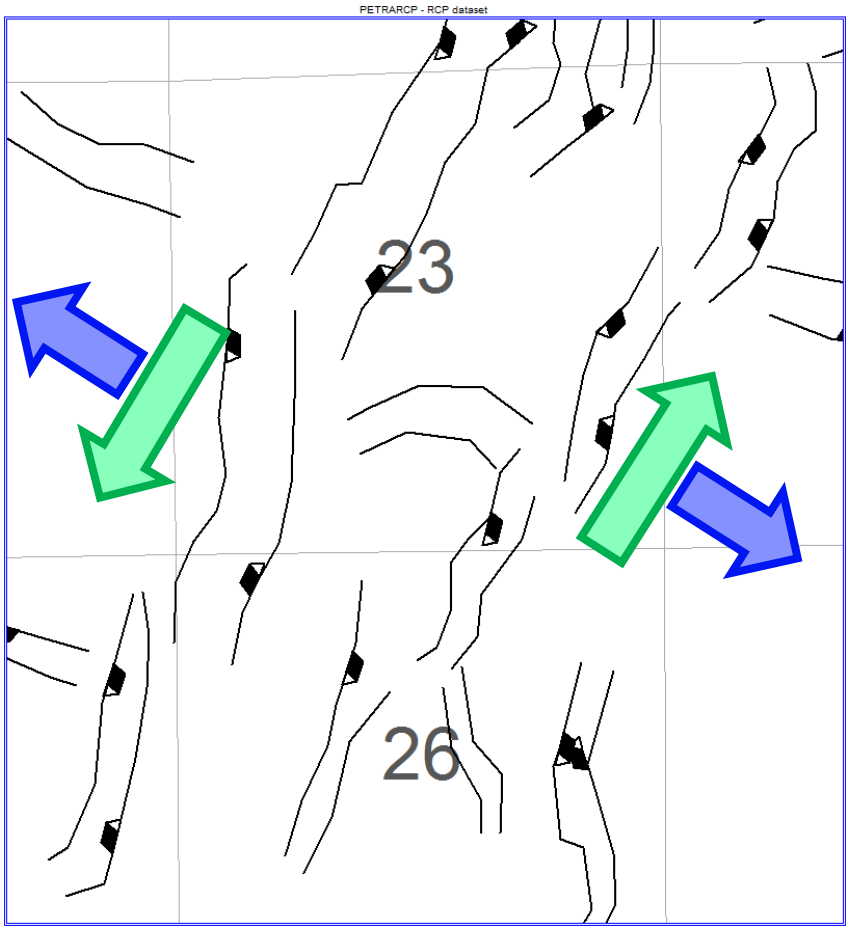

Figure 6.2. En echelon grabens showing transtension. Blue arrows show direction of extension and green arrow show direction of simple shear.

6.3 Log Data Trends

Log-derived TOC calculations and subsequent mapping allow for the creation of an exploration tool. However, since the small-scale average TOC maps are generally a reflection of the maturity in the GWA, they have limited use in exploration. Examining TOC at other scales (e.g., Figure 5.5) or in areas of the Denver Basin with a smaller range in maturity is of more use

to exploration. Additionally, it should be noted that the versions of the equations used in this study only give accurate values for the TOC of the marls and not the chalks of the Niobrara. To look at the chalks, or carbonate-poor source rocks like the Sharon Springs, these equations will need to be modified and recalibrated. Finally, the resistivity low recognized in Wattenberg Field also impacts the log-derived TOC because resistivity is one of the variables in the TOC calculation. Anomalously low resistivity values of 5 Ω-m can affect the calculations by up to about -0.5% TOC (depending on the other parameters).

The anomalous resistivity low in the center of Wattenberg Field correlates with various other parameters. Many of these are related to maturity, like vitrinite reflectance, GOR, and oil gravity, but the correlation to overpressuring is not related to maturity. Although resistivity correlates to stratigraphic thins in the B Chalk and C Chalk, it does not correlate to a thin in the B Marl, suggesting stratigraphy does not play a role in the presence of this feature.

To understand the nature of this anomaly, it is necessary to look beyond correlations and consider possible causes of the resistivity low. One hypothesis for the cause of the low resistivity is related to formation water in mature, high temperature rocks. At high temperature, significant volumes of water vapor may be dissolved in the hydrocarbon gas (Yarrison et al., 2006; Newsham and Rushing 2009). The remaining water in the system would become more saline, therefore reducing resistivity (Cumella and Sheevel, 2012). However, it has been shown that in rocks of high shale content, salinity does not significantly affect resistivity (Wang et al., 2006). This effect is independent of water saturation. Since the Niobrara has a high enough clay content to mask the effect of salinity on resistivity, this hypothesis is rejected.

A second hypothesis for the cause of the resistivity low is the formation of conductive pyrobitumen at high maturities. Pyrobitumen is the residual insoluble organic compounds after

oil thermally decomposes into gas. Some of the components of pyrobitumen are conductive (e.g., shungite and precursors to graphite) (Shaw et al., 1997). This relationship is mentioned by Passey et al., (2010), who concludes that conductive mineral phases (but no graphite) are present and reduce resistivity in very mature (Ro>3) rocks. However, Passey et al. (2010) are studying rocks at a higher maturity than Wattenberg (Ro>3 vs. Ro≈1.1) and no pyrobitumen has been documented or studied in Wattenberg (Cumella and Sheevel, 2012). Therefore this hypothesis is unlikely, but not rejected.

The third, and most likely, hypothesis for the cause of the low resistivity is overpressuring. Overpressuing is known to cause low resistivity anomalies in other basins, such as the Anadarko Basin (Nelson and Gianoutsos, 2011). Given the high spatial correlation between the resistivity low and overpressure data from Birmingham et al. (2001), this is the most probably explanation for this feature. Since the resistivity low is limited to the B Chalk, B Marl, and C Chalk, these units may have the largest changes in overpressuring. However, since some units (like the Codell) show overpressuring but no resistivity low, other causes must also influence the resistivity of the Niobrara in Wattenberg.

CHAPTER 7

CONCLUSIONS AND RECOMMENDATIONS

From this research, the following conclusions about the characteristics and spatial variability of the Niobrara Formation in Wattenberg Field can be reached. Stratigraphic variations across Wattenberg are primarily due to differential compaction and compensational sedimentation (Drake and Hawkins, 2012). The largest structural feature is a paleo-high running east-west across the field. Its presence is related to igneous intrusions in the basement. Parts of the A Chalk, A Marl, and B1 Chalk are missing, primarily due to submarine erosion, giving the feature a maximum relief of about 100 ft. Normal faults are similar to those previously characterized as part of a PFS (Sonnenberg and Underwood, 2013), with the exception of a strong northeast-southwest trend. The presence of en echelon grabens is due to transtension. The faults mapped in this study are attributed to a PFS, and their scale emphasizes the importance of 3D seismic data in exploration. Log-derived TOC data is heavily influenced by the Wattenberg Thermal Anomaly and is only accurate across a wide range in maturity in the marls. Due to the range of maturity in the GWA, log-derived TOC is of limited exploration use at this scale. The resistivity low in the middle of the field is limited to the B Chalk, B Marl, and C Chalk and is primarily related to overpressuring due to increased thermal maturation.

The two datasets in this study provide enough detail for a significant volume of future work. A petrophysical analysis of the digital logs and detailed geophysical work on the seismic data are recommended. This work is currently underway by students in both the Colorado School of Mines Niobrara Consortium and Reservoir Characterization Project.

REFERENCES

Beitz, M. K., R. Cunningham, and L. E. LaChance, 2013, Utilizing the Delta Log R method for determining total organic carbon of the Niobrara Formation, B Bench, Denver-Julesburg Basin, Colorado and Wyoming: AAPG Search and Discovery Article 10532: http://www.searchanddiscovery.com/pdfz/documents/2013/10532beitz/ndx_beitz.pdf.html (accessed January 10, 2014).

Birmingham, T. J., D. M. Lytle, and R. N. Sencenbaugh, 2001, Enhanced recovery from a tight gas sand through hydraulic refracturing: Codell Formation, Wattenberg Field, Colorado: Gas in the Rockies.

Cartwright, J. A., 1996, Polygonal fault systems: a new type of fault structure revealed by 3-D seismic data from the North Sea Basin, *in* Weimer, P., and Davis, T.L., eds., AAPG Studies in Geology No. 42 and SEG Geophysical Development Series No. 5: Tulsa, American Association of Petroleum Geologists, p. 225-230.

Cartwright, J. A., 2011, Diagenetically induced shear failure of fine-grained sediments and the development of polygonal fault systems: Marine and Petroleum Geology v. 28, no. 9, p. 1593–1610.

Cumella, S. and J. Scheevel, 2012, Mesaverde tight gas sandstone sourcing from underlying Mancos-Niobrara shales: AAPG Search and Discovery Article 10450: http://www.searchanddiscovery.com/documents/2012/10450cumella/ndx_cumella.pdf (accessed March 4, 2014).

Dean, W. E., and M. A. Arthur, 1998, Geochemical expressions of cyclicity in Cretaceous pelagic limestone sequences: Niobrara Formation, Western Interior Seaway: Stratigraphy and Paleoenvironments of the Cretaceous Western Interior Seaway, USA, SEPM Concepts in Sedimentology and Paleontology, no. 6, p. 227–255.

Drake, W. R., and S. J. Hawkins, 2012, A sequence stratigraphic framework for the Niobrara Formation in the Denver-Julesburg Basin: AAPG Search and Discovery Article 50757: http://www.searchanddiscovery.com/documents/2012/50757drake/ndx_drake.pdf (accessed February 2, 2014).

Higley, D. K. and D. O. Cox, 2005, Oil and gas exploration and development along the Front Range in the Denver Basin of Colorado, Nebraska, and Wyoming, *in* N. S. Fishman, ed., Energy resource studies, Northern Front Range, Colorado, UGSG Professional Paper 1698, p. 9–53.

Higley, D. K., D. O. Cox, and R. J. Weimer, 2003, Petroleum system and production characteristics of the Muddy (J) Sandstone (Lower Cretaceous) Wattenberg continuous gas field, Denver basin, Colorado: AAPG Bulletin, v. 87, no. 1, p. 15–37.

Higley, D. K., D. L. Gautier, and M. J. Pawlewicz, 1992, Influence of regional heat flow variation on thermal maturity of the Lower Cretaceous Muddy ("J") sandstone, Denver Basin, Colorado, *in* L. B. Magoon, ed., The petroleum system—Status of research and methods, 1992: U.S. Geological Survey Bulletin 2007, p. 66–69.

IHS Energy, 2013, U.S. well and production database: IHS Energy, 15 Inverness Way East, Englewood, CO 80112.

Jarvie, D. M., 2012, Shale resource systems for oil and gas: Part 2—Shale-oil resource systems, *in* J. A. Breyer, ed., Shale reservoirs—Giant resources for the 21st century: AAPG Memoir 97, p. 89–119.

Johnson, R. A., and R. T. Bartshe, 1991, Using resistivity to assess Niobrara fracture patterns for horizontal wells: Oil & Gas Journal, v. 89, p. 99–103.

Kauffman, E.G., 1977, Geological and biological overview; Western Interior Cretaceous Basin: The Mountain Geologist, v. 14, p. 75–99.

Ladd, J. H., 2001, An overview and development history of the Wattenberg Field: Gas in the Rockies, p. 29.

Locklair, R. E., and B. B. Sageman, 2008, Cyclostratigraphy of the Upper Cretaceous Niobrara Formation, Western Interior, U.S.A.: A Coniacian-Santonian orbital timescale: Earth and Planetary Science Letters, v. 269, p. 540–553.

Longman, M. W., B. A. Luneau, and S. M. Landon, 1998, Nature and distribution of Niobrara lithologies in the Cretaceous Western Interior Seaway of the Rocky Mountain Region: The Mountain Geologist, v. 35, no. 4, p. 137–170.

Luneau, B., M. Longman, P. Kaufman, and S. Landon, 2011, Stratigraphy and petrophysical characteristics of the Niobrara Formation in the Denver Basin, Colorado and Wyoming: AAPG Search and Discovery Article 50469: http://www.searchanddiscovery.com/ documents/2011/ 50469luneau/ndx_luneau.pdf (accessed February 2, 2014).

Magoon, L. B. and W. G. Dow, 1994, The petroleum system, *in* L. B. Magoon and W. G. Dow, eds., The petroleum system—from source to trap: AAPG Memoir 60, p. 3–24.

Matthews, V., 2011, Colorado's new oil boom—the Niobrara: CGS Rocktalk, v. 13, no. 1, p. 1–12.

Nelson, P. H., and N. J. Gianoutsos, 2011, Evolution of overpressured and underpressured oil and gas reservoirs, Anadarko Basin of Oklahoma, Texas, and Kansas—Overview: USGS Open-File Report 2011-1245.

Nelson, P. H., and S. L. Santus, 2011, Gas, oil, and water production from Wattenberg Field in the Denver Basin, Colorado, 2011–1175: U.S. Geological Survey, 23 p.

Newsham, K. E., and J. A. Rushing, 2009, Laboratory and field observations of an apparent sub-capillary-equilibrium water saturation distribution in a tight gas sand reservoir: AAPG Search and Discovery Article 40400: http://www.searchanddiscovery.com/documents/2009/40400newsham/images/newsham_ppt.pdf (accessed August 29, 2013).

Passey, Q. R., K. M. Bohacs, W.L. Esch, R. Klimentidis, and S. Sinha, 2010, From oil-prone source rock to gas-producing shale reservoir – Geologic and petrophysical characterization of unconventional shale-gas reservoirs: SPE International Oil & Gas Conference and Exhibition, Beijing, China.

Passey, Q. R., S. Creaney, J. B. Kulla, F. J. Moretti, and J. D. Stroud, 1990, A practical model for organic richness from porosity and resistivity logs: AAPG Bulletin, v. 74, no. 12, p. 1777–1794.

Pittman, E. D., 1989, Nature of the Terry Sandstone reservoir, Spindle Field, Colorado, *in* E. B. Coalson and S. S. Kaplan, eds., Petrogenesis and petrophysics of selected sandstone reservoirs of the Rocky Mountain Region, Rocky Mountain Association of Geologists, p. 245–254, 338–339.

Shaw, J. C., R. Tsuen, and S. M. Leggitt, 1997, Well productivity improvement by chemical removal of pyrobitumen: SPE Oilfield Chemistry International Symposium, p. 161–168.

Sims, P. K. and C. A. Finn, 2001, Precambrian basement map of Colorado—A geologic interpretation of an aeromagnetic anomaly map: GSA Joint Annual Meeting: Tectonics of the Rocky Mountain Region (Posters), Albuquerque, NM, May 1, 2001.

Smagala, T. M., C. A. Brown, and G. L. Nydegger, 1984, Log-derived indicator of thermal maturity, Niobrara Formation, Denver Basin, Colorado, Nebraska, Wyoming, *in* J. Woodward, F. F. Meissner, and J. L. Clayton, eds., Hydrocarbon source rocks of the greater Rocky Mountain Region, Rocky Mountain Association of Geologists, p. 355–363.

Sonnenberg, S. A., 2012, The Niobrara Petroleum System, Rock Mountain Region: AAPG Search and Discovery Article 80206: http://www.searchanddiscovery.com/documents/2012/80206sonnenberg/ndx_sonnenberg.pdf (accessed February 2, 2014).

Sonnenberg, S. A. and D. F. Underwood, 2013, Polygonal fault systems—A new structural style for the Niobrara Formation and Pierre Shale, Denver Basin, Colorado: The Rocky Mountain Geologist, v. 50, no. 4, p. 127–142.

Sonnenberg S. A. and R. J. Weimer, 1993, Oil production from Niobrara Formation, Silo Field, Wyoming: Fracturing associated with a possible wrench fault system (?): The Mountain Geologist, v. 30, no. 3, p. 39–53.

Underwood, D., 2013, Polygonal fault systems, a new structural style for the Niobrara and Lower Pierre Shale, Denver Basin, Colorado, Master's thesis, Colorado School of Mines, Golden, Colorado, 68 p.

USGS, 2013, Core library number D859, Central Region Core Research Center Administration, http://my.usgs.gov/crcwc/core/report/12065 (accessed November 11, 2013).

Wang, K. W., J. M. Sun, S. C Geng, and J. L. Wu, 2006, Percolation network study of shale effects on rock electrical properties under different salinity: Chinese Journal of Geophysics, v. 49, no. 6, p. 1710–1717.

Weimer, R. J., 1996, Guide to the petroleum geology and Laramide Orogeny, Denver Basin and Front Range, Colorado: Denver, Colorado Geological Survey, 127 p.

Weimer, R. J., and S. A. Sonnenberg, 1982, Wattenberg Field, paleostructure-stratigraphic trap, Denver Basin Colorado: Oil and Gas Journal, v. 80, p. 204–210.

Weimer, R. J., S. A. Sonnenberg, and G. C. Young, 1986, Wattenberg Field, Denver Basin, Colorado, *in* C. W. Spencer and R. F. Mast, eds., Geology of tight gas reservoirs: Tulsa, Oklahoma, American Association of Petroleum Geologists, p. 143–164.

Yarrison, M., K. R. Cox, and W. G. Chapman, 2006, Measurement and modeling of the solubility of water in supercritical methane and ethane from 310 to 477 K and pressures from 3.4 to 110 MPa: Industrial & Engineering Chemistry Research, v. 45, p. 6770-6777.